



Universitat Autònoma de Barcelona

# Hemilabile Phosphine Ligands in Molybdenum and Tungsten Octahedral Environments

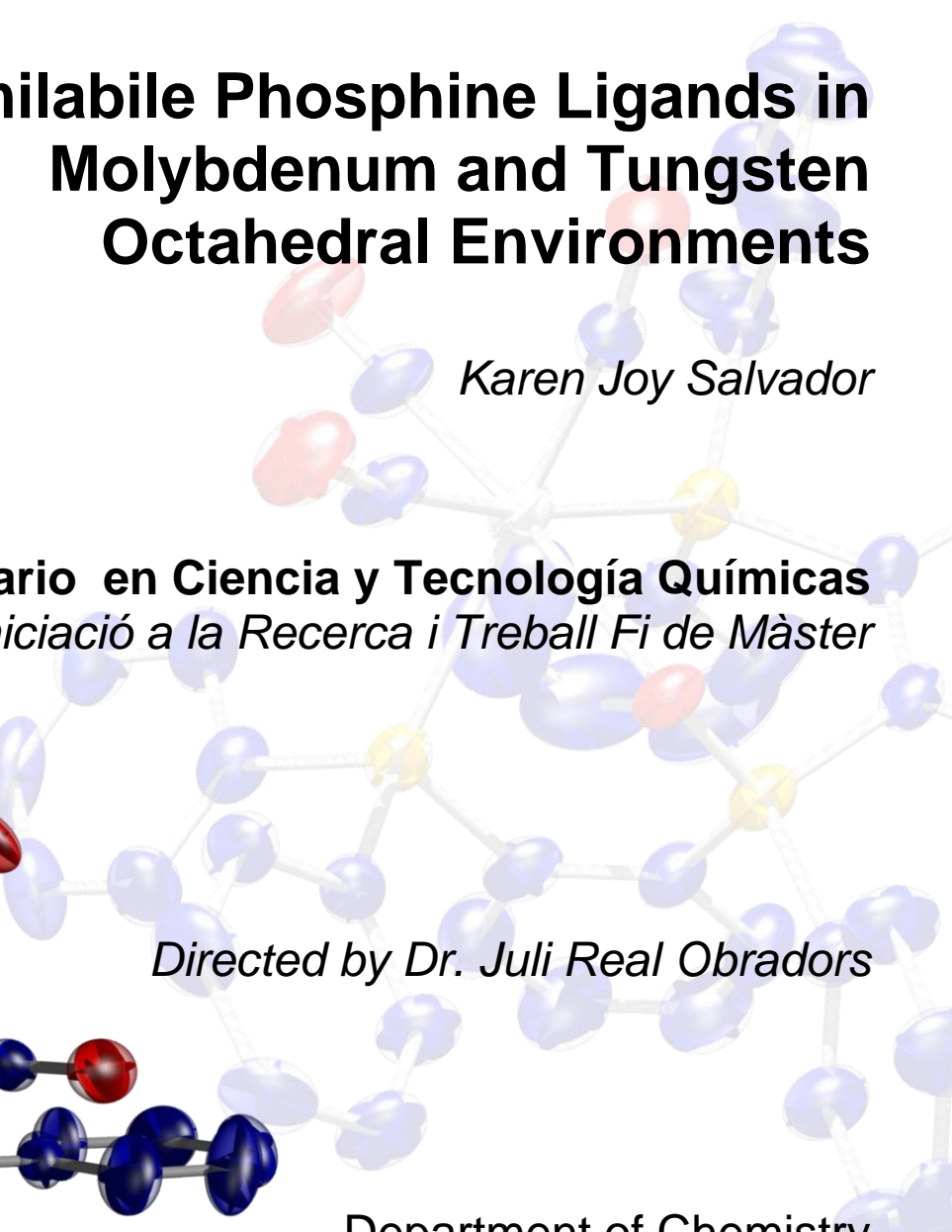
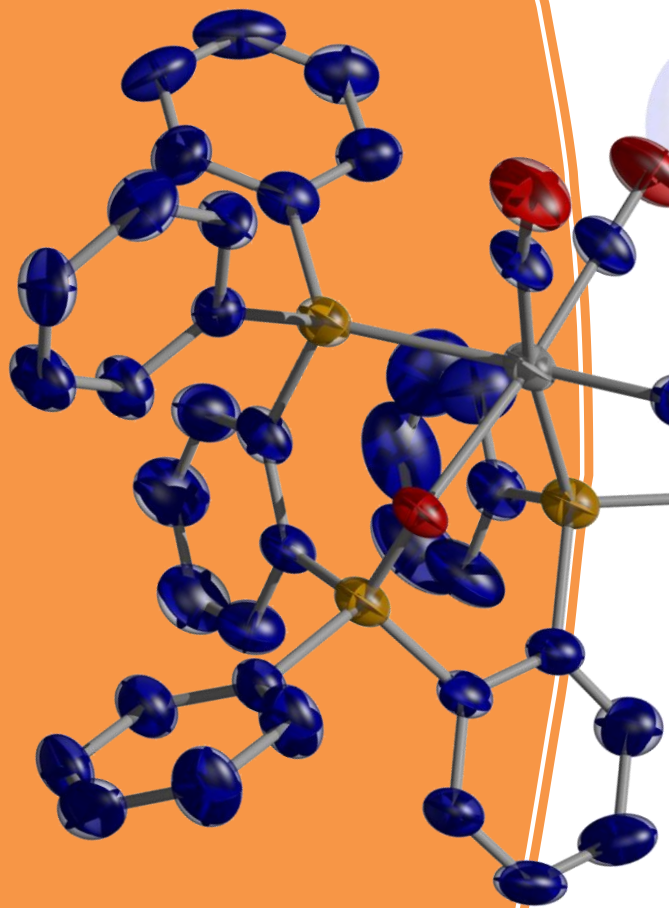
*Karen Joy Salvador*

**Máster Universitario en Ciencia y Tecnología Químicas**  
*Iniciació a la Recerca i Treball Fi de Màster*

*Directed by Dr. Juli Real Obradors*

Department of Chemistry  
Faculty of Science

September 2010





Memòria presentada per superar el mòdul Laboratori d'Iniciació a la Recerca  
correspondent al Màster Universitari Ciència i Tecnologia Químiques

**Karen Joy Salvador**

Vist i plau

**Dr. Juli Real i Obradors**  
Bellaterra, 30/07/2010

To the people who have put their hands on this work  
and to the people who shared their time and believed in me...

Juli, Joan Carles, Nacho, Dani, Ori,  
Laia, Joan, Fran, Jordi, Adu,  
*Nanay, Tatay, Manong, Ading, Anti, Pinsan.*

Thank you...Salamat...

This one is for you all...

## ABSTRACT

The synthesis of three bidentate, hemilabile phosphine ligands, newly synthesized in the research group (**TPOdiphos**, **DPPrPOdiphos** and **SODPdiphos**), has been up-scaled and optimized. The ligand substitution reaction on Mo(CO)<sub>6</sub> and W(CO)<sub>6</sub> has been studied and the corresponding complexes *fac*-[**MTPOdiphos**(CO)<sub>3</sub>], *fac*-[**MDPPrPOdiphos**(CO)<sub>3</sub>], and *fac*-[**MSODPdiphos**(CO)<sub>3</sub>], (M= Mo, W) have been isolated in good yields and characterized by NMR, IR and HR MS. In the case of *fac*-[**MoTPOdiphos**(CO)<sub>3</sub>] the XRD crystal structure was resolved. The complexes were found to be octahedral, neutral molecules, with the metal in the zero oxidation state and the ligand adopting a *facial* P,P,O-coordination. The hard ligand atom (oxygen) is expected to exhibit special features the future applications of these novel ligands.

## TABLE OF CONTENTS

	<b>Page</b>
<b>TITLE PAGE</b>	i
<b>ACKNOWLEDGEMENTS</b>	iii
<b>ABSTRACT</b>	iv
<b>TABLE OF CONTENTS</b>	v
<b>1 INTRODUCTION</b>	1
<b>2 OBJECTIVES</b>	4
<b>3 RESULTS AND DISCUSSION</b>	5
<b>3.1. Synthesis and Characterization of the Ligands L1, L2 and L3</b>	5
Synthetic routes ( <b>Route 1</b> and <b>Route 2</b> )	
NMR Studies	
IR Studies	
<b>3.2. Synthesis and Characterization Mo(0) and W(0) Complexes of L1-L3</b>	11
NMR Studies	
IR Studies	
HRMS of <b>C1, C3, C4</b> and <b>C5</b>	
Crystal Structure of <i>fac</i> -[Mo(TPOdiphos)(CO) <sub>3</sub> ]	
<b>4 EXPERIMENTAL</b>	20
<b>4.1. General Procedures and Characterization of Products</b>	20
NMR and IR Spectroscopy	
High Resolution Mass Spectroscopy – ESI <sup>+</sup>	
X-Ray Diffraction Analysis	
<b>4.2. Synthesis of Ligands</b>	21
2-bromodiphenylphosphine, <b>L0</b>	
bis{2-(diphenylphosphino)phenyl}(phenyl)phosphine oxide, <b>L1</b>	
bis(2-(diphenylphosphino)phenyl)(propyl)phosphine oxide, <b>L2</b>	
(sulfonylbis(3-methyl-6,1-phenylene))bis(diphenylphosphine), <b>L3</b>	
<b>4.3. Synthesis of Metal Complexes</b>	24
<i>fac</i> -[Mo(TPOdiphos)(CO) <sub>3</sub> ]	
[W(TPOdiphos)(CO) <sub>3</sub> ]	
Reaction of [Mo(CO) <sub>6</sub> ] with <b>L2</b>	
[Mo(SODPdiphos)(CO) <sub>3</sub> ]	
[W(SODPdiphos)(CO) <sub>3</sub> ]	
<b>ANNEX</b>	
<b>A-I. NMR Spectra</b>	A-1
<b>A-II. IR Spectra</b>	A-11
<b>A-III. HRMS Spectra</b>	A-16
<b>A-IV. Crystallographic Data for <i>fac</i>-[Mo(TPOdiphos)(CO)<sub>3</sub>]</b>	A-18

## 1 INTRODUCTION

For the past decade, high attention has been given to phosphine chemistry as shown by an extensive number of studies conducted to synthesize new ligands and to study their properties and applications.<sup>1,2,3,4</sup> From time to time, new phosphines are announced and the regularity of reports including combinatorial synthetic procedures, reaffirm the current intense interest in phosphine science. A “renaissance” of activity is underway as scientists seek not only to find new ligands and improve those existing ones but the process of ligand design itself. But what makes these phosphine ligands so attractive?

To begin with, thousands of P-ligands have been prepared and tested in various selective reactions.<sup>5,6,7</sup> Secondly, one of the key aspects is the great potential for both electronic and steric modification of these ligands. One can easily change the properties of a phosphine by changing the substituents attached to the phosphorous. Another key advantage is the facile characterization by <sup>31</sup>P NMR.

And among these phosphine ligands, lies a group of phosphines with both soft and hard nucleophilic centers within the molecule. These ligands would bind well enough but would readily dissociate the “hard” ligand component, thus generating a vacant site for substrate binding. They are called *hemilabile* phosphines. The first hemilabile ligands emerged in 1970s.<sup>8</sup>

In this work, 3 new bidentate, hemilabile phosphine ligands developed by our group such as TPOdiphos, DPPrPOdiphos and SODPdiphos were studied and their syntheses optimized. These ligands bear the same skeleton structure as shown below. They differ depending on which electron withdrawing groups (i.e., PO and SO<sub>2</sub>) bridge the two phosphine bearing aryls and if these aryls bear any other substituent as in **L3** which bears methyl groups at the para- position.

<sup>1</sup> Chengye, Y., Weizhen, Y., Chengming, Z., Yongzheng, H. *Phosphorus Chem.* **1981**: 615.

<sup>2</sup> Delacroix, O and Gaumont, A. C. *Curr. Org. Chem.*, **2005**, 9: 1851.

<sup>3</sup> Harris, J. R., Haynes II, M.T., Thomas, A. M., Woerpel, K. A. J. *Org. Chem.* DOI: 10.1021/jo1008367. Publication Date (Web): July 6, 2010

<sup>4</sup> Honaker, M., Hovland, J. and Salvatore, R. N. *Curr. Org. Chem.* **2007**, 4: 31.

<sup>5</sup> Sun, J. and Fu, G. *J. Am. Chem. Soc.* **2010**, 132: 4568.

<sup>6</sup> Chung, Y. K. and Fu, G. *Angew. Chem. Int. Ed. Engl.* **2009**; 48: 2225.

<sup>7</sup> Vallcorba V., O.; Tesis Doctoral, **2010**.

<sup>8</sup> (a) Bader, A. and Lindner, E. *Coord. Chem. Rev.* **1991**, 108: 27. (b) Slone, C. S., Weinberger, D. A., Mirkin, C. A. *The Transition Metal Coordination Chemistry of Hemilabile Ligands*. In *Progres in Inorganic Chemistry*; Karlin, K. D., Ed. Wiley: New York, **1999**, 48: 233. (c) Braunstein, P. and Naud, F. *Angew. Chem., Int. Ed.* **2001**, 40, 680. (d) Bassetti, M. *Eur. J. Inorg. Chem.* **2006**, 4473.

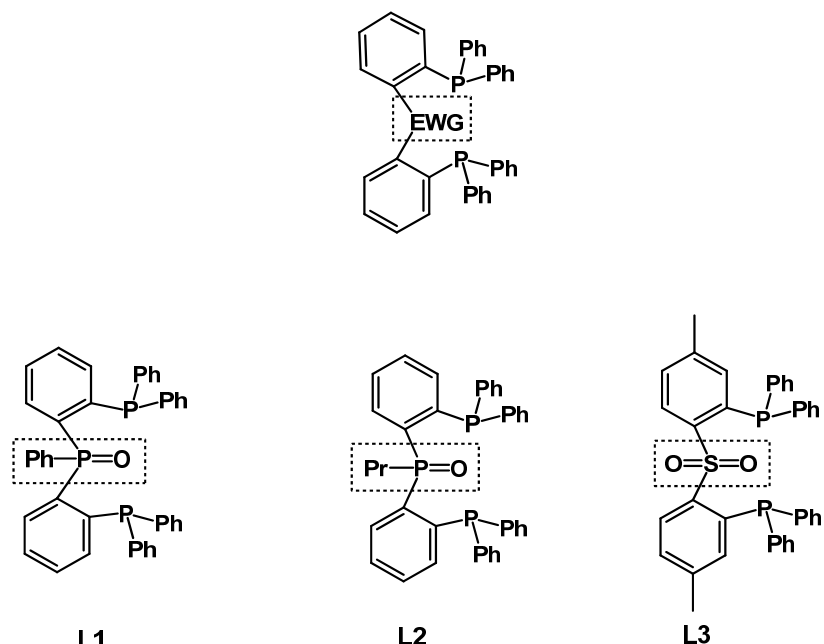


**Figure 1.1.** Ligands developed by the group and are used in the current study.

The advantage of these bidentate ligands is it has a better effect in stabilizing a complex than monodentate ligands. Moreover, the presence of E=O oxygen bearing moieties may give rise to a weaker and labile metal-oxygen (E=O–M) bond and a phosphorus atom closely coordinated to the central atom.

These types of compounds hold a promising future to a wide variety of reactions especially those catalyzed by transition metals.<sup>9,10</sup> Complexes containing hemilabile ligands have been winning lots of attention and has been applied to homogeneous catalysis and in the synthesis of complex organic molecules.<sup>11,12</sup> More recently, they have been found as potential candidates for the reversible binding of analytes to the transition metal center. These are hybrid ligands of the general formula P–E=O where the two groups, P (phosphorus) and E=O, exhibit different donor properties toward the metal center (Figure 1.2). And due to their dynamic chelating capability, they have found a good application in chemical sensing.<sup>13</sup>

<sup>9</sup> Grushin, V. *Organometallics*, **2001**, *20*: 3950.

<sup>10</sup> Grushin, V. *J. Am. Chem. Soc.*, **1999**, *121*:5831.

<sup>11</sup> Rothenberg, G. *Catalysis. Concepts and Green Applications*. Wiley. **2008**.

<sup>12</sup> Hegedus, L. *Transition metals in the synthesis of complex organic molecules*. Univ. Science Books, **1994**.

<sup>13</sup> Angell, S., Rogers, C., Zhang, Y., Wolf, M. and Jones Jr., W. *Coord. Chem. Rev.* **2006**, *250*: 1829.

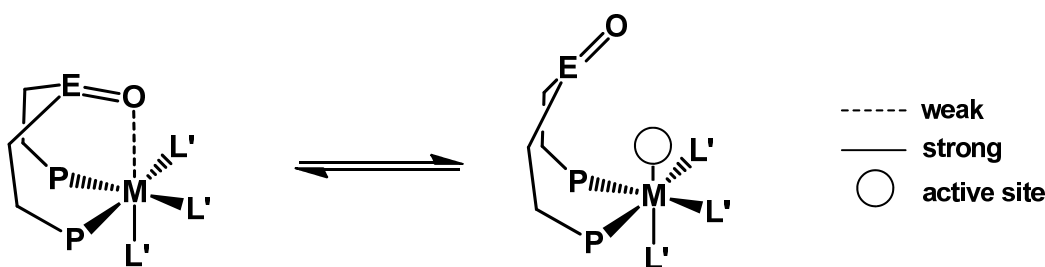


**Figure 2.1.** Figure showing the dynamic chelating ability of hemilabile ligands.

There are a number of labile groups reported in the literature, and in general, oxygen-based substituents, such as ethers, esters, and phosphine oxides, are the most labile.<sup>8(a,b)</sup> Another interesting application taking advantage of this feature is additive oxidation which may have various applications in the field of catalysis and organic synthesis.<sup>14</sup>

More and more applications are discovered for these types of compounds and more and more studies are conducted to get even more results. This work has been done as a contribution to the study of metal/ligand systems relevant to homogeneous catalysis. Specifically this study concentrates to the synthetic methodology and some modifications for obtaining hemilabile, bidentate phosphine ligands bridged by electron withdrawing groups, to obtain quantitative amounts and to study its complexing behavior with molybdenum(0) and tungsten(0).

---

<sup>14</sup> McDonough, J., Weir, J., Sukcharoenphon, K., Hoff, C., Kryatova, O., Rybak-Akimova, E., Scott, B., Kubas, G., Mendiratta, A. and Cummins, C. *J. Am. Chem. Soc.*, **2006**, 128: 31, 10295.

## 2 OBJECTIVES

This work has been done as a contribution to the study of metal/ligand systems relevant to homogeneous catalysis. The first objective of this work has been the optimization of the synthesis of three new hemilabile, bidentate phosphine ligands developed by our research group: **L1**, **L2** and **L3**.

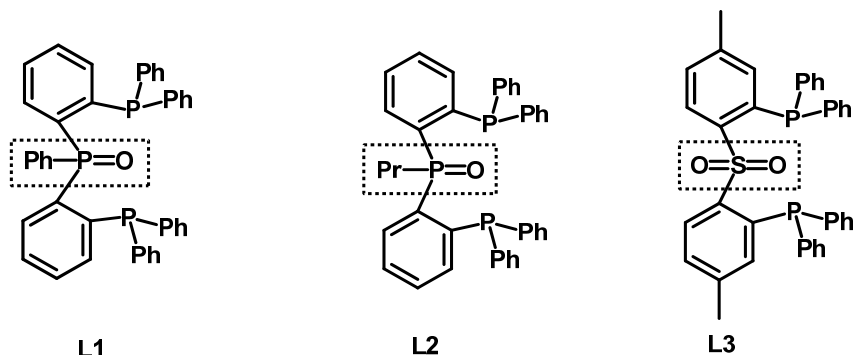


**Figure 2.1** Ligands **L1**, **L2** and **L3**.

These ligands bear a similar skeleton structure but differ on the central electron withdrawing group. Ph-P=O, Pr-P=O and O=S=O groups bridge the two phosphine bearing aryls or “wings” and define a very large P,P-bite angle. This part of the study was aimed to synthesize and purify these three ligands easily and in “*large amounts*”, in the laboratory scale. For these ligands, the starting materials are cheap and readily available from commercial sources.

The second objective has been to asses the coordination character of ligands **L1**, **L2** and **L3** with group 6 metals (Mo and W) that typically prefer octahedral structures. Preliminary results in our group have shown that these ligands coordinate to square planar metal ions (Pd<sup>II</sup> and Pt<sup>II</sup>, Figure 2.2) in a cis-P,P mode, but with the oxygen atoms strongly oriented towards the metal. This has suggested that with the earlier, more electropositive, transition metals fac-P,P,O (facial octahedral) coordination compounds could be obtained. However, it is impossible to predict if **L1**, **L2** or **L3** will act as bidentate cis-P,P or tridentate fac-P,P,O ligands (Figure 2.2).

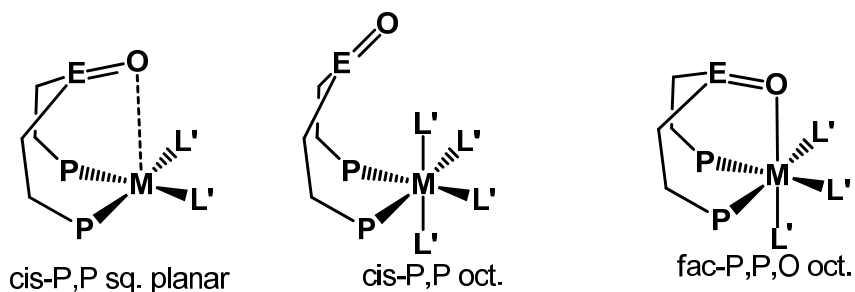
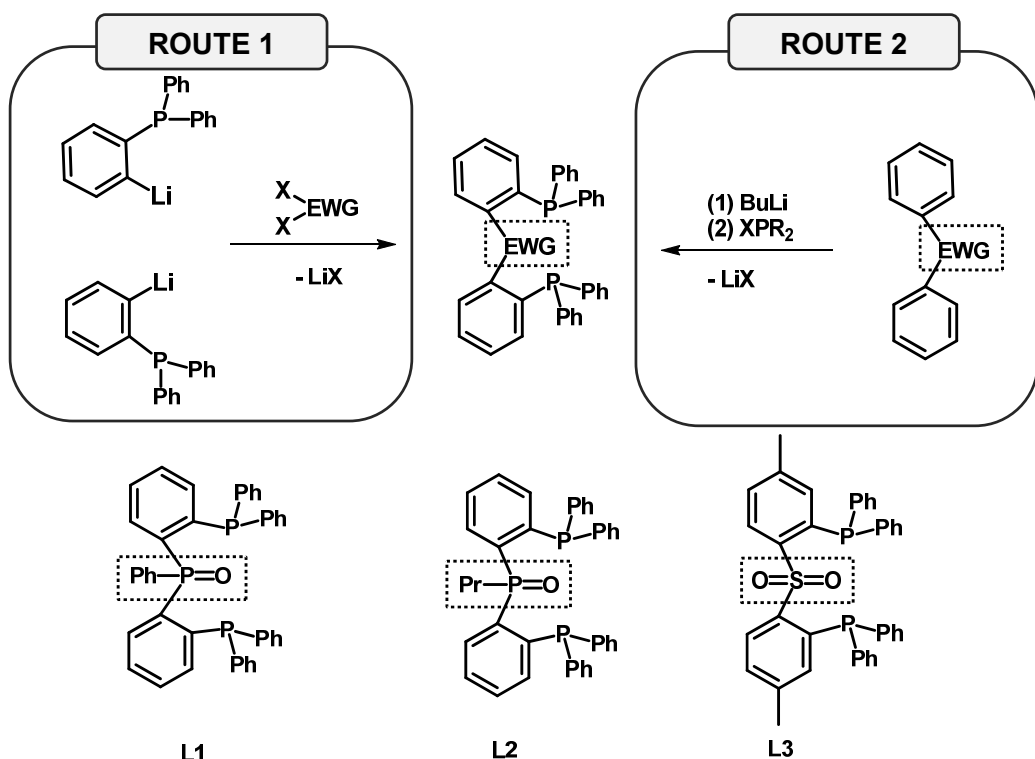


**Figure 2.2** Coordination modes of **L1-L3** with square planar and octahedral centers.

### 3 RESULTS AND DISCUSSIONS

#### 3.1. Synthesis and Characterization of the Ligands L1, L2 and L3

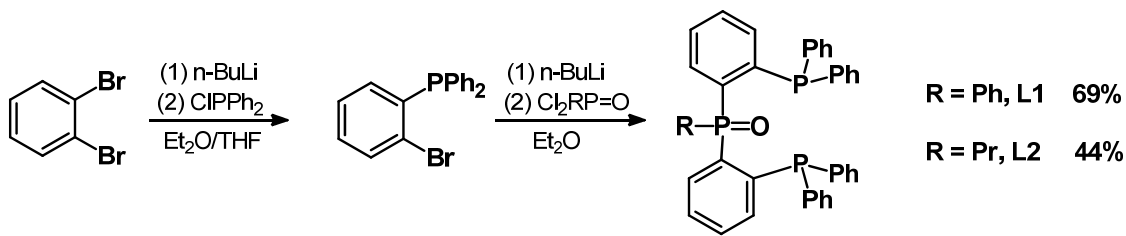
For the synthesis of the ligands, two routes have been developed (Scheme 3.1): **Route 1** includes a two-step synthesis where the “wings” of the ligand must be prepared first and later on attached to a bridging group which bears the electron withdrawing group (EWG) R-P=O or O=S=O. On the other hand, **Route 2** is a simple, one-step reaction wherein the ligand skeleton is directly lithiated and reacted with chlorodiphenylphosphine to form the desired ligand.



**Scheme 3.1.** New hemilabile diphosphine ligands bridged by electronegative groups.

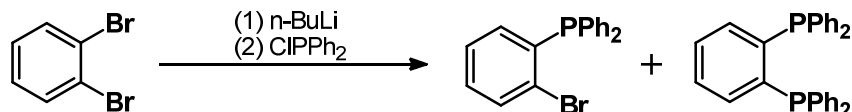
Ligands **L1** and **L2** were synthesized using **Route 1** and ligand **L3** using **Route 2** (Scheme 3.1). The synthesis and characterization of these ligands will be discussed in this section.

**Route 1** involves the prior synthesis of the aryl peripheries. For **L1** and **L2** o-bromodiphenylphosphine is a common intermediate that has to be prepared and then lithiated and reacted with the core group bearing the electronegative moiety. The essential part of the synthesis is the lithiation step. During the addition of the reactants, temperatures were kept low to avoid possible formation of byproducts.



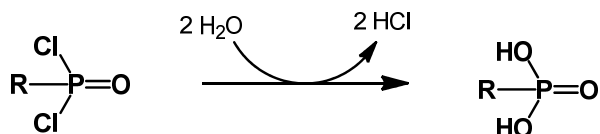
**Scheme 3.2.** Reactions for the synthesis of ligands **L1** and **L2**.

In the lithiation of 1,2-dibromobenzene (Scheme 3.3), an excess of n-BuLi could cause lithium exchange of both bromo substituents and would lower the yield of the o-bromodiphenylphosphine, and give rise to the possible formation of 1,2-bis(diphenylphosphino)benzene at the end of the procedure. Therefore, the addition of n-BuLi was done via syringe with 2% mmols less than the stoichiometric equivalent of 1,2-dibromobenzene. It was added slowly allowing the n-BuLi to react first so as to ensure complete mono-lithiation (Scheme 3.2). Successively, PCl(Ph)<sub>2</sub> was added via slow addition using syringe.



**Scheme 3.3.** Possible products given by the addition of excess BuLi.

In second step, o-bromodiphenylphosphine was reacted with an excess amount of n-BuLi and then with 0.5 equivalents of P(O)Cl<sub>2</sub>Ph for **L1** or P(O)Cl<sub>2</sub>Pr for **L2** (Scheme 3.2). This step presents a problem that can be solved by using carefully dried, distilled and degassed solvents. Dichlorophosphine oxide reactants are prone to hydrolysis (Scheme 3.4) and may produce other potentially hazardous decomposition products. Therefore, the step was strictly done under the hood and in minimum moisture conditions to avoid accident and to achieve maximum yield of the desired phosphine ligand.



**Scheme 3.4.** Hydrolysis of dichlorophosphine oxide derivatives.

Taking this into consideration, **Route 1**, however presents a greater advantage through the possibility of modification of the central group substituent, **R** and further modifications on the aryl substituents of the ligand. In this case, **R = Ph** for **L1** and **n-Pr** for **L2**. Through this, **Route 1** allows easy electronic and steric modifications. It is also suggested that any dichlorophosphine oxide derivative (i.e., **R = alkyl, aryl, etc.**) should yield

the corresponding ligand using this synthetic route under proper reaction conditions. The lower reaction yield was observed with the synthesis of **L2** (44%) which may be attributed to the high reactivity of dichloropropylphosphine oxide.

The ligands were characterized through  $^{31}\text{P}$ ,  $^1\text{H}$  NMR, and other techniques, but  $^{31}\text{P}$  was most useful. The phosphines were designed to display a unique set of NMR signals. Where **L1** and **L2** should display a triplet and doublet signal signifying the success of the synthesis. The spectrum of **L1** shows peaks at  $\delta_{\text{P}} -11.86$ , d, and  $\delta_{\text{PO}} 34.15$ , t with  $J_{\text{PP}}= 19$  Hz (Figure 3.5). Some peak broadening was observed in the spectrum but the peaks integrate to a ratio of 1:2 which pertains to the one  $\text{Ar}_3\text{P}=\text{O}$  and two  $\text{PAr}_3$ .

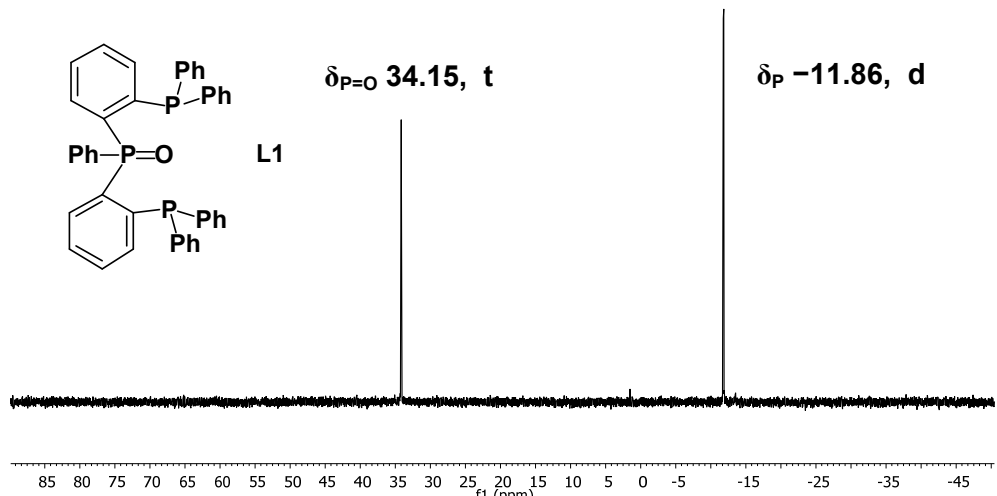


**Figure 3.5.**  $^{31}\text{P}\{^1\text{H}\}$  NMR showing the triplet-doublet pattern of **L1**.

**L1** was oxidized with  $\text{H}_2\text{O}_2$  for referencing purposes (Figure 3.6). The spectrum shows peaks for **L1O<sub>2</sub>** at the usual  $\text{P}^{\vee}=\text{O}$  “oxidized P range”. We see that the spectrum has preserved the same triplet ( $\delta_{\text{P}} 35.13$ ) and doublet ( $\delta_{\text{P}} 32.38$ ) pattern, with  $J_{\text{PP}}= 8\text{Hz}$ . The triplet was displaced only a few ppm but the oxidized Ps were displaced 44 ppm. The shifts were in congruence with the literature (t,  $\delta$  36.78 and d, 33.65).<sup>1</sup> Peaks are sharp and well defined and integrate to a ratio of 1:2.

<sup>1</sup> Miyata, K., Hasegawa, Y., Kuramochi, Y., Nakagawa, T., Yokoo, T. and Kawai, T. *Eur. J. Inorg. Chem.* **2009**, 4777–4785

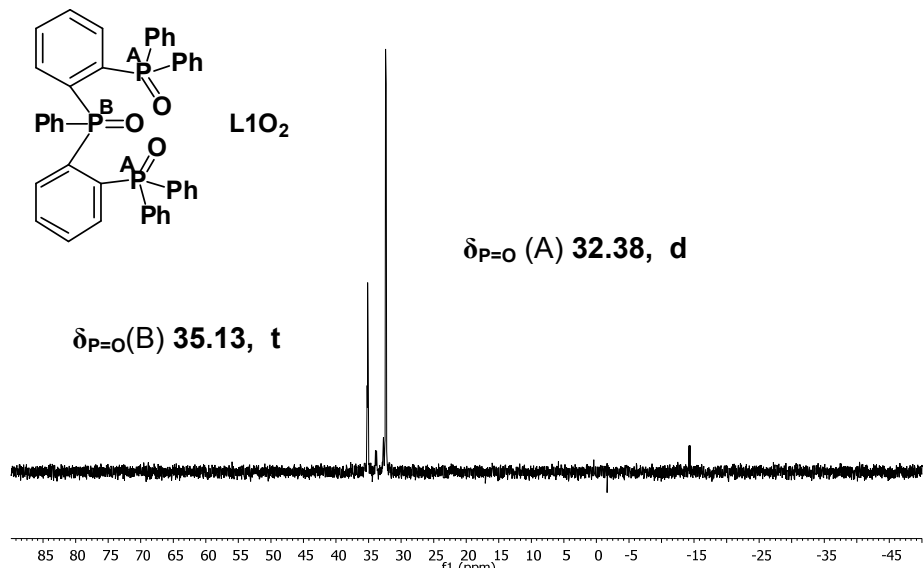
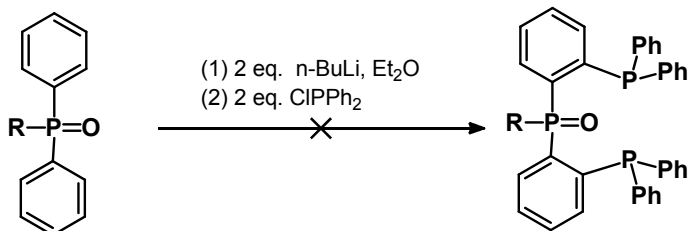


**Figure 3.6.**  $^{31}\text{P}\{\text{H}\}$  NMR showing the triplet-doublet pattern of **L1O<sub>2</sub>**.

**L2**, bearing almost the same structure but only differs with the phosphine oxide substituent, shows the same triplet-doublet pattern and at a very slightly different shift. The  $^{31}\text{P}$  NMR peaks of the free ligand were observed at  $\delta_{\text{P}} -14.88$ , d, and  $\delta_{\text{P=O}} 34.48$ , t.

**Route 2** is a direct lithiation and substitution reaction, a one-pot reaction. Triphenylphosphine oxide could not be lithiated directly, consequently, this route could not be used for ligands such as **L1** or **L2** (Scheme 3.7).



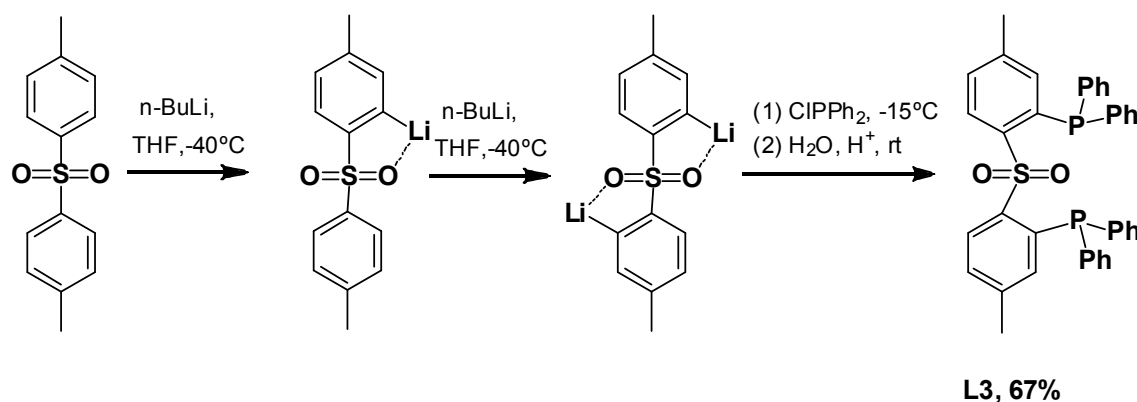
**Scheme 3.7.** Scheme showing the reaction of  $\text{RPh}_2\text{P=O}$  with  $\text{BuLi}$  and  $\text{CIPPh}_2$

However, preliminary work in our group has shown that aryl sulfones can be lithiated.<sup>2</sup> The availability of p-tolyl sulfone and its property to favor direct dilithiation in the ortho positions selectively was taken into advantage. Hence, **L3** was synthesized using this route.

n-BuLi was added to the reaction solution in a slow manner and allowing it to react at a time. The amount of n-BuLi added is important to obtain the desired ligand. That is, both mono- and di- lithiation are possible by controlling the amount of the reagent. However in this case, we opted to add 2 eqs. of n-BuLi to lithiate both ortho positions of the two “wings”. Ortho- lithiation is favored due to the presence of two oxygens of the sulfone group. These

<sup>2</sup> Tello, I., Tesis Doctoral, 2010

oxygens produce an inductive effect and cause the stabilization of lithiation at the otho-position (Scheme 3.8).



**Scheme 3.8.** Reaction route for **L3** synthesis.

The easy control of the synthetic route at low temperatures makes the synthesis of **L3** the easiest among the three ligands. After a fast purification through flash chromatography, a singlet peak during the  $^{31}\text{P}\{\text{H}\}$  NMR analysis of the ligand was observed at  $\delta = 13.98$ . To further characterize and reference the ligand, it was oxidized with H<sub>2</sub>O<sub>2</sub>. The oxidized ligand shows a single peak at  $\delta = 33.46$  (Figure 3.9).

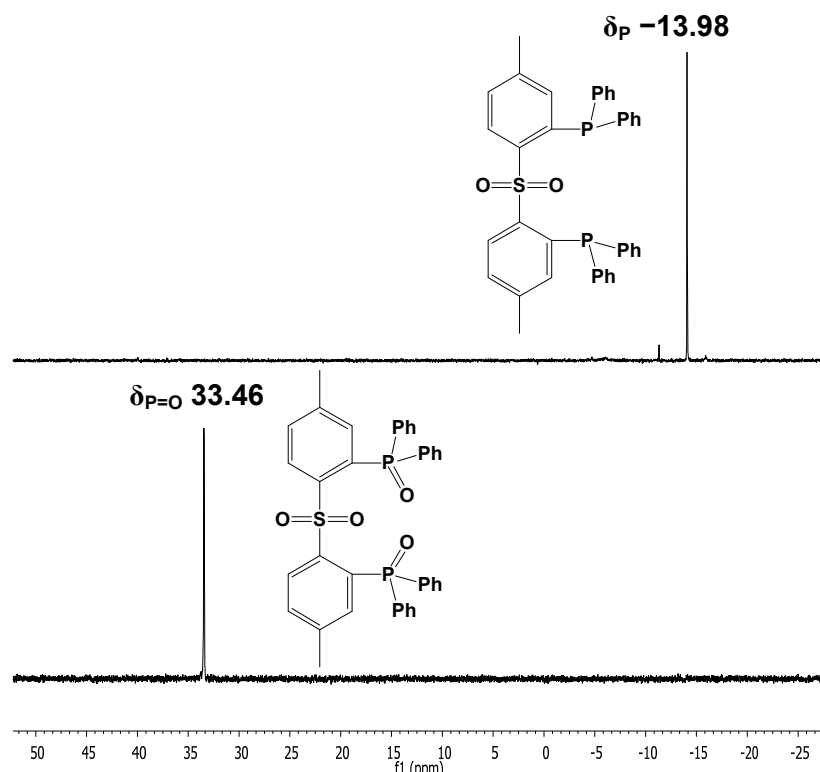


**Figure 3.9.**  $^{31}\text{P}\{\text{H}\}$  NMR comparison of **L3** and its oxidized analogue.

The IR spectra of the ligands **L1**, **L2**, **L3** and **oxidized L3** was also obtained and the data gathered are shown on the table below.

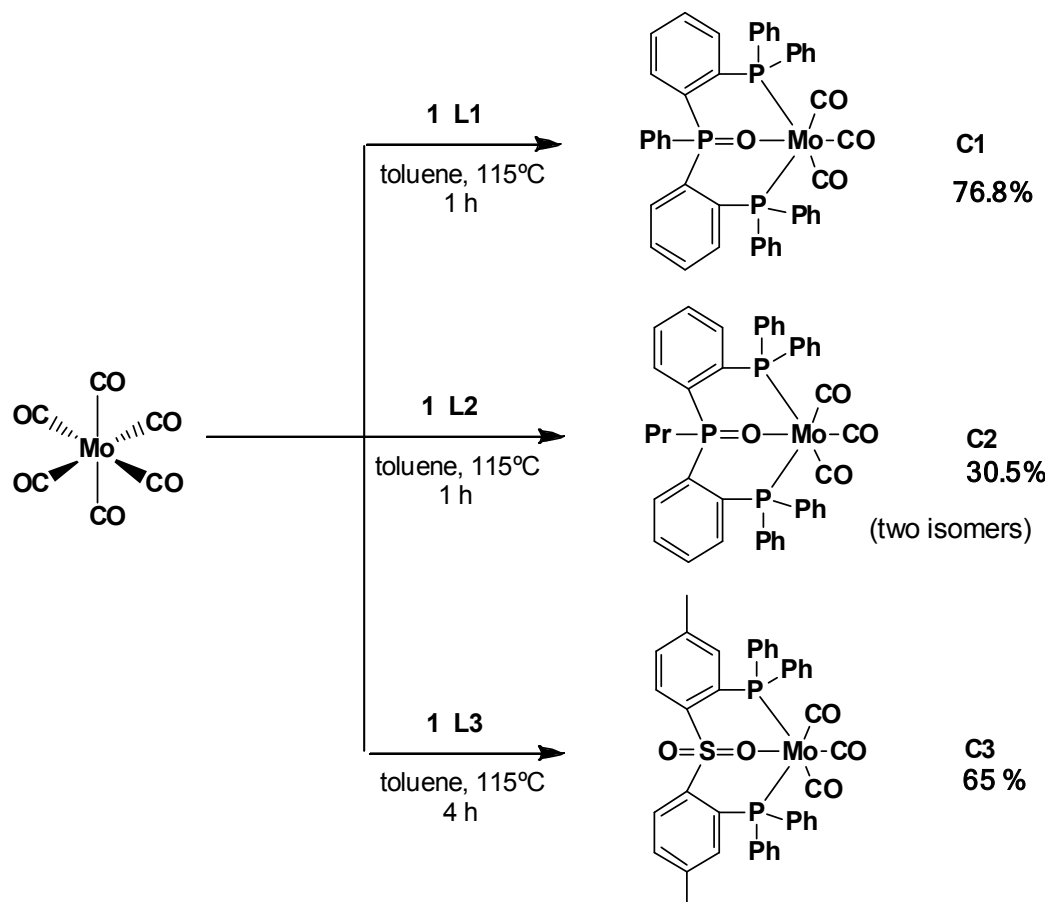
**Table 3.10.** Characteristic IR stretching data [cm<sup>-1</sup>] for the E=O double bonds in sulfone and phosphine oxide compounds.

Ligands	P=O stretching	SO <sub>2</sub> stretching	
		Symmetric	Assymmetric
<b>L1</b> , TPOdiphos	1198		
<b>L2</b> , DPPrPOdiphos	1173		
<b>L3</b> , SODPdiphos		1148	1300
<b>L3O<sub>2</sub></b> , ( <b>L3</b> -P,P-oxide)	1176	1117	1380
Ph <sub>2</sub> SO <sub>2</sub> <sup>a</sup>		1156	1310
Ph <sub>3</sub> PO <sup>a</sup>	1180		

<sup>a</sup> I. Tello, Tesis Doctoral, 2010.

### 3.2. Synthesis and Characterization of Mo(0) and W(0) Complexes of L1-L3

In the current study, reactions involving the successful compexation of molybdenum carbonyl fragments with the ligand were accomplished by refluxing a 1:1 stoichiometric mixtures of  $\text{Mo}(\text{CO})_6$  and **L1-L3**, using toluene as the solvent (Scheme 3.11). Given these conditions, complexes **C1**, **C2** and **C3** were produced from the reactions. On the other hand, attempted reactions performed at room temperature or by refluxing using low boiling point solvents such as  $\text{CH}_2\text{Cl}_2$  proved to be unsuccessful. No change in the physical aspects of the reaction solutions were observed after >6 hours of refluxing or by continuous agitation for >72 hours, respectively.



**Scheme 3.11.** Reaction scheme employed to synthesize molybdenum carbonyl complexes of **L1**, **L2** and **L3**.

Variable completion time for the reactions was observed with molybdenum complexes, from 1 to 4 hours reaction time. The NMR of **C1** shows peaks at  $\delta_{\text{P}=\text{O}}$  37.27, t, and  $\delta_{\text{PO-Mo}}$  30.49, d. A considerable shift of the signal pertaining to the coordinated phosphine group (Figure 3.12) was observed. In the case of **C2**, a mixture of two molybdenum containing products was obtained after an hour of reaction (Figure 3.13). Interestingly the signals of the phosphine-phosphorus (P-Mo) are very close in both the major and the minor products, but the signal of the phosphine oxide-phosphorus are shifted: this will be interpreted as the minor product being cis-P,P-[Mo(**L2**)(CO)<sub>4</sub>], a complex in which

the P=O oxygen remains uncoordinated. The NMR of **C3**, however, shows a single peak at  $\delta_{\text{P}}$  31.12. The formation of **C3** with respect to time is shown in Figure 3.14.

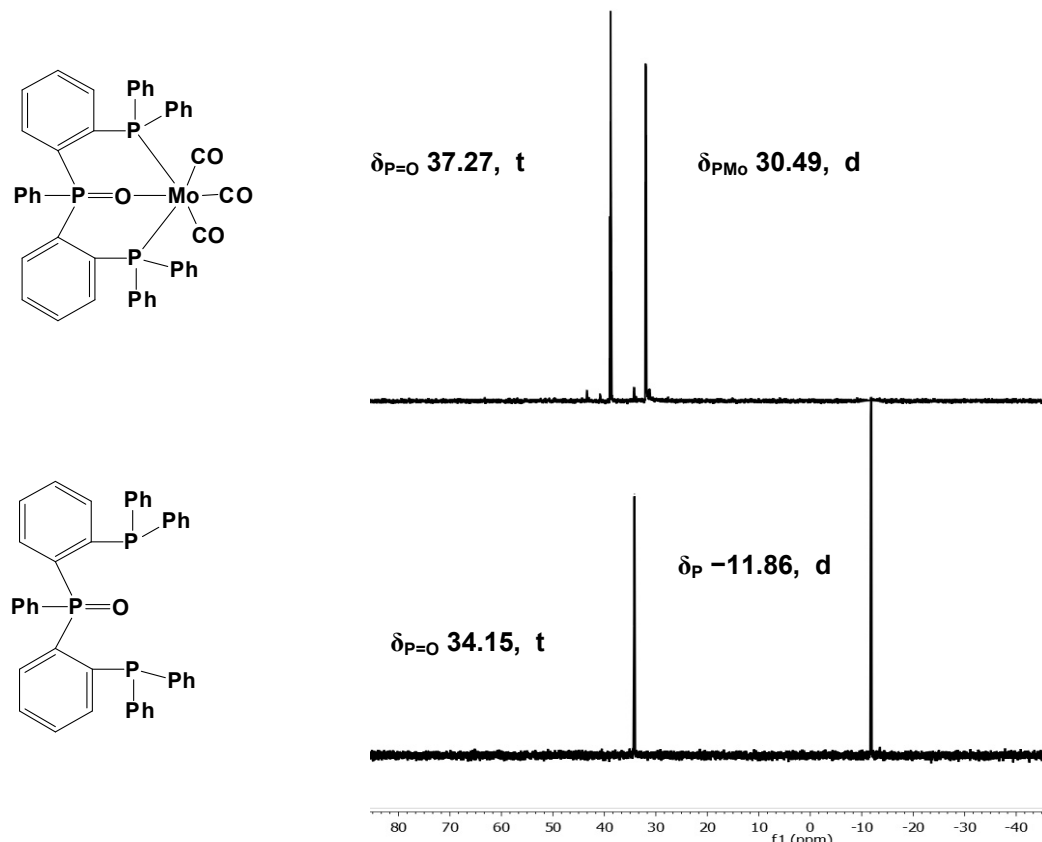


**Figure 3.12.**  $^{31}\text{P}\{\text{H}\}$  signal displacement upon complexation ( $t = 1\text{ h}$ ) of **L1** with  $[\text{Mo}(\text{CO})_6]$

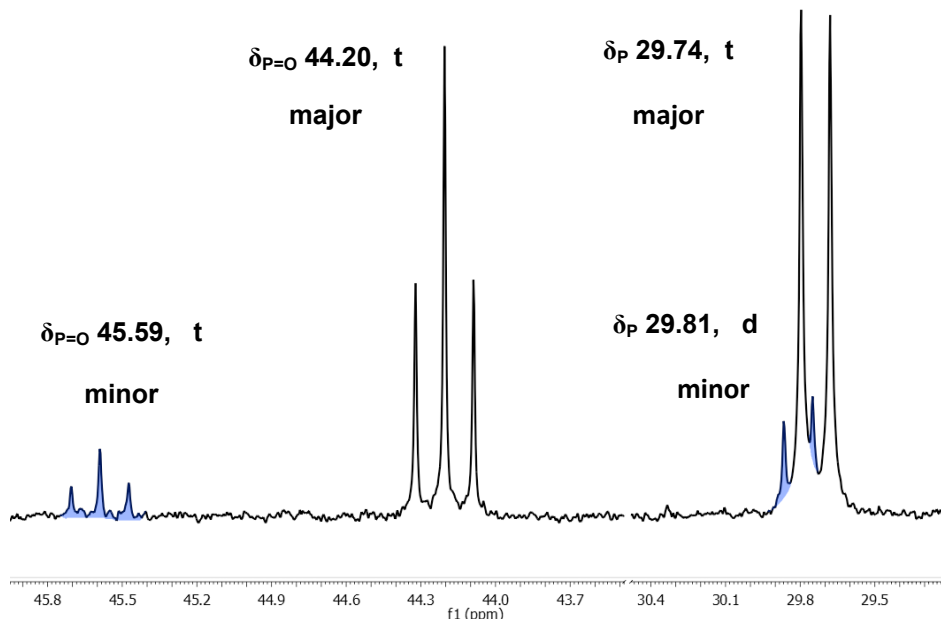


**Figure 3.13.**  $^{31}\text{P}\{\text{H}\}$  NMR of reaction mixture of  $[\text{Mo}(\text{CO})_6]$  and **L2** showing the major and minor products

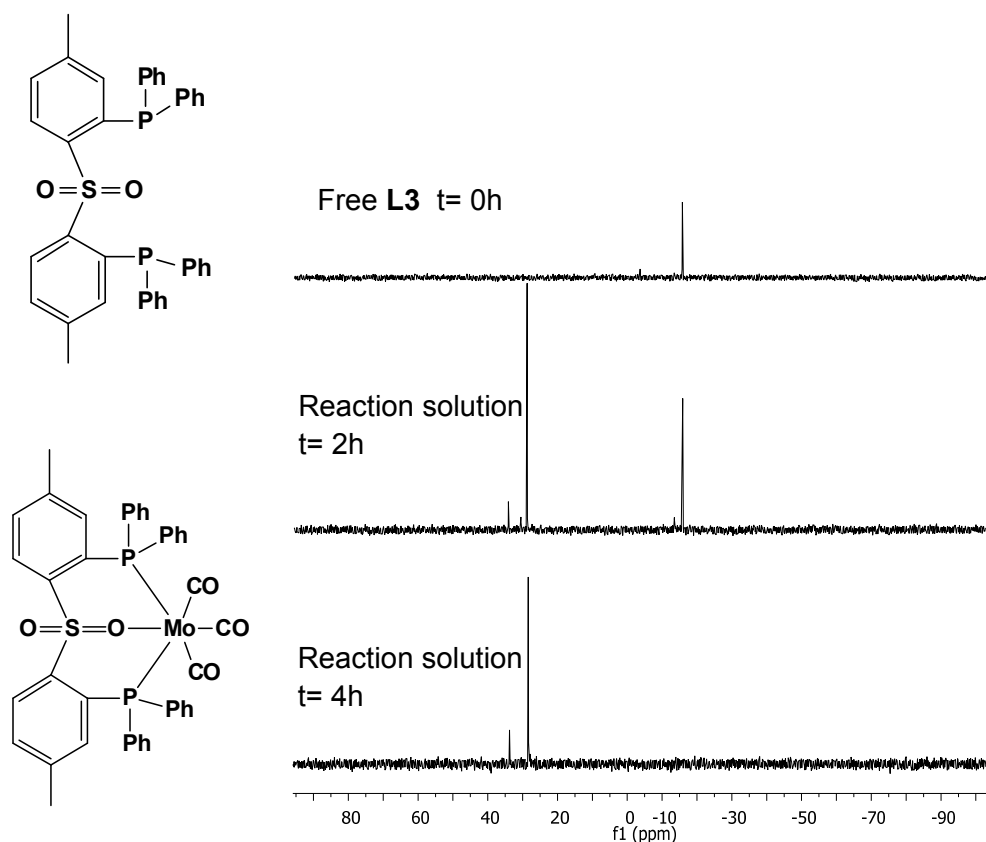
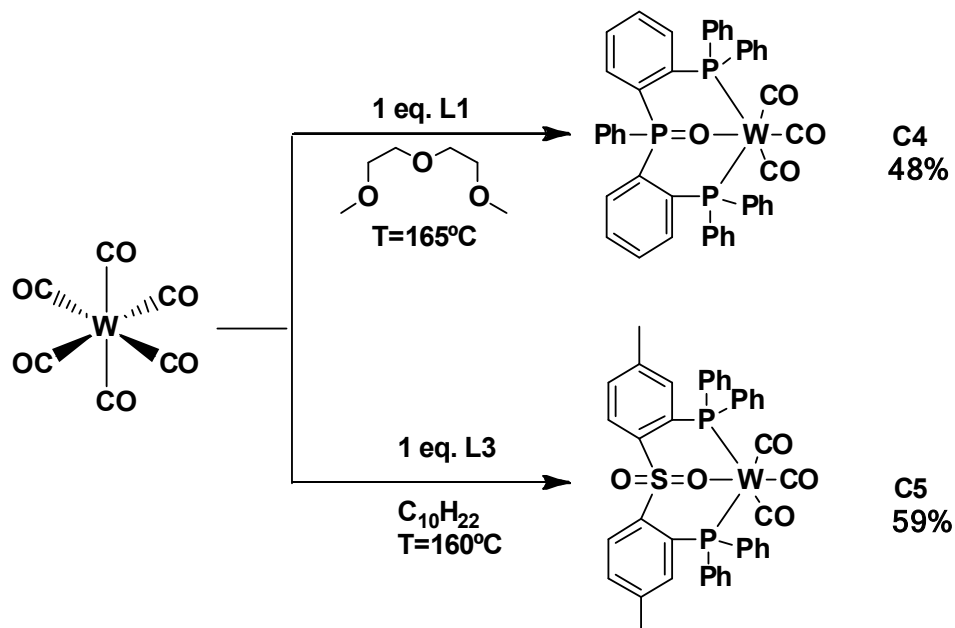


**Figure 3.14.**  $^{31}\text{P}\{\text{H}\}$  showing the formation of  $[\text{Mo}(\text{SODPdiphos})(\text{CO})_3]$  with time.

Tungsten complexes were harder to obtain owing to the fact that  $\text{W}(\text{CO})_6$  is more kinetically inert than  $\text{Mo}(\text{CO})_6$ . **C4** and **C5** were generally formed, after four hours of reflux, regardless of the solvent used (Scheme 3.15). Higher temperatures were employed to allow complexation of **L1** and **L3** with  $\text{W}(\text{CO})_6$ .



**Scheme 3.15.** Reactions of ligands with octahedral,  $d^6 \text{W}(0)$ .

Reaction progress was monitored by performing  $^{31}\text{P}$  NMR tests of homogeneous samples taken from the reaction mixtures at 2 and 4 hours reaction times.

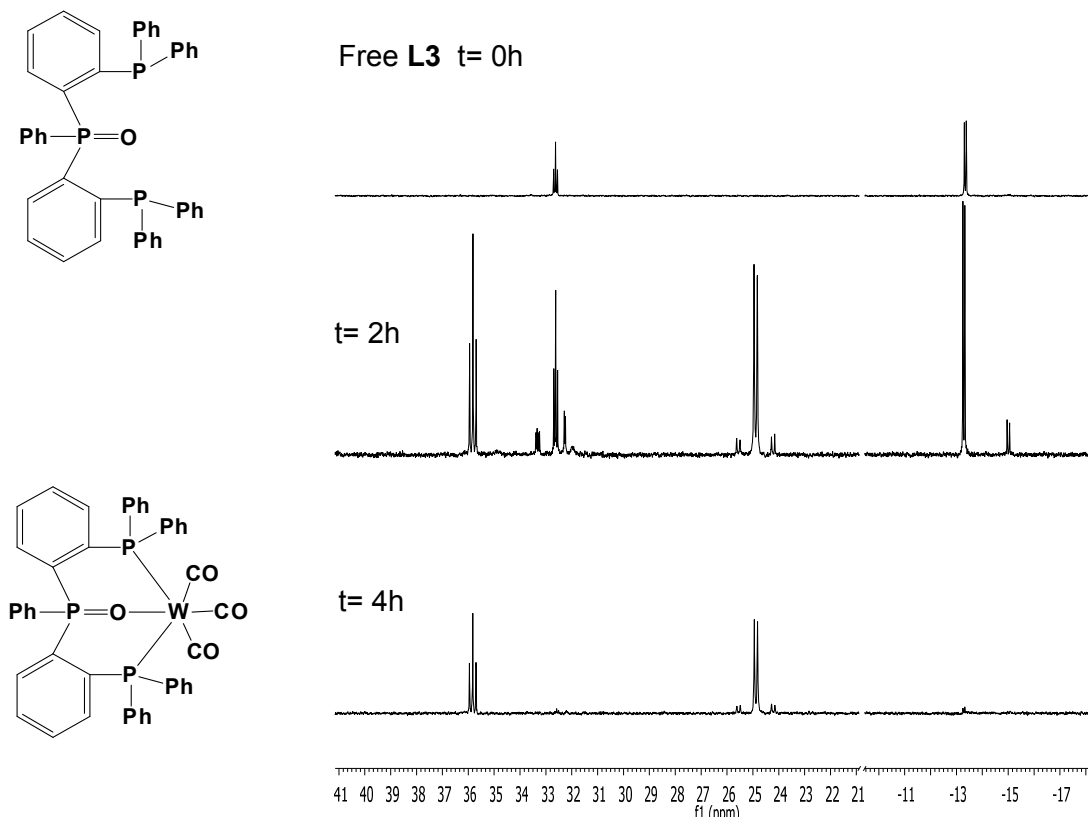


**Figure 3.16.**  $^{31}\text{P}\{^1\text{H}\}$  showing the formation of  $[\text{W}(\text{TPOdiphos})(\text{CO})_3]$  with time.

NMR peaks corresponding to the P directly coordinated with W were observed at  $\delta_{\text{P}}$  25.58, s, for **C4** and at  $\delta_{\text{P}}$  22.83, s, for **C5**. The spin active  $^{183}\text{W}$  ( $I=1/2$ , abundance 14%) gives rise to satellites by coupling to phosphorus in the  $^{31}\text{P}\{^1\text{H}\}$  spectra, for **C4**  ${}^1\text{J}_{\text{P-W}} = 217$  Hz and for **C5**  ${}^1\text{J}_{\text{P-W}} = 233$  Hz. Both conforming to the values found in previous studies.<sup>3,4</sup>

The complexes displayed varying solubilities in various halogenated solvents (i.e.,  $\text{CHCl}_3$  and  $\text{CH}_2\text{Cl}_2$ ) – **C2**, **C3** and **C5** being the more soluble products and **C1** and **C4** as the complexes with the lower solubility. A property that can be attributed to the difference in the core group and the substituent groups attached to the central phosphine oxide. **C1** and **C4** are only slightly soluble in  $\text{CH}_2\text{Cl}_2$  and in  $\text{CHCl}_3$ . Complexes **C2**, **C3** and **C5** are more soluble in both solvents.

<sup>3</sup> Martínez Cuevas, F. *Treball de Recerca; Laboratori d’Iniciació a la Recerca, Máster en Ciencia y Tecnología Químicas, 2007*

<sup>4</sup> Craig Taylor, R., Keiter, R., and Cary, L. W. *Inorg. Chem.*, **1974**, 1928–1932

## IR study of ligands L1, L2 and L3 and their Mo(0) and W(0) complexes

IR spectroscopy is a classical tool for the characterization of organic and inorganic molecules that has IR active groups such as CO, SO<sub>2</sub> and PO. The analysis of spectra of the complexes allowed us to obtain additional information on the coordinating property of the central oxygen. Generally, a coordination of the O in SO<sub>2</sub> or PO would cause a decrease in the frequency of the vibration between the phosphorous and oxygen. Hence, a displacement of spectral band pertaining to these groups suggests a change in the environment of the bonds involved, thus a possible coordination. Furthermore, the number of expected CO stretches in an IR spectrum depends on the number of IR active groups present and the orientation of the coordinating ligand.

All molybdenum (**C1**, **C2** and **C3**) and tungsten complexes (**C4** and **C5**) each showed three new intense peaks between 1775 cm<sup>-1</sup> to 1920 cm<sup>-1</sup> which pertain to the terminal CO groups. Also, spectral data for the complexes were compared to the IR spectra of their corresponding free ligands. Aside from the appearance of the 3 CO bands, a noticeable decrease in the frequency of the PO band of **C1**, from 1198 cm<sup>-1</sup> to 1154 cm<sup>-1</sup> (Figure 3.17), may suggest metal–O coordination. The absence of the characteristic weak peak at  $\nu \sim 2000$  cm<sup>-1</sup> also suggests the absence of trans- COs in the molecule. With regards to the case of **C2**, which is a mixture of two products, we also observed three intense CO peaks between the ranges 1775 cm<sup>-1</sup> to 1920 cm<sup>-1</sup>. And at the PO region, there is a noticeable displacement from 1173 cm<sup>-1</sup> to 1150 cm<sup>-1</sup> while the other peak positions remain unchanged. **C4** also shows a decrease in the PO vibration frequency from 1198 cm<sup>-1</sup> to 1151 cm<sup>-1</sup>, almost the same decrease as in **C1**.

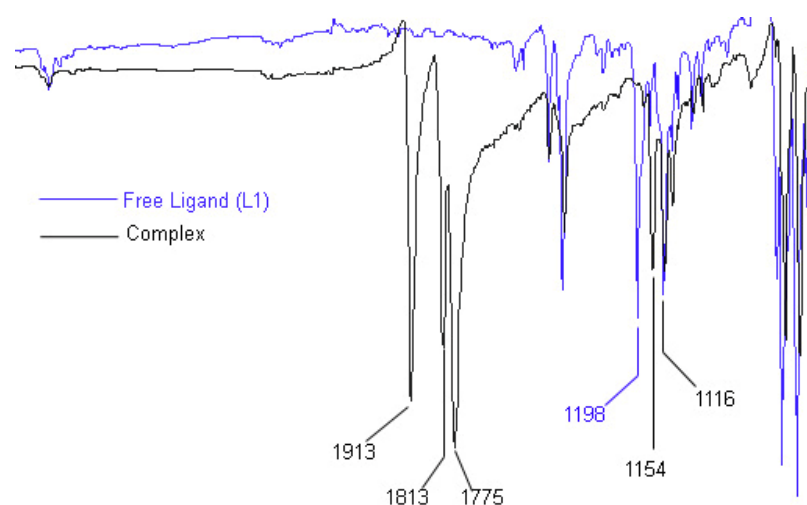


**Figure 3.17.** IR Spectral overlay of **C1** and **L1** showing the M(CO)<sub>3</sub> characteristic pattern and the  $\nu(P=O)$  peak displacement (values in cm<sup>-1</sup>).

With the complexes bearing **L3**, **C3** and **C5**, we also observed the same CO stretches and the same displacement but for the SO<sub>2</sub> group. For **C3** and **C5**, the SO<sub>2</sub> asymmetric stretch was retained at ~1300 cm<sup>-1</sup>. On the other hand, the symmetric stretches were displaced from 1148 cm<sup>-1</sup> to 1134 cm<sup>-1</sup> and 1148 cm<sup>-1</sup> to 1129 cm<sup>-1</sup> for **C3** and **C5**, respectively. Table 3.18 shows a summary of the characteristic E=O peaks of the complexes compared to that of their corresponding ligands.

**Table 3.18. Characteristic IR stretching data [cm<sup>-1</sup>] for the E=O double bonds for the free ligands and their Mo(0) and W(0) octahedral complexes.**

Ligands/Complexes	P=O stretching	SO <sub>2</sub> stretching	
		Symmetric	Assymmetric
<b>L1</b> , TPOdiphos	1198		
<b>L2</b> , DPPrPOdiphos	1173		
<b>L3</b> , SODPdiphos		1148	1300
<b>C1</b> , [Mo(CO) <sub>3</sub> (TPOdiphos)]	1154*		
<b>C2</b> , [Mo(CO) <sub>3</sub> (DPPrPOdiphos)]	1150*		
<b>C3</b> , [Mo(CO) <sub>3</sub> (SODPdiphos)]		1134*	1300
<b>C4</b> , [W(CO) <sub>3</sub> (TPOdiphos)]	1150*		
<b>C5</b> , [W(CO) <sub>3</sub> (SODPdiphos)]		1129*	1297

\*displaced peaks

#### HRMS of C1, C3, C4 and C5

The conclusions formulated from the IR data were further supported by the determination of the exact masses of the complexes. The found and calculated exact mass envelopes for **C1**, **C3**, **C4** and **C5** were in congruence with the proposed composition, including the number of COs in the complexes (n=3). For all complexes, the data is presented in the annex. In the case of **C1**, the spectra are shown below (Figure 3.19).

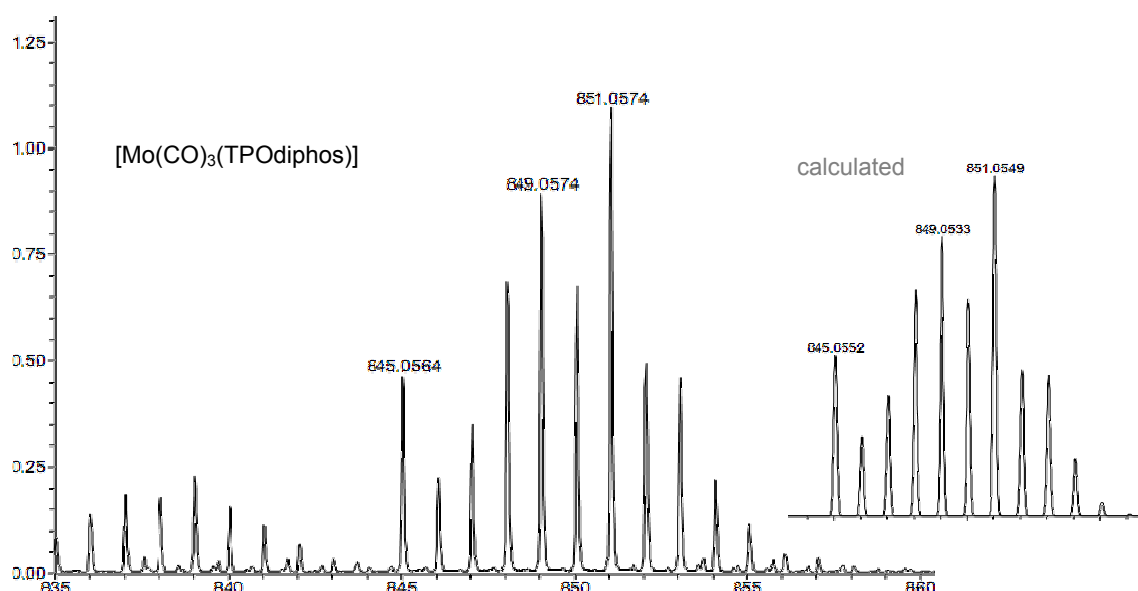


**Figure 3.19.** Experimental and calculated HRMS of **C1**

The simulated isotopic pattern for **C1**, **C3**, **C4** and **C5** calculated for complexes match the experimental data and were within the margin of 3% deviation. This strengthens the pre-conclusions that the ligands were able to complex the O in the E=O group to the metal center Mo and W.

### Crystal Structure of *fac*-[Mo(TPOdiphos)(CO)<sub>3</sub>]

Crystals of *fac*-[Mo(TPOdiphos)(CO)<sub>3</sub>] were obtained by the slow diffusion of diethyl ether to a saturated solution of the complex in CH<sub>2</sub>Cl<sub>2</sub>. To be able to confidently conclude what configuration the complex bears, an XRD study was undertaken. This section of the study is focused with the discussion of crystallographic data and its implications. A complete CIF file can be found in the Annex. Table 3.20 contains the relevant crystal and refinement data. Table 3.21 collects selected distances and Table 3.22 selected angles. Figure 3.23 shows an ORTEP plot of the molecule.

**Table 3.20.** Crystal data and structure for *fac*-[Mo(TPOdiphos)(CO)<sub>3</sub>]

Empirical Formula	C <sub>45</sub> H <sub>35</sub> MoO <sub>4</sub> P <sub>3</sub>
Formula weight	828.58
Crystal System	Monoclinic
Space group	P2 <sub>1</sub> /a
Unit cell dimensions [Å]	a = 19.7966(14) $\alpha$ = 90° b = 9.8803(7) $\beta$ = 95.880(2)° c = 39.196(3) $\gamma$ = 90°
Formula Units per cell	8
Crystal size [mm]	0.18 x 0.13 x 0.12
Crystal color	Transparent orange
Cell volume, Å <sup>3</sup>	7626.257(6)
Density, $\rho_{\text{calc}}$ (g/cm <sup>3</sup> )	1.44
Measurement temperature (K)	295(2)
Wavelength MoKa, $\lambda$ [Å]	0.71073
Absorption coefficient, $\mu$ , cm <sup>-1</sup>	0.514
R factor (all)	0.2143
R Factor (gt)	0.0795
wR Factor (ref)	0.219
wR Factor (gt)	0.16
Goodness of Fit	0.867

The unit cell contains two chemically equivalent but crystallographically different molecules of *fac*-[Mo(TPOdiphos)(CO)<sub>3</sub>], labeled type 1 and type 2 in the tables. The coordination of molybdenum is octahedral, albeit distorted by the fact that the ligand atoms are of a very different nature. The bond lengths of Mo to P have a median value of 2.56 Å. The Mo-P distances are somewhat long owing to the fact that they are trans to the CO ligands which form a very strong bond to molybdenum(0), an electron rich d<sup>6</sup> metal. This is in agreement to the short Mo-CO distance in the facial Mo(CO)<sub>3</sub> group.

It is interesting to see how the oxygen of the phosphine oxide part of L1 has displaced CO in the coordination sphere of the soft, electron rich molybdenum(0). The bond lengths between Mo and O have a median value of 2.26 Å. This value is considerably longer than

that reported for most oxo-molybdenum complexes.<sup>5</sup> This implies a role on the hemilability of this part of the ligand. It is suggested that this bond between Mo and O will be the first to break and will be able to generate an active site during catalysis. Another interesting feature of the complex is the relationship between the CO bond lengths that are trans to the P,P,O coordination. The CO bonds trans- to the Ps has an average distance of 1.16 Å and the CO bonds trans- to the E=O group has an average value of 1.18 Å.

**Table 3.21.** Selected distances [Å]

	MoL1 (type 1) <sup>1</sup>	MoL1 (type 2) <sup>2</sup>
Mo <sub>1</sub> -P <sub>1</sub> (Mo <sub>2</sub> -P <sub>4</sub> )	2.567(2)	2.560(2)
Mo <sub>1</sub> -P <sub>3</sub> (Mo <sub>2</sub> -P <sub>6</sub> )	2.568(2)	2.548(2)
Mo <sub>1</sub> -O <sub>1</sub> (Mo <sub>2</sub> -O <sub>2</sub> )	2.263(4)	2.266(5)
Mo <sub>1</sub> -C <sub>11</sub> (Mo <sub>2</sub> -C <sub>26</sub> )	1.922(8)	1.925(9)
Mo <sub>1</sub> -C <sub>12</sub> (Mo <sub>2</sub> -C <sub>22</sub> )	1.902(8)	1.899(8)
Mo <sub>1</sub> -C <sub>13</sub> (Mo <sub>2</sub> -C <sub>24</sub> )	1.936(8)	1.951(8)
P <sub>2</sub> -O <sub>1</sub> (P <sub>5</sub> -O <sub>2</sub> )	1.501(5)	1.493(5)
C <sub>11</sub> -O <sub>11</sub> (C <sub>26</sub> -O <sub>26</sub> )	1.174(8)	1.179(9)
C <sub>12</sub> -O <sub>12</sub> (C <sub>22</sub> -O <sub>22</sub> )	1.183(8)	1.176(8)
C <sub>13</sub> -O <sub>13</sub> (C <sub>24</sub> -O <sub>24</sub> )	1.155(8)	1.154(8)

**Table 3.22.** Selected angles [deg]

MoL1 (struct. 1) <sup>1</sup>	MoL1 (struct. 2) <sup>2</sup>
C <sub>12</sub> -Mo <sub>1</sub> -C <sub>11</sub>	86.6(3)
C <sub>12</sub> -Mo <sub>1</sub> -C <sub>13</sub>	86.5(3)
C <sub>12</sub> -Mo <sub>1</sub> -P <sub>1</sub>	100.0(3)
O <sub>1</sub> -Mo <sub>1</sub> -P <sub>1</sub>	73.90(13)
O <sub>1</sub> -Mo <sub>1</sub> -C <sub>11</sub>	99.9(2)
O <sub>1</sub> -Mo <sub>1</sub> -P <sub>3</sub>	85.82(12)
C <sub>11</sub> -Mo <sub>1</sub> -P <sub>3</sub>	90.4(2)
C <sub>12</sub> -Mo <sub>1</sub> -P <sub>3</sub>	92.6(2)
P <sub>1</sub> -Mo <sub>1</sub> -P <sub>3</sub>	98.05(7)
O <sub>1</sub> -Mo <sub>1</sub> -C <sub>13</sub>	96.1(2)
C <sub>11</sub> -Mo <sub>1</sub> -C <sub>13</sub>	80.7(3)
P <sub>1</sub> -Mo <sub>1</sub> -C <sub>13</sub>	90.9(3)
Mo <sub>1</sub> -C <sub>11</sub> -O <sub>11</sub>	170.7(7)
Mo <sub>1</sub> -C <sub>12</sub> -O <sub>12</sub>	178.3(7)
Mo <sub>1</sub> -C <sub>13</sub> -O <sub>13</sub>	172.2(7)
C <sub>11</sub> -Mo <sub>1</sub> -P <sub>1</sub>	169.0(2)
O <sub>1</sub> -Mo <sub>1</sub> -C <sub>12</sub>	173.4(3)
P <sub>3</sub> -Mo <sub>1</sub> -C <sub>13</sub>	171.1(3)
P <sub>2</sub> -O <sub>1</sub> -Mo <sub>1</sub>	124.8(3)
C <sub>22</sub> -Mo <sub>2</sub> -C <sub>26</sub>	82.0(3)
C <sub>22</sub> -Mo <sub>2</sub> -C <sub>24</sub>	84.7(3)
C <sub>22</sub> -Mo <sub>2</sub> -P <sub>6</sub>	90.2(3)
O <sub>2</sub> -Mo <sub>2</sub> -P <sub>6</sub>	86.03(13)
O <sub>2</sub> -Mo <sub>2</sub> -C <sub>26</sub>	102.1(3)
O <sub>2</sub> -Mo <sub>2</sub> -P <sub>4</sub>	72.24(12)
C <sub>26</sub> -Mo <sub>2</sub> -P <sub>4</sub>	90.3(2)
C <sub>22</sub> -Mo <sub>2</sub> -P <sub>4</sub>	104.8(2)
P <sub>6</sub> -Mo <sub>2</sub> -P <sub>4</sub>	97.97(6)
O <sub>2</sub> -Mo <sub>2</sub> -C <sub>24</sub>	96.9(3)
C <sub>26</sub> -Mo <sub>2</sub> -C <sub>24</sub>	84.7(3)
P <sub>6</sub> -Mo <sub>2</sub> -C <sub>24</sub>	88.3(2)
Mo <sub>2</sub> -C <sub>26</sub> -O <sub>26</sub>	169.7(7)
Mo <sub>2</sub> -C <sub>22</sub> -O <sub>22</sub>	176.2(7)
Mo <sub>2</sub> -C <sub>24</sub> -O <sub>24</sub>	174.7(8)
C <sub>26</sub> -Mo <sub>2</sub> -P <sub>6</sub>	169.8(2)
O <sub>2</sub> -Mo <sub>2</sub> -C <sub>22</sub>	174.8(3)
P <sub>4</sub> -Mo <sub>2</sub> -C <sub>24</sub>	166.9(2)
P <sub>5</sub> -O <sub>2</sub> -Mo <sub>2</sub>	125.2(3)

The P-Mo-P bond angle measures an average of 98° while the equatorial C-Mo-C bond angles measures a little acute: 80.7(3)° for molecule 1 and 84.7(3)° for molecule 2. It was also evident that the axial bonds were oriented towards the E=O group, the trans C-Mo-O angle measures an average value of 174°. Distortions of the equatorial CO bonds were supposed to have been affected by the bulky diphenyl substituent of the phosphine groups. The ORTEP plots of the complexes are shown below. Hydrogen atoms were removed to simplify the structure.

<sup>5</sup> Cotton, F. A. and Wilkinson, G., *Advanced Inorganic Chemistry*, Wiley, 5<sup>th</sup> Ed

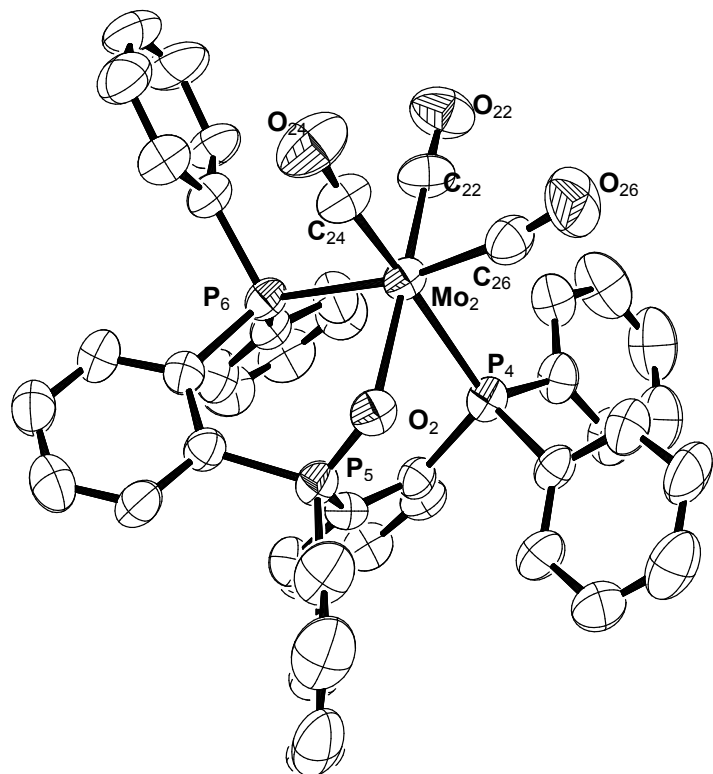
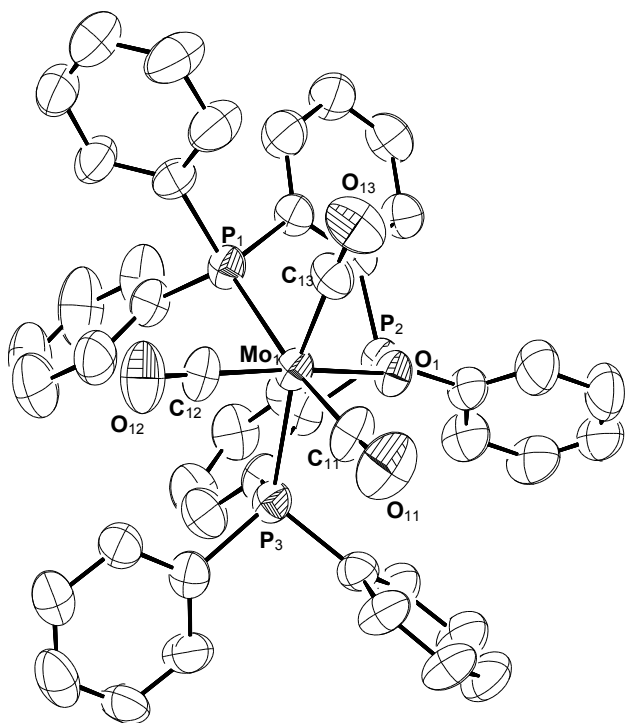


**Figure 3.23.** ORTEP visualizations of the molecules 1 and 2 of *fac*-[Mo(TPOdiphos)(CO)<sub>3</sub>]

## 4 EXPERIMENTAL

### 4.1. General Procedures and Characterization of Products

All routinary synthetic procedures including reaction handling and the handling and purification of solvents were done under inert atmosphere (i.e., N<sub>2</sub>/vacuum). Solvents employed for air sensitive steps were generally dried, distilled over the necessary reagents and degassed prior to use. Toluene, THF, hexane and ethyl ether were distilled over sodium and benzophenone; CH<sub>2</sub>Cl<sub>2</sub> was distilled over CaH<sub>2</sub>. All other reagents were of commercial sources or prepared according to established methods and checked spectroscopically whenever necessary.

#### 4.1.1. NMR and IR Spectroscopy

Reaction progress was monitored through <sup>1</sup>H and <sup>31</sup>P{<sup>1</sup>H} NMR. Final reaction products were characterized employing spectroscopic techniques: <sup>1</sup>H and <sup>31</sup>P{<sup>1</sup>H} NMR. The chemical shifts are reported in the  $\delta$  scale. <sup>1</sup>H are referenced to TMS and <sup>31</sup>P spectra are referenced by using a capillary tube containing 85% H<sub>3</sub>PO<sub>4</sub> as external standard. The NMR spectra were recorded at 250MHz and 400MHz using Bruker DPX250-Auto and AV400, respectively, at the *Servei de Ressonància Magnètica Nuclear* (SeRMN), UAB. Characterization of the ligands and the coordination complexes through IR spectroscopy was carried out on a Bruker TENSOR27<sup>TM</sup> infrared spectroscope employing ATR mode at the *Servei de Análisis Química* (SAQ), UAB.

#### 4.1.2. High Resolution Mass Spectroscopy – Electrospray Ionization (HRMS-ESI<sup>+</sup>)

High resolution determination of the masses was performed at the SAQ, UAB using a micrOTOF-Q mass spectroscope equipped with electrospray ionizer (ESI<sup>+</sup>) in positive ion mode. The determinations were performed by Dr. M<sup>a</sup> Jesús Ibarz Esteva.

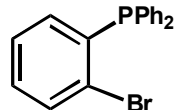
#### 4.1.3. X-Ray Diffraction Analysis

Crystals grown by solvent diffusion were found appropriate for crystal structure determination. They were mounted on a MicroMount<sup>TM</sup> and were analyzed at room temperature on a Bruker SMART APEX by X-Ray Diffraction spectroscopy (XRD) at the *Servei de Difracció de RX* de la UAB.

## 4.2 Synthesis of Ligands

### 4.2.1. Synthesis of 2-bromophenyldiphenylphosphine (**L0**)

This ligand was synthesized by slightly modifying the procedure developed at our group by I. Tello, which in turn, was obtained from the literature.<sup>1</sup>



In a side arm flask charged with 1,2-dibromobenzene (FluoroChem, 96%, 51 mmol, 12.03 g) dissolved in dry, degassed 50:50 ether/THF mixed solvent (100 ml), n-BuLi (Aldrich, 2.5 M in hexanes, 20 mL, 50 mmol) was added drop wise at -120°C (85:10:5, ether:acetone:pentane/liquid N<sub>2</sub> slush bath). The reaction was stirred for an hour at -120°C. Maintaining the same condition, chlorodiphenylphosphine (Aldrich, 96%, 51 mmol, 11.4 g) was added slowly via syringe and was allowed to react for an hour. The temperature was slowly increased to -80°C (acetone/liquid N<sub>2</sub>) and a degassed aqueous solution of NH<sub>4</sub>Cl was added (5 g in 50 ml H<sub>2</sub>O). The organic and aqueous layers were separated and the aqueous layer was discarded. The organic layer was washed with degassed water (10 mL x 3). The solution was filtered through anhydrous MgSO<sub>4</sub> and the solvent was evaporated to dryness under reduced pressure. The product was obtained as a white solid that was further purified by flash chromatography over silica gel using CH<sub>2</sub>Cl<sub>2</sub> as eluent. Yield: 17 g, 96%.

<sup>31</sup>P{<sup>1</sup>H} NMR (162 MHz, CDCl<sub>3</sub>, 298 K) δ -4.47 (s, PAr<sub>3</sub>).

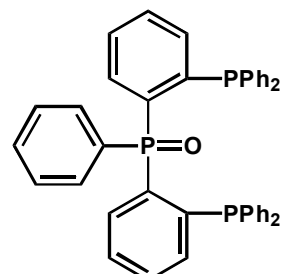
<sup>1</sup>H NMR (250 MHz, CDCl<sub>3</sub>, 298 K) δ 6.75-6.83 (m, 1H), 7.16-7.45 (m, 12H), 7.62 (m, 1H).

### 4.2.2. Synthesis of bis{2-(diphenylphosphino)phenyl}(phenyl)phosphine oxide

#### TPOdiphos, (**L1**)

This ligand was prepared according to the experience of our group, and its synthesis optimized.

A side-arm flask was charged with **L0** (C<sub>18</sub>H<sub>14</sub>BrP, 14.27 g, 41.8 mmol) dissolved in degassed, dry ether (120 mL). The solution was cooled down to -80°C (acetone/liquid N<sub>2</sub> slush bath) and n-BuLi was added drop wise (Aldrich, 2.5 M in hexanes, 16.8 mL, 42 mmol). The mixture was stirred for 1 hr at -80°C and 3 more h at rt. The temperature was again decreased to -80°C and dichlorophenylphosphine oxide (Aldrich, 98%, 4.10 g, 20.92 mmol) was slowly added via syringe. The reaction was gradually warmed up to room temperature and was stirred for 24 hours. The solvent was removed through cannula



<sup>1</sup> (a) Luo, X., Zhang, H., Duan, H., Liu, Q., Zhu, L., Zhang, T. and Lei, A. *Org. Lett.*, **2007**, 9, 4571. (b) Gelman, D.; Jiang, L.; Buchwald, S. L. *Org. Lett.* **2003**, 5, 2315.

filtration at  $-80^{\circ}\text{C}$  and the white product was washed with ether (20 mL x 3) and degassed water (50 mL). Dry methanol (60 ml) was then added and it was refluxed for 2 hours. The solvent was again removed through cannula filtration and the residue was washed with ether (50 mL) and dried under reduced pressure to obtain a white solid product. Yield: 18.8 g, 69%.

**$^{31}\text{P}\{\text{H}\}$  NMR** (162 MHz,  $\text{CDCl}_3$ , 298 K)  $\delta$  33.29 (t,  $\text{Ar}_3\text{P}=\text{O}$ ,  $J_{\text{PP}} = 12.0$  Hz),  $-12.68$  (d,  $\text{Ar}_3\text{P}$ ,  $J_{\text{PP}} = 12.0$  Hz).

**$^1\text{H}$  NMR** (250 MHz,  $\text{CDCl}_3$ , 298 K):  $\delta$  6.78-6.83 (m, 1 H), 7.21-7.40 (m, 12 H), 7.60-7.66 (m, 1 H).

**IR [cm $^{-1}$ ]** ( $\nu \text{ P=O}$ , strong) 1198.

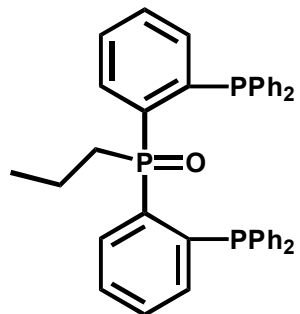
#### 4.2.3. Synthesis of bis(2-(diphenylphosphino)phenyl)(propyl)phosphine oxide (L2),

This ligand was prepared according to the experience of our group, and its synthesis optimized.

In a Schlenk flask charged with of **L0** (15.20 g, 44.55 mmol) dissolved in 100 mL of degassed dry ether, an excess amount of n-BuLi (Aldrich, 2.5 M in hexanes, 17.80 mL, 44.55 mmol) was added dropwise at  $-80^{\circ}\text{C}$ . The solution was allowed to react for an hour at this temperature and for three more hours at room temperature. The formation of white precipitate was observed as the reaction goes. The temperature was again lowered to  $-80^{\circ}\text{C}$  and dichloropropylphosphine oxide (Alfa Aesar, 98%, 3.60 g, 22.27 mmol) was added drop by drop. The solution was gradually warmed and allowed to react at room temperature for 24 hours. The suspension was brought to reflux temperature and was refluxed for 6 hours. The solvent was entirely removed and the white precipitate was washed with degassed water (50 ml) and ether (3 x 20 ml). All the solvent was removed and the white product was allowed to dry under reduced pressure. Yield: 6 g, 44%.

**$^{31}\text{P}\{\text{H}\}$  NMR** (162 MHz,  $\text{CDCl}_3$ , 298 K)  $\delta$  34.48 (t,  $J_{\text{PP}} = 20$  Hz, 1  $\text{P=O}$ ),  $-14.88$  (d,  $J_{\text{PP}} = 20$  Hz, 2  $\text{PAr}_3$ ).

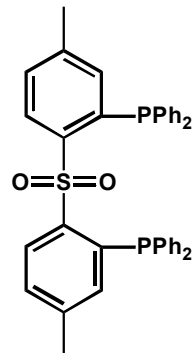
**IR [cm $^{-1}$ ]** ( $\nu \text{ P=O}$ , strong) 1173.



#### 4.2.4. Synthesis of (sulfonylbis(3-methyl-6,1-phenylene))bis(diphenylphosphine) SODPdiphos (**L3**)

This ligand was prepared according to the experience of our group, and its synthesis optimized.

p-Tolyl sulfone (Acros, 6.15 g, 25 mmol) was dissolved in dry, degassed THF (100 ml) in a 250 ml side arm flask. The solution was cooled down to  $-41^{\circ}\text{C}$  ( $\text{CH}_3\text{CN}$ /liquid  $\text{N}_2$ ) and n-BuLi (2.5 M in hexane, Aldrich, 22.5 ml, 55 mmol) was added drop wise. The mixture was stirred at  $-41^{\circ}\text{C}$  for an hour and two more hours at  $-15^{\circ}\text{C}$  (ethylene glycol/liquid  $\text{N}_2$  slush bath). A solution of chlorodiphenylphosphine (Aldrich, 10.75 ml, 58.75 mmol) in dry THF (25 ml) was added slowly. The solvent was evaporated and the resulting white residue was treated with degassed HCl (1% aq soln) and was extracted with  $\text{CH}_2\text{Cl}_2$  (3 x 30 ml). The aqueous layer was discarded and the organic layer was filtered through  $\text{Na}_2\text{SO}_4$  and the resulting solution was dried under reduced pressure to yield a yellowish to yellow-green oil that was purified by flash chromatography over silica gel with dry  $\text{CH}_2\text{Cl}_2$  and washing with ether. The solution was dried under reduced pressure producing a white solid product. Yield: 10 g, 67%.



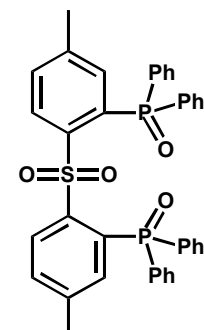
$^{31}\text{P}\{\text{H}\}$  NMR (101 MHz,  $\text{CDCl}_3$ , 298 K)  $\delta$  –13.98 (s, PAr<sub>3</sub>).

$^1\text{H}$  NMR (400 MHz,  $\text{CDCl}_3$ , 298 K)  $\delta$  8.60–8.39 (m, 1H), 7.27–7.11 (m, 7H), 7.02–6.86 (m, 4H), 6.79 (s, 1H), 2.16 (s, 3H).

IR [ $\text{cm}^{-1}$ ] 3051, 1583, 1477, 1433, 1378, 1300 ( $\nu$  SO<sub>2</sub> asymm stretch), 1148 ( $\nu$  SO<sub>2</sub> symm stretch), 1114, 1091, 821, 742, 721, 692, 673, 629.

#### 4.2.5. Synthesis of (sulfonylbis(3-methyl-6,1-phenylene))bis(diphenyl phosphine oxide)

In an open 50 ml round bottom flask charged with **L3** (500 mg, 814 mmol), glacial acetic acid (2.5 ml, Panreac) and acetone (3 ml) were added. The suspension was stirred and cooled down to 0°C and  $\text{H}_2\text{O}_2$  (35%, J.T. Baker, 0.5 ml) was added. The suspension was left to react for 20 minutes at 0°C and the suspension was heated until all the acetone was evaporated. The suspended solids were dissolved and the solution became transparent as it was heated. The solution was cooled down to room temperature. Cold  $\text{H}_2\text{O}$  (20 ml) was added to precipitate the product. The white insoluble product was filtered off using a glass sintered filter and was washed with water (15 ml) and ether (3 x 10 ml). The white product was dried under reduced pressure. Yield: 169 mg, 32%.



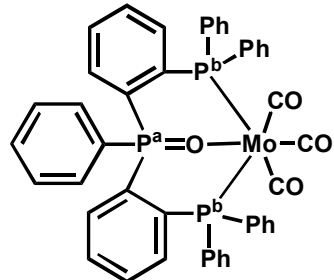
$^{31}\text{P}\{\text{H}\}$  NMR (162 MHz,  $\text{CDCl}_3$ , 298 K)  $\delta$  33.46 (s, PAr<sub>3</sub>).

IR [cm<sup>-1</sup>] 3061, 1436, 1326, 1176 ( $\nu$  P=O), 1158, 1380 ( $\nu$  SO<sub>2</sub> asymm stretch), 1117 ( $\nu$  SO<sub>2</sub> symm stretch), 1102, 874, 833, 753, 723, 704, 692, 671, 625.

#### 4.3. Synthesis of Metal Complexes

##### 4.3.1. Synthesis of *fac*-[Mo(TPOdiphos)(CO)<sub>3</sub>]

A side arm flask was charged with Mo(CO)<sub>6</sub> (Strem, 98%, 204 mg, 0.77 mmol) and with a suspension of **L1** (500 mg, 0.77 mmol) in dry, degassed toluene (30 ml). The solution was refluxed for an hour and the formation of an orange, transparent solution was observed as the reaction proceeds. After 1 hr at reflux temperature, the solvent was evaporated at rt under reduced pressure and the remaining residue was dissolved in CH<sub>2</sub>Cl<sub>2</sub>. Cold, dry ether was added to cause the formation of the product as a precipitate. The yellow-orange solid product was filtered, washed with dry ether (3 x 5 ml) and dried under reduced pressure. Yield: 491 mg, 76.8%.



$^{31}\text{P}\{\text{H}\}$  NMR (162 MHz,  $\text{CDCl}_3$ , 298 K)  $\delta$  37.24 (t,  $J_{\text{PP}} = 19.6$  Hz, P<sub>a</sub>), 30.44 (d,  $J_{\text{PP}} = 19.4$  Hz, 2P<sub>b</sub>).

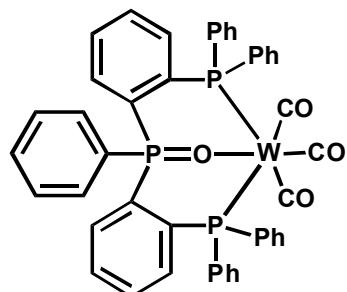
IR [cm<sup>-1</sup>] 1913, 1813, 1775, 1479, 1433, 1154 ( $\nu$  P=O), 1116, 1093, 737, 690, 661

HRMS ESI<sup>+</sup> Experimental m/z, Int. % (calculated m/z, Int. % for C<sub>45</sub>H<sub>33</sub>O<sub>4</sub>P<sub>3</sub>Mo, M+Na<sup>+</sup>): 851.0574, 100 (851.0549, 100); 849.0574, 81.7 (849.0533, 82.1); 850.0592, 61.8 (850.0546, 63.8); 845.0564, 42.5 (845.0552, 47.4)

**XRD** The crystals grown by the diffusion of diethyl ether into a saturated solution of the complex in CH<sub>2</sub>Cl<sub>2</sub> were found to be suitable for X-Ray diffraction. The data was successfully gathered and the structure of the crystal was resolved.

##### 4.3.2. Synthesis of [W(TPOdiphos)(CO)<sub>3</sub>]

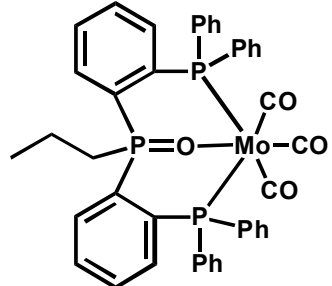
A flask was charged with W(CO)<sub>6</sub> (275 mg, 0.79 mmol) and with a solution of **L1** (500 mg, 0.77 mmol) in anhydrous diglyme (MeOCH<sub>2</sub>CH<sub>2</sub>OCH<sub>2</sub>CH<sub>2</sub>OMe, Aldrich, 30 ml). The solution was refluxed at 165°C for four hours. The formation of a deep red solution and a brown precipitate was observed as the reaction proceeds. The solvent was removed and the *terra cotta* colored product was washed



with hexane (10 ml) and ether (3 x 20 ml). The product was purified by repeated crystallization by dissolving the product in  $\text{CH}_2\text{Cl}_2$  and adding cold, dry ether to precipitate the solid. The product was filtered and dried under reduced pressure. Yield: 341 mg, 48%  
 $^1\text{P}\{^1\text{H}\}$  NMR (162 MHz,  $\text{CDCl}_3$ , 298 K)  $\delta$  36.46 (t), 25.51 (d with  $^{183}\text{W}$  sat.,  $^1J_{\text{PW}} = 217$  Hz).  
IR [ $\text{cm}^{-1}$ ] 1905, 1805, 1770, 1480, 1433, 1150 ( $\nu \text{ P=O-W}$ ), 1117, 1092, 816, 738, 690.  
HRMS ESI<sup>+</sup> Experimental m/z, Int. % (calculated m/z, Int. % for  $\text{C}_{45}\text{H}_{33}\text{O}_4\text{P}_3\text{W}$ , M+Na<sup>+</sup>): 937.1011, 100 (937.1001, 100); 939.1047 (939.1028, 79.7); 936.1010, 70.9 (936.0987, 66.7); 935.0988, 67.4 (935.0966, 64.6)

#### 4.3.3. Reaction of $\text{Mo}(\text{CO})_6$ with L2

A flask was charged with  $\text{Mo}(\text{CO})_6$  (Strem, 98%, 214 mg, 827 mmol) and with **L2** (500 mg, 816 mmol) in dry, degassed toluene (30 ml). The solution was refluxed at 110°C for an hour and the formation of a transparent, yellow solution was observed as the reaction proceeds. All the solvent was removed under reduced pressure. The yellow residue was re-dissolved in dry  $\text{CH}_2\text{Cl}_2$  and the product was precipitated with cold, dry, ether. The yellow impure product was washed with ether (3 x 20 ml), filtered and dried under reduced pressure. Yield: 198 mg, 30.5%

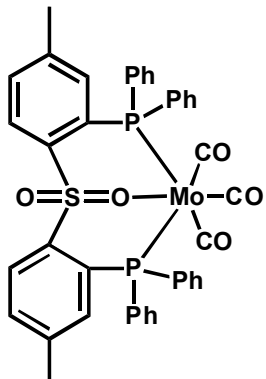


$^{31}\text{P}\{^1\text{H}\}$  NMR (162 MHz,  $\text{CDCl}_3$ , 298 K) Major Product (ca. 90%)  $\delta$  44.20 (t,  $J_{\text{PP}} = 19$  Hz), 29.74 (d,  $J_{\text{PP}} = 19$  Hz). Minor Product (ca. 10%)  $\delta$  45.59 (t,  $J_{\text{PP}} = 18$  Hz), 29.81 (d,  $J_{\text{PP}} = 18$  Hz).

IR [ $\text{cm}^{-1}$ ] 1909, 1804, 1776, 1479, 1433, 1151 ( $\nu \text{ P=O}$ ), 1120, 744, 691

#### 4.3.4. Synthesis of $[\text{Mo}(\text{SODPdiphos})(\text{CO})_3]$

A flask was charged with  $\text{Mo}(\text{CO})_6$  (53.4 mg, 0.202 mmol) and with a solution of **L3** (120 mg, 0.202 mmol) in dry, degassed toluene (30 ml). The solution was refluxed at 120°C for four hours. The formation of a yellow, transparent solution was observed. Eventually, a yellow precipitate was formed as the reaction proceeds. The solvent was removed and the solid was washed with cold, dry ether (3 x 5 ml). The product was purified by repeated recrystallizations by dissolving the product in  $\text{CH}_2\text{Cl}_2$  (5 ml) and by adding cold dry, degassed ether (30 ml). The precipitated product was filtered and was dried under reduced pressure. Yield: 97 mg, 65 %



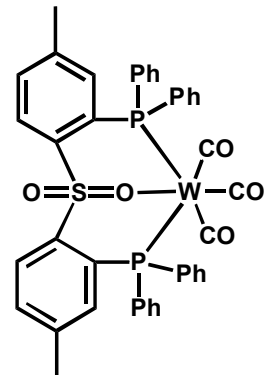
$^{31}\text{P}\{^1\text{H}\}$  NMR (101 MHz,  $\text{CDCl}_3$ )  $\delta$  31.12 (s, PAr<sub>3</sub>).

**IR** [ $\text{cm}^{-1}$ ] 1920, 1830, 1778, 1584, 1480, 1434, 1300 ( $\nu \text{SO}_2$  asymm stretch), 1134 ( $\nu \text{SO}_2$  stretch), 1090, 830, 748, 696, 669.

**HRMS ESI<sup>+</sup>** Experimental m/z, Int. % (calculated m/z, Int. % for  $\text{C}_{41}\text{H}_{32}\text{O}_5\text{SP}_2\text{Mo}$ , M+Na<sup>+</sup>): 819.0376, 100 (819.0400, 100); 817.034, 81.0 (817.0387, 80.2); 813.0381, 49.0 (813.0406, 46.6); 821.0396, 47.7 (821.0413, 43.8).

#### 4.3.5. Synthesis of $[\text{W}(\text{SODPdiphos})(\text{CO})_3]$

A flask was charged with  $\text{W}(\text{CO})_6$  (275 mg, 0.781 mmol) and with a solution of **L3** (500mg, 0.774 mmol) in degassed decane (30 ml). The solution was refluxed at 160°C for a total of four hours. The formation of a yellow, transparent solution was observed. Eventually, the formation of a yellow precipitate was observed as the reaction proceeds. The solvent was removed and the product was washed with cold, ether (3 x 5 ml). The yellow product was purified by repeated recrystallizations in  $\text{CH}_2\text{Cl}_2$  and the addition of dry ether. Yield: 412 mg, 59%



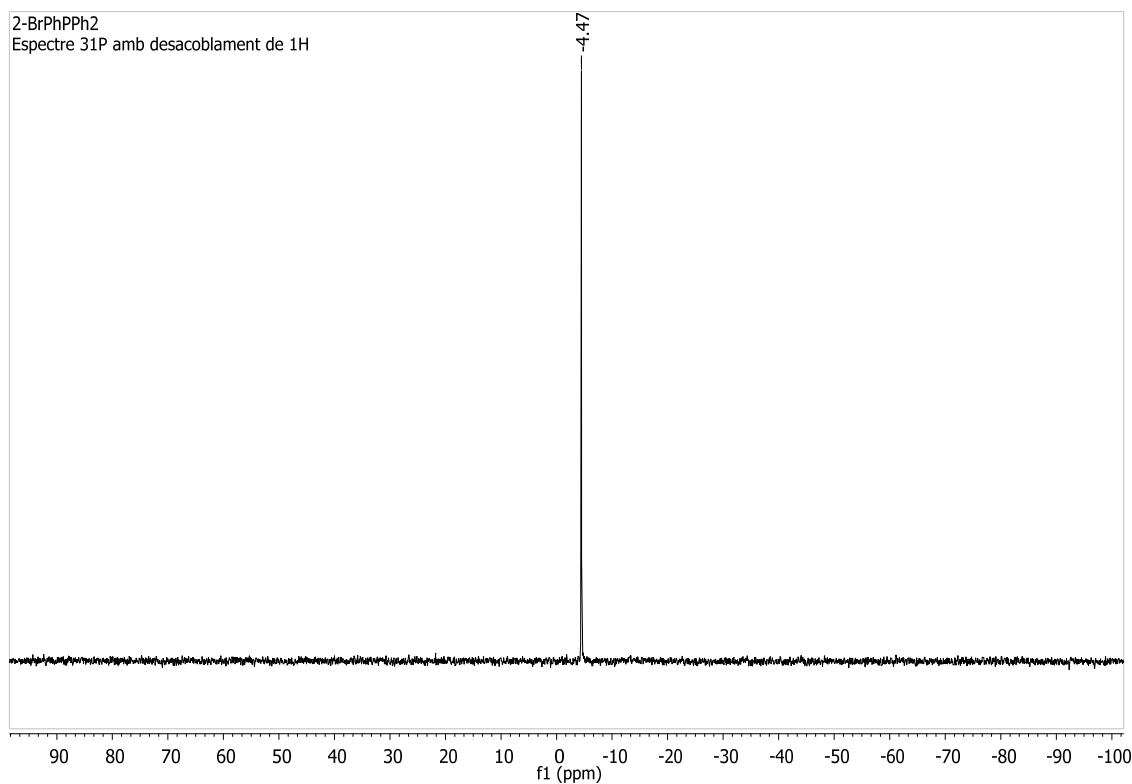
**$^{31}\text{P}\{\text{H}\}$  NMR** (101 MHz,  $\text{CDCl}_3$ , 298 K)  $\delta$  22.83 (s with  $^{183}\text{W}$  sat.,  $^1J_{\text{PW}}=233$  Hz).

**IR** [ $\text{cm}^{-1}$ ] 1905, 1805, 1770, 1572, 1481, 1434, 1297 ( $\nu \text{SO}_2$  asymm stretch), 1130 ( $\nu \text{SO}_2$  stretch), 1092, 1027, 831, 749, 695, 670, 639.

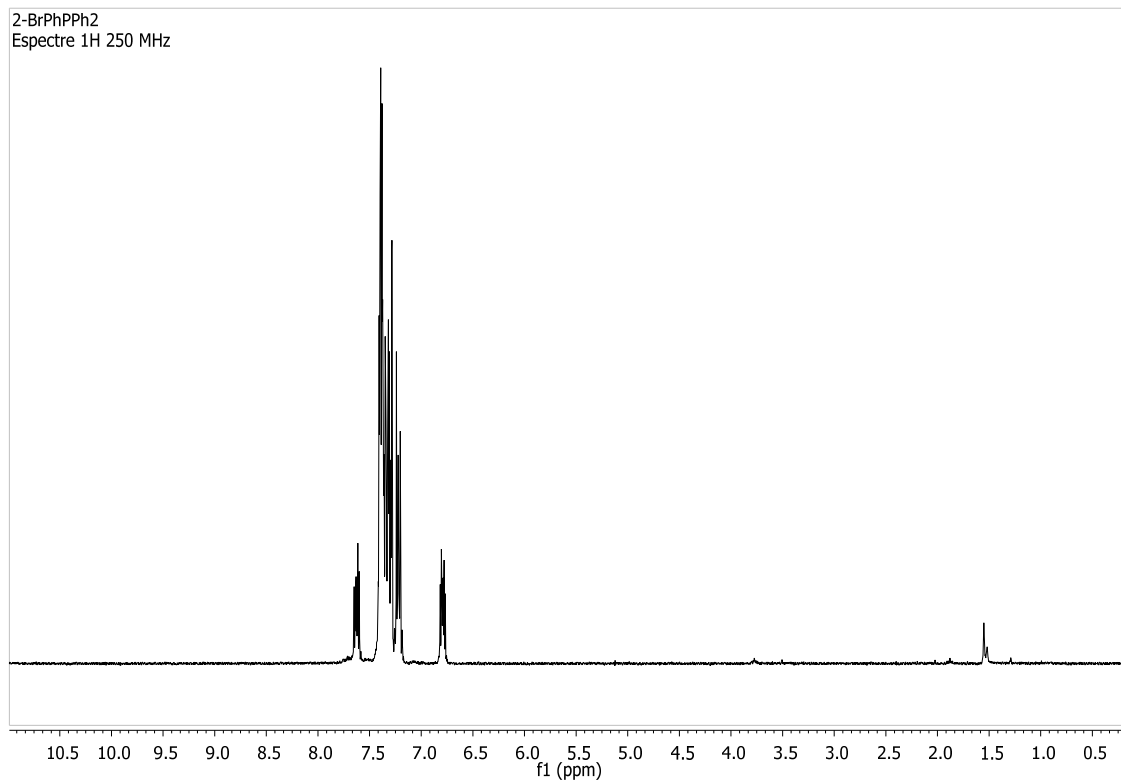
**HRMS ESI<sup>+</sup>** Experimental m/z, Int. % (calculated m/z, Int. % for  $\text{C}_{41}\text{H}_{32}\text{O}_5\text{SP}_2\text{W}$ , M+Na<sup>+</sup>): 905.0840, 100.0 (905.0852, 100.0); 907.0863, 77.2 (907.0881, 82.3); 904.0825, 61.5 (904.0841, 63.9).

# **ANNEX**

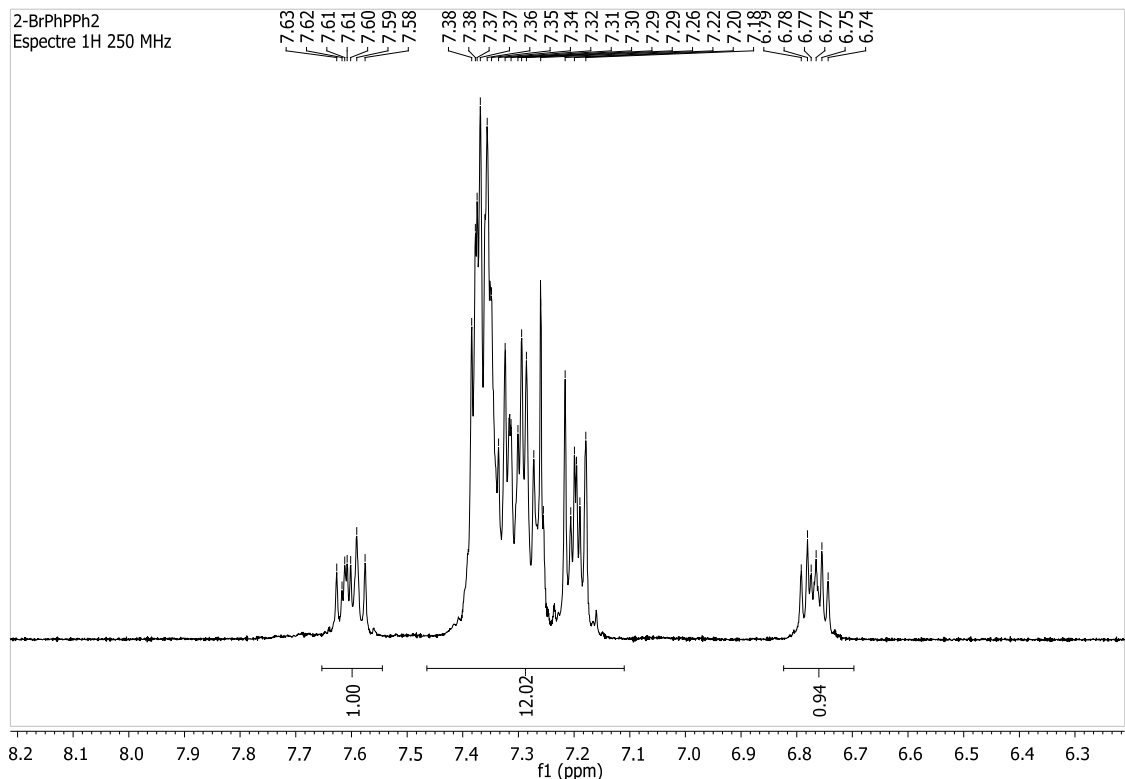
## ANNEX I. NMR Spectra



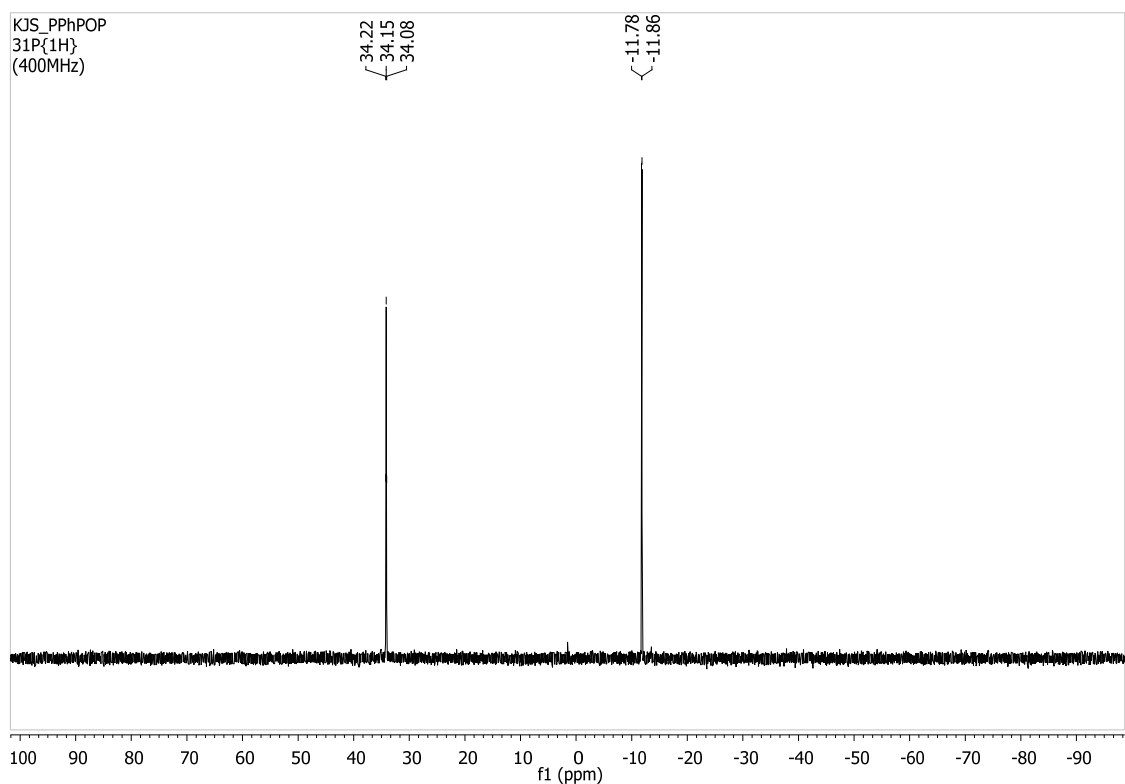
**Annex 1.1.** <sup>31</sup>P{<sup>1</sup>H} NMR of 2-bromophenyldiphenylphosphine (C<sub>18</sub>H<sub>14</sub>PBr), L0



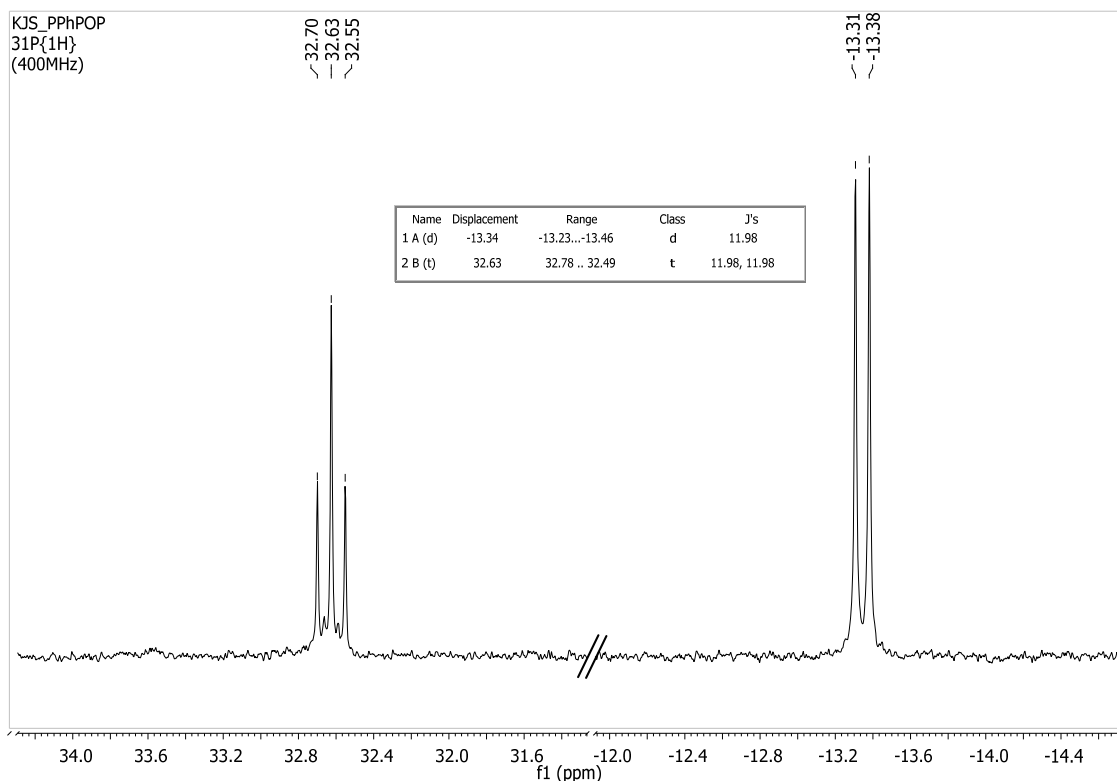
**Annex 1.2.** <sup>1</sup>H NMR of 2-bromophenyldiphenylphosphine (C<sub>18</sub>H<sub>14</sub>PBr), L0



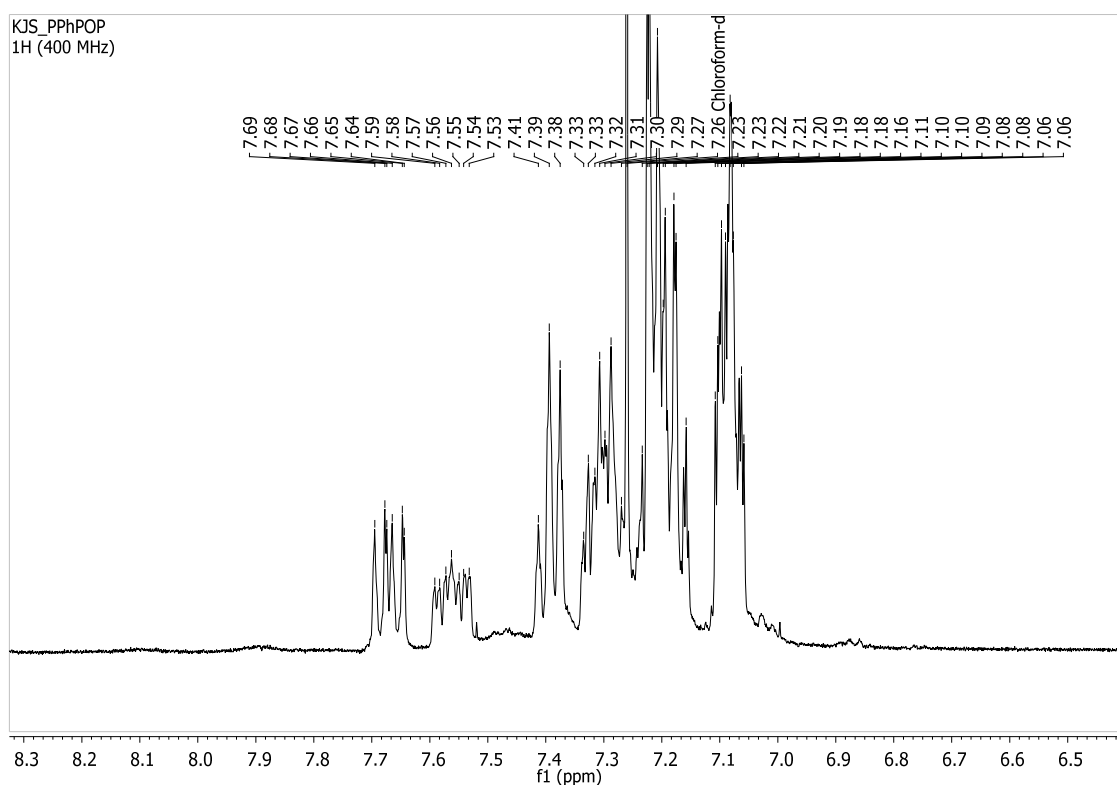
### **Annex 1.3. Amplification of the $^1\text{H}$ NMR of 2-bromophenyldiphenyl phosphine ( $\text{C}_{18}\text{H}_{14}\text{PBr}$ ), L0**



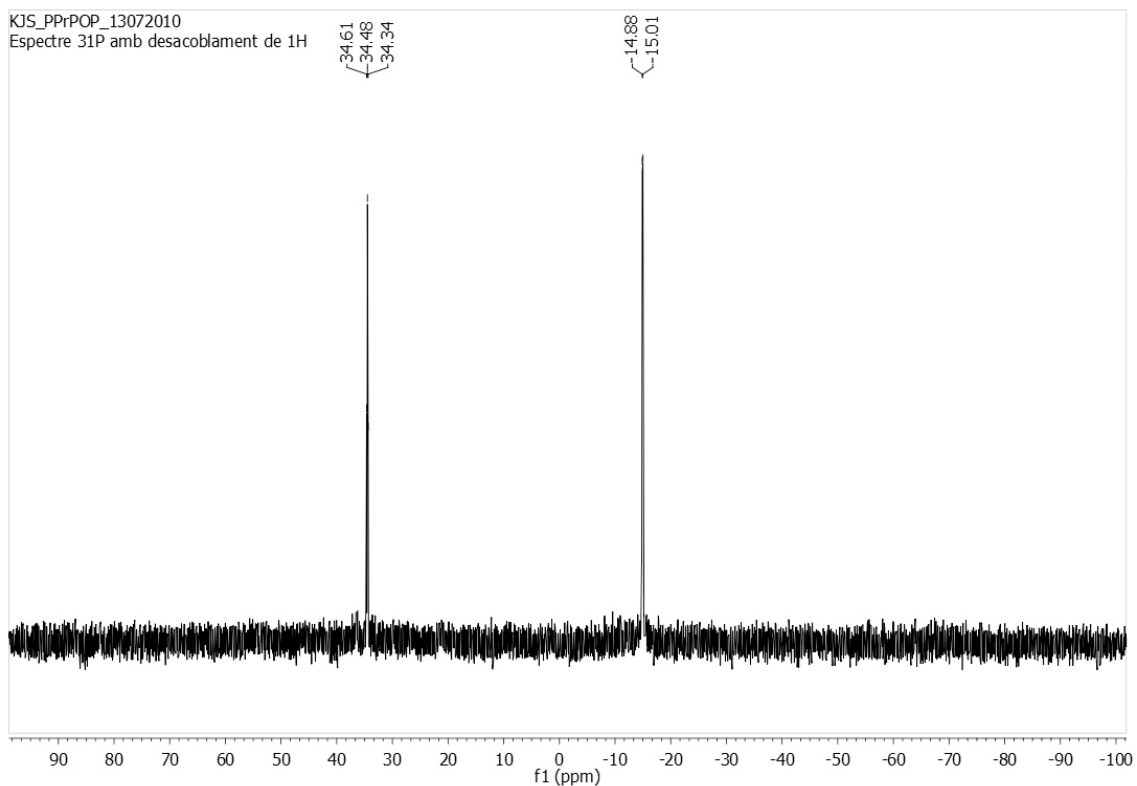
**Annex 1.4.  $^{31}\text{P}\{\text{H}\}$  NMR of bis(2-(diphenylphosphino)phenyl)(phenyl)phosphine oxide (TPOdiphos), L1**



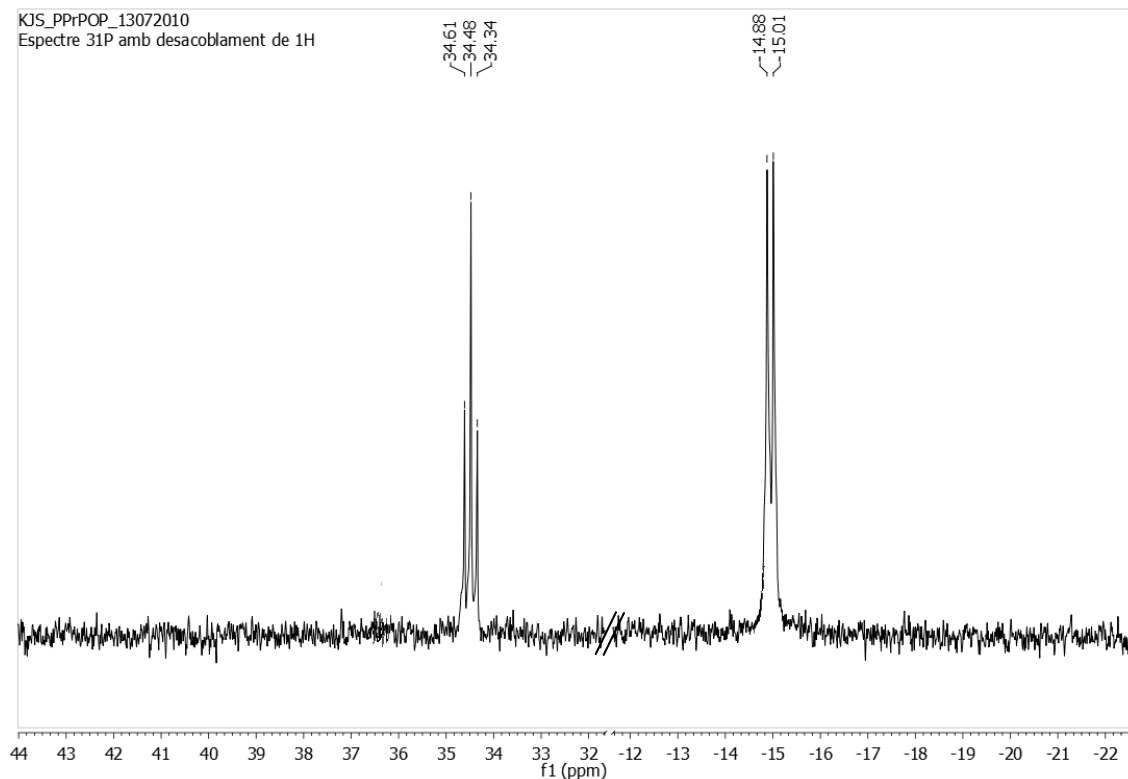
**Annex 1.5.** Amplification of the  $^{31}\text{P}\{\text{H}\}$  NMR of bis(2-diphenylphosphino)phenyl(phenyl)phosphine oxide (TPOdiphos), **L1**



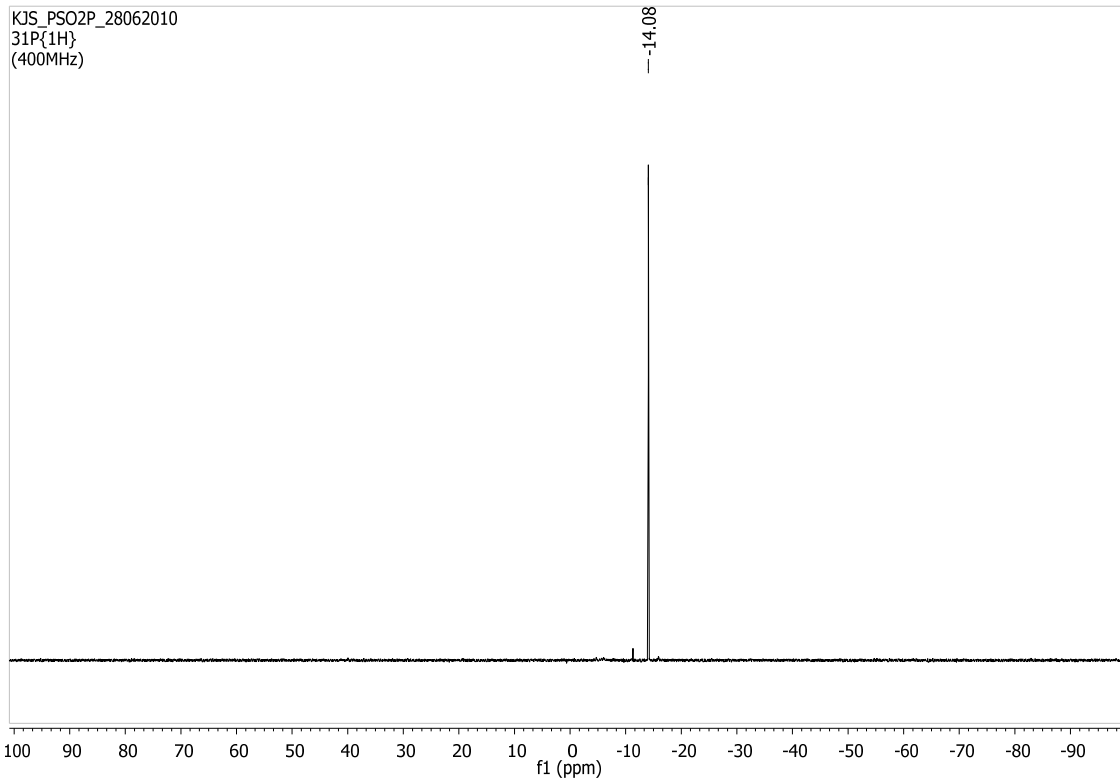
**Annex 1.9.**  $^1\text{H}$  NMR of bis(2-diphenylphosphino)phenyl(phenyl)phosphine oxide (TPOdiphos), **L1**



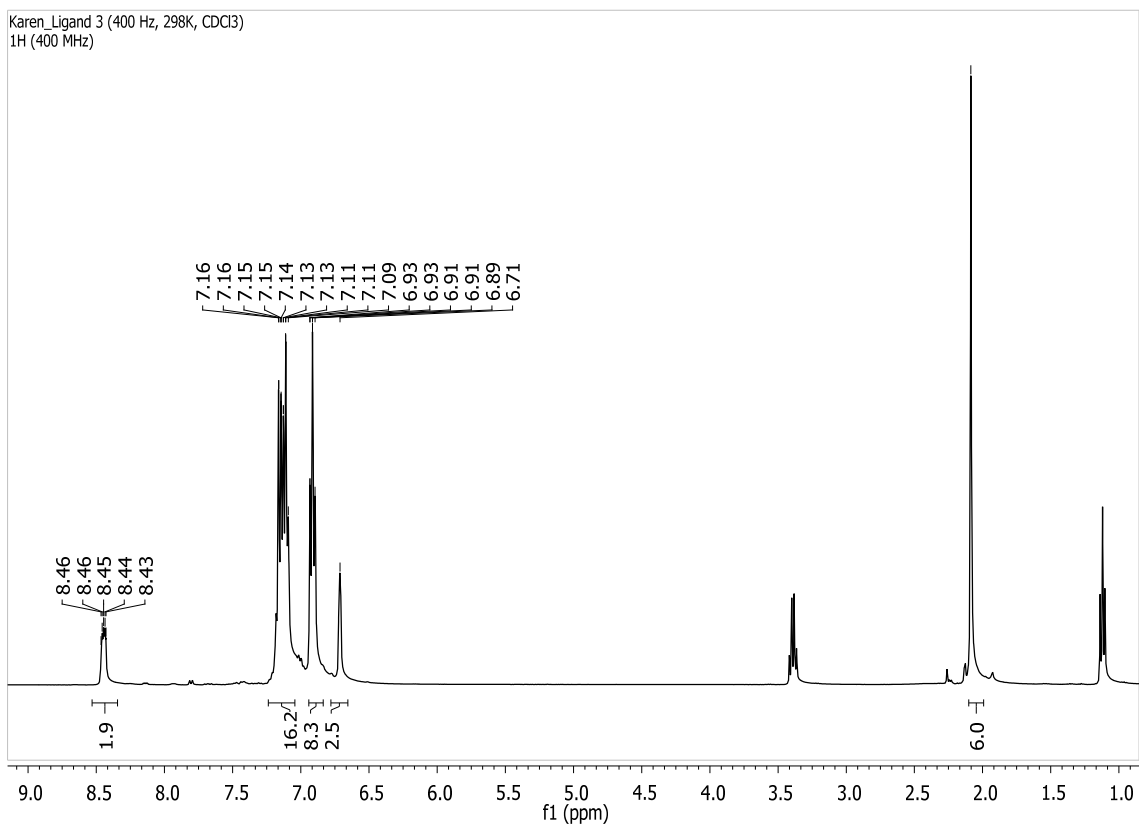
**Annex 1.8.**  $^{31}\text{P}\{\text{H}\}$  NMR of bis(2-(diphenylphosphino)phenyl) (propyl)phosphine oxide (DPPrOdiphos), **L2**



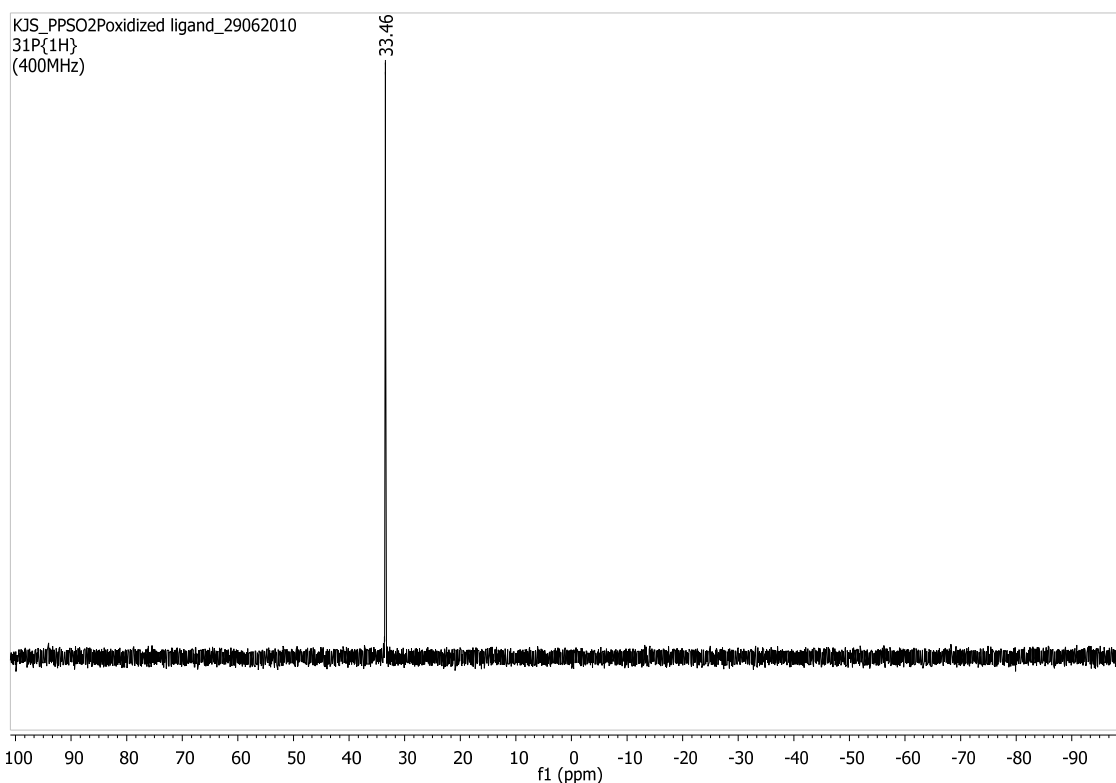
**Annex 1.9.** Amplification of the  $^{31}\text{P}\{\text{H}\}$  NMR of bis(2-diphenylphosphino)phenyl (propyl)phosphine oxide (DPPrOdiphos), **L2**



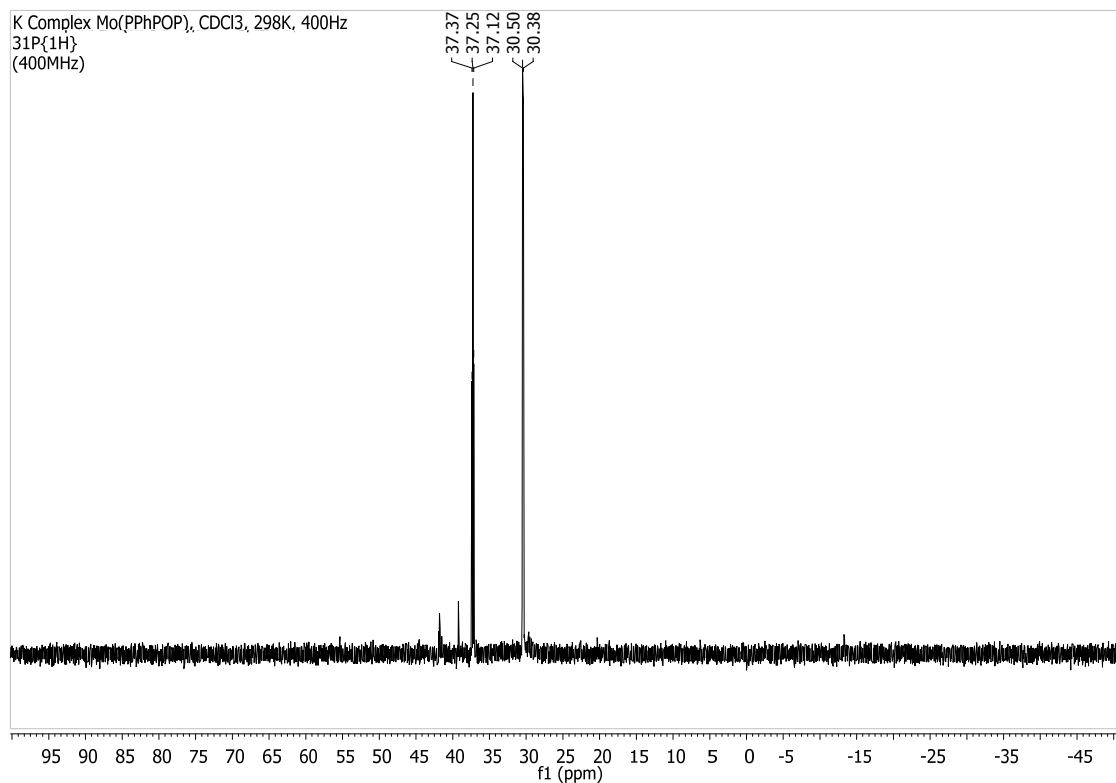
**Annex 1.10.**  $^{31}\text{P}\{\text{H}\}$  NMR of (sulfonylbis (3-methyl-6,1-phenylene)) bis(diphenyl phosphine) (SODPdiphos), **L3**



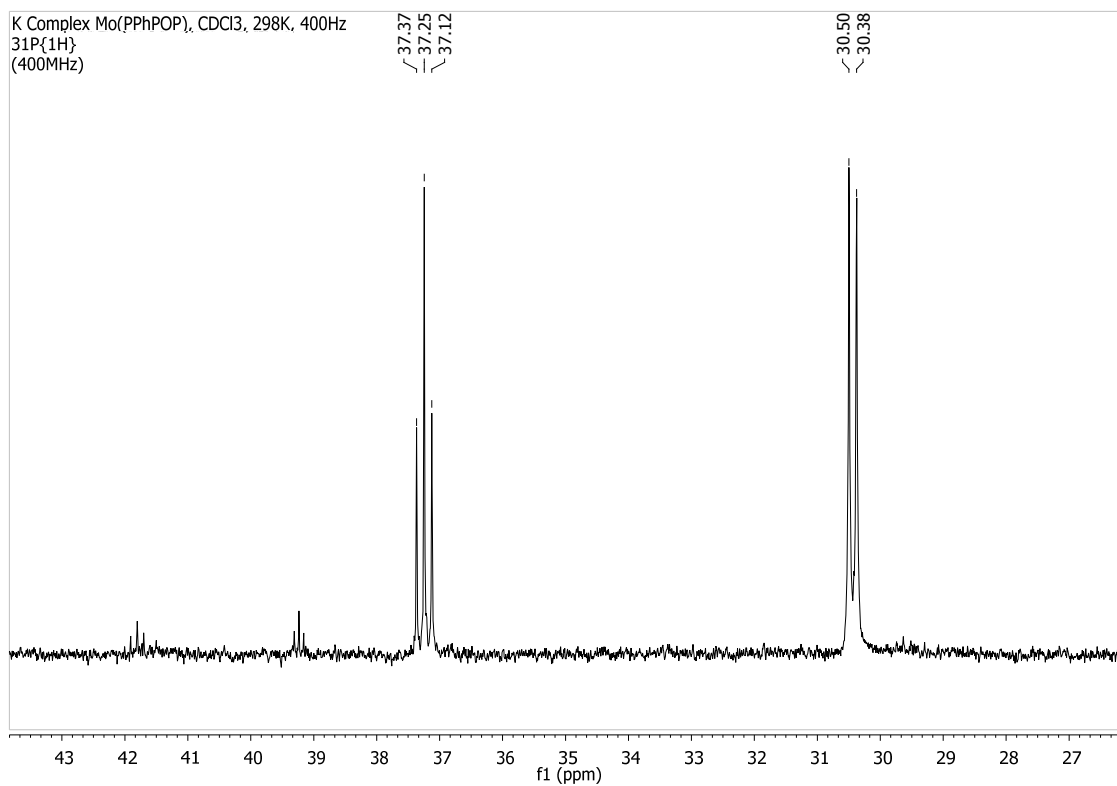
**Annex 1.11.**  $^1\text{H}$  NMR of (sulfonylbis (3-methyl-6,1-phenylene)) bis(diphenyl phosphine) (SODPdiphos), **L3**



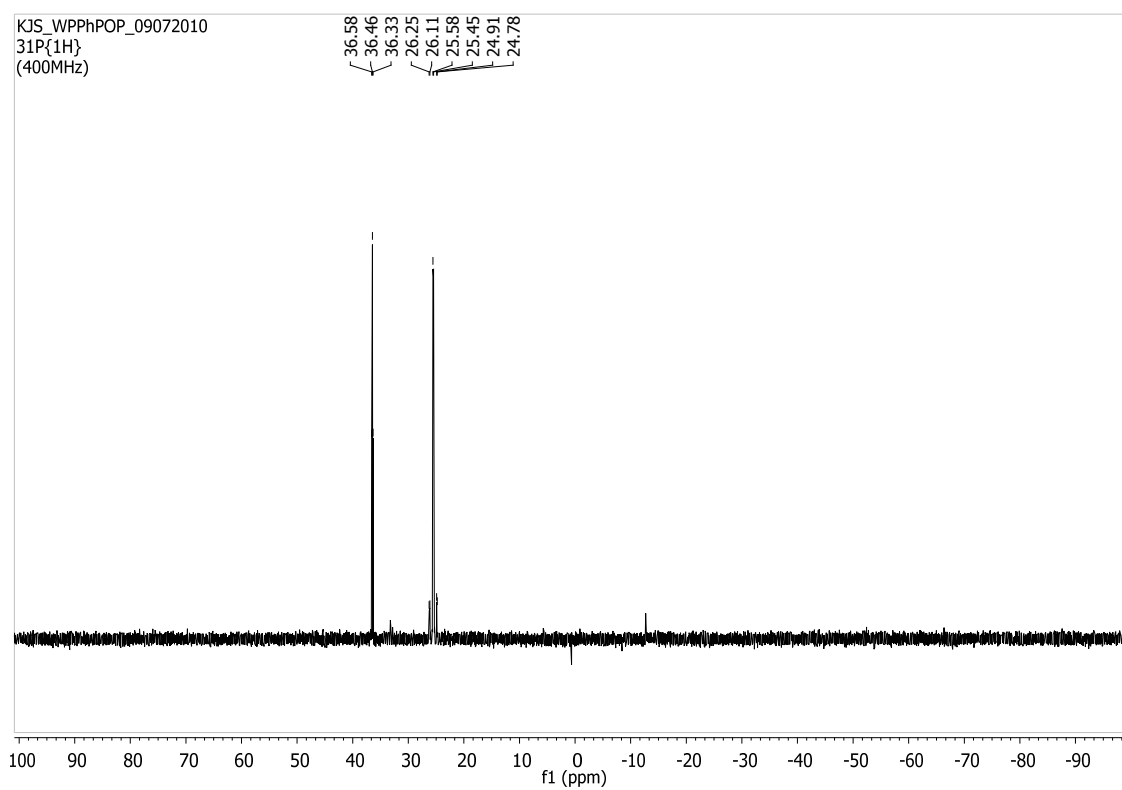
**Annex 1.12.**  $^{31}\text{P}\{^1\text{H}\}$  NMR of (sulfonylbis(3-methyl-6,1-phenylene)bis(diphenyl phosphine oxide) (SODPdiphos oxide )



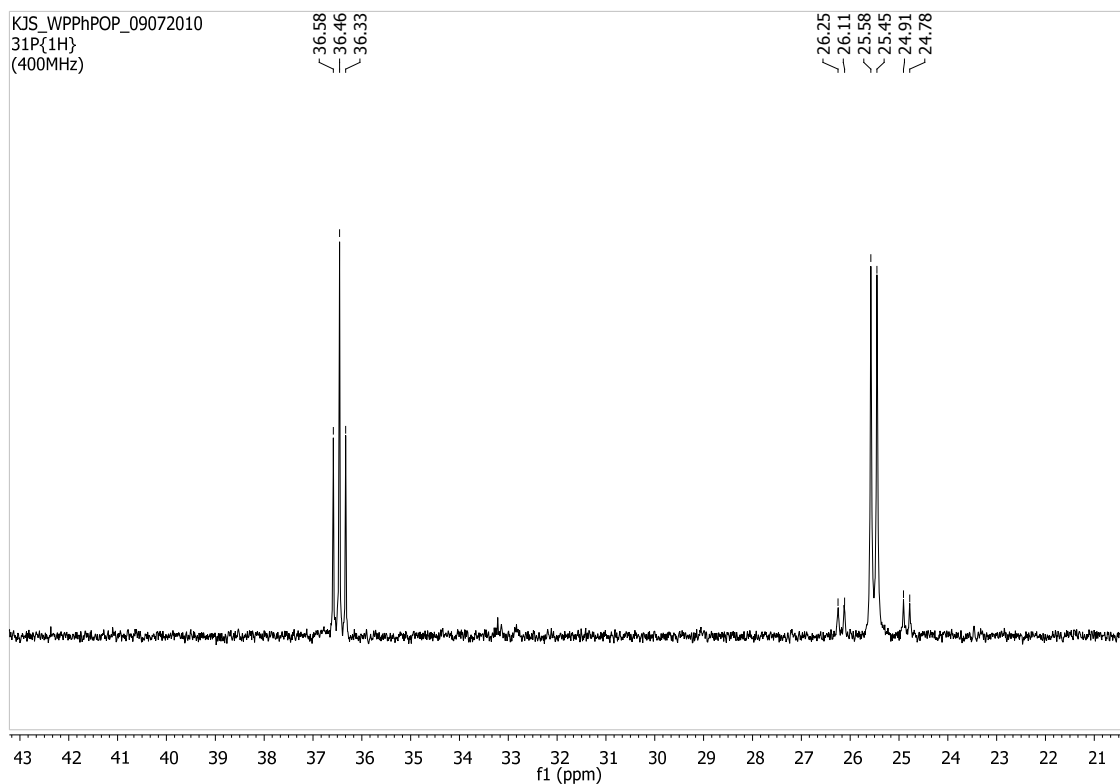
**Annex 1.13.**  $^{31}\text{P}\{^1\text{H}\}$  NMR of [Mo(TPOdiphos)(CO)<sub>3</sub>]



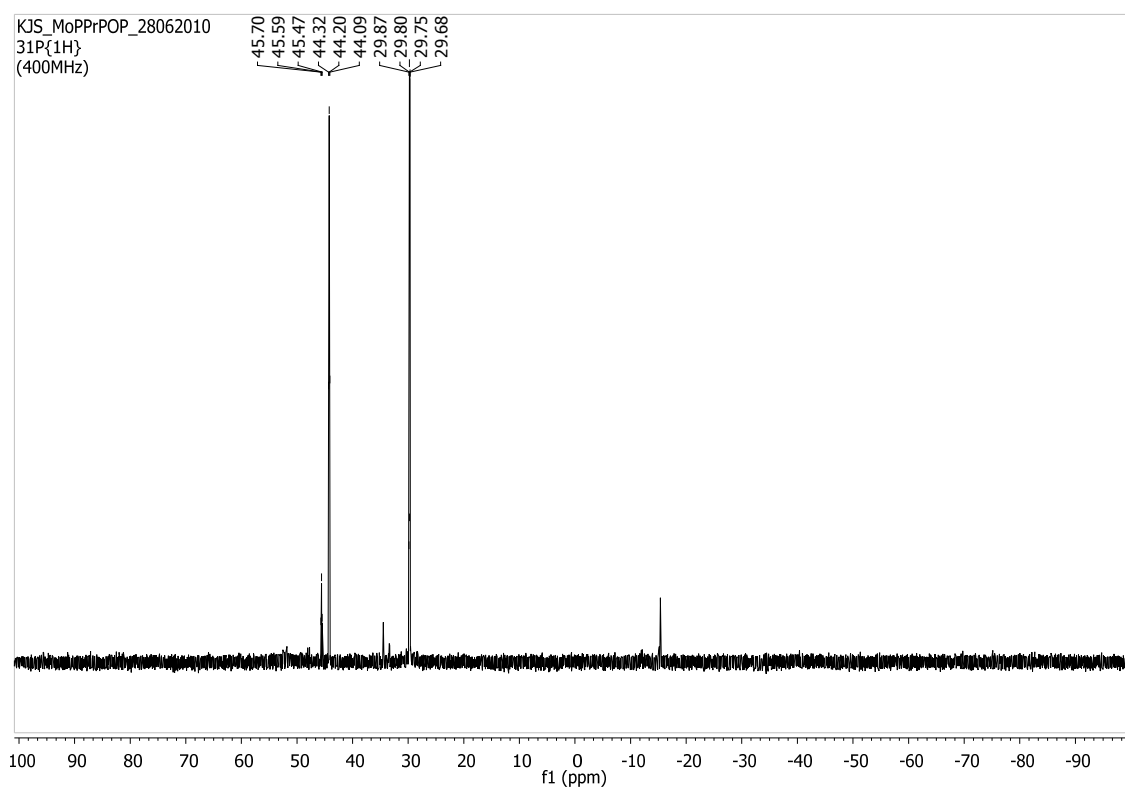
**Annex 1.14.** Amplification of the  $^{31}\text{P}\{^1\text{H}\}$  NMR of [Mo(TPOdiphos)(CO)<sub>3</sub>]



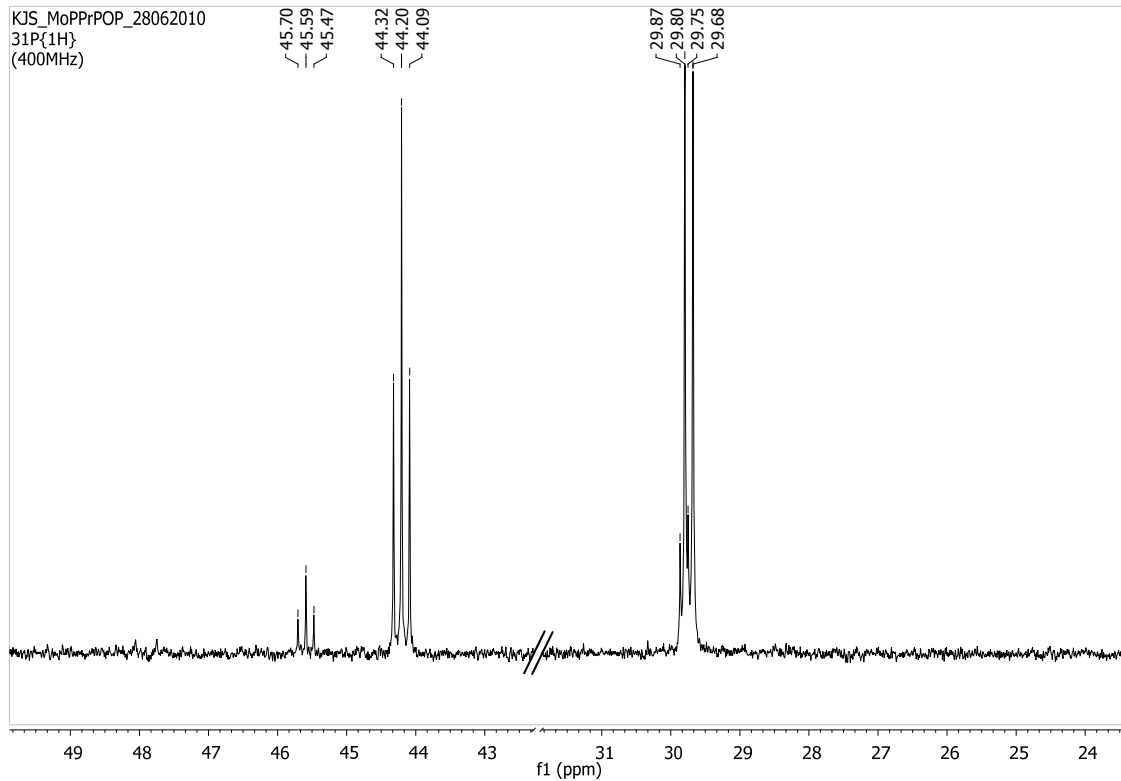
**Annex 1.15.**  $^{31}\text{P}\{^1\text{H}\}$  NMR of [W(TPOdiphos)(CO)<sub>3</sub>]



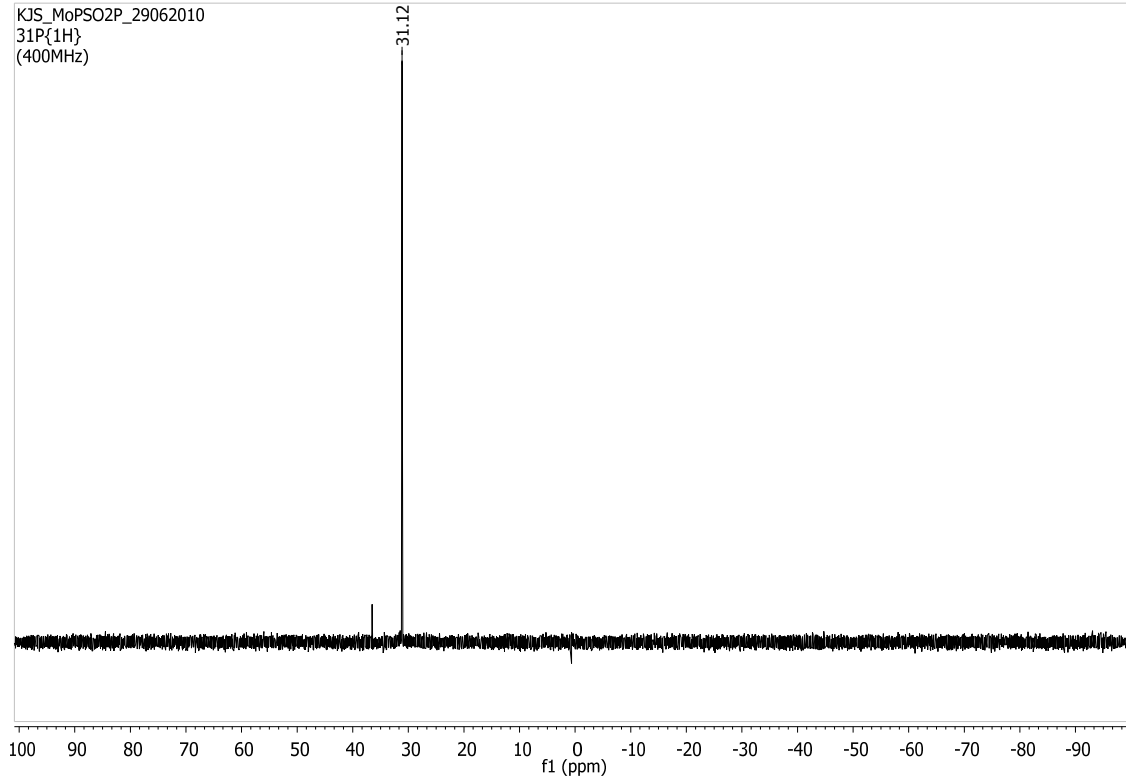
**Annex 1.16.** Amplification of the  $^{31}\text{P}\{\text{H}\}$  NMR of  $[\text{W}(\text{TPOdiphos})(\text{CO})_3]$



**Annex 1.17.**  $^{31}\text{P}\{\text{H}\}$  NMR of the reaction mixture of  $[\text{Mo}(\text{CO})_6]$  and **L2**

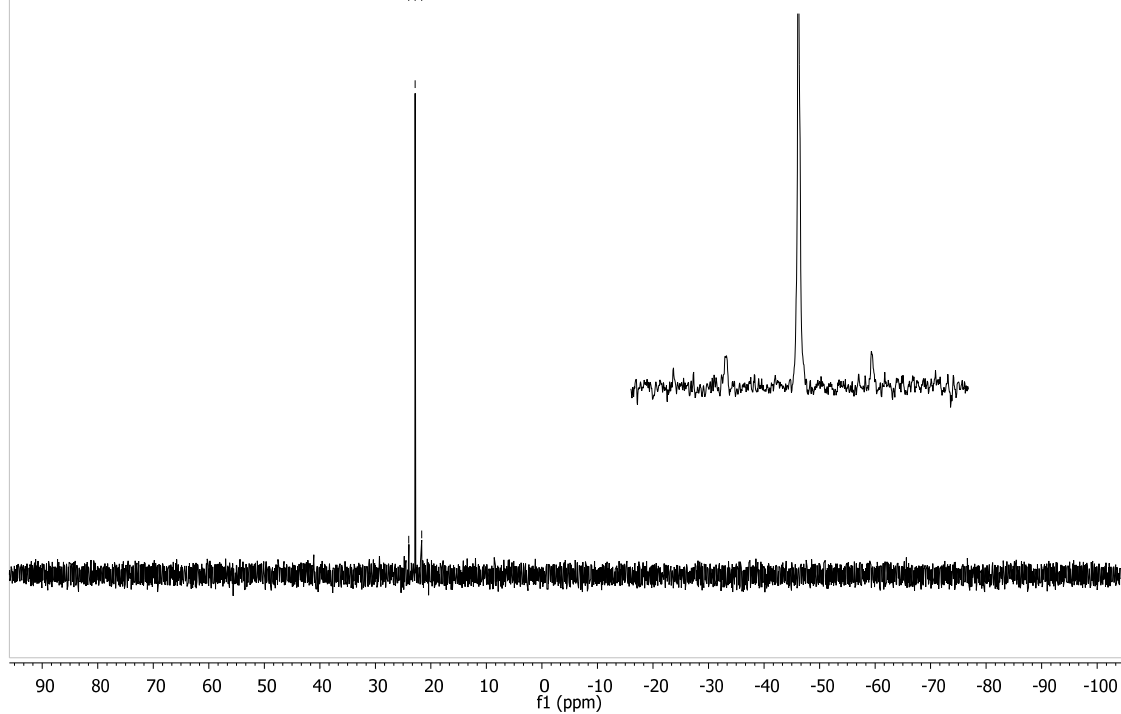


**Annex 1.18.** Amplification of the  $^{31}\text{P}\{\text{H}\}$  NMR of the reaction mixture of  $[\text{Mo}(\text{CO})_6]$  and **L2**



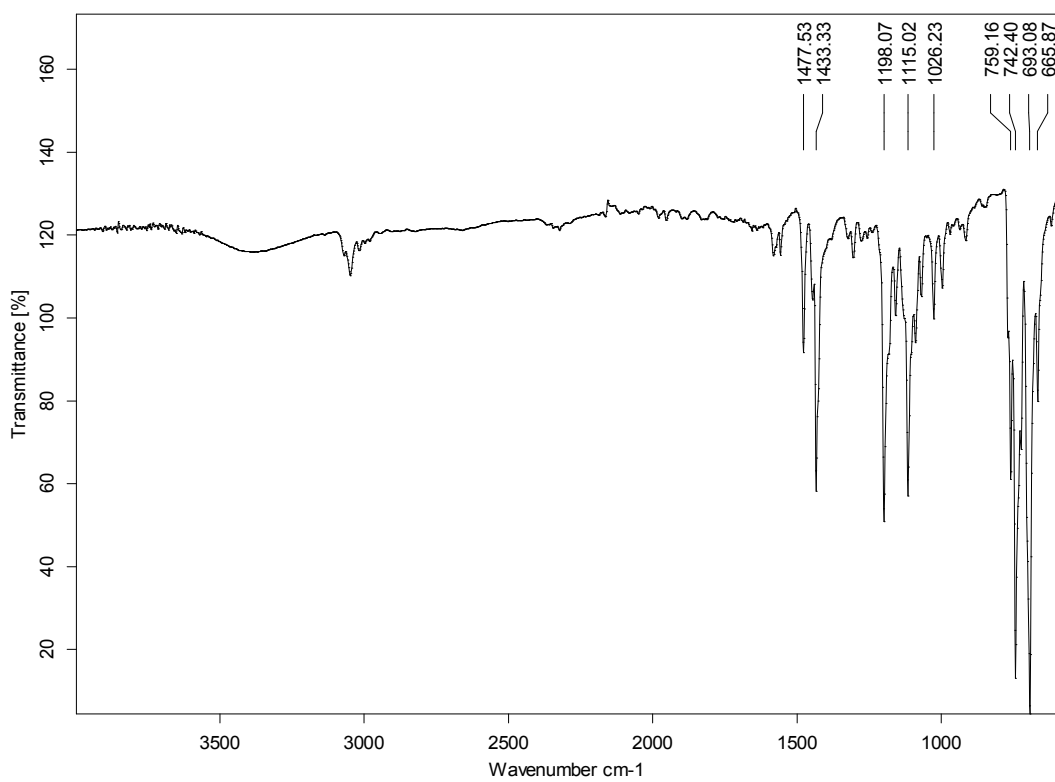
**Annex 1.21.**  $^{31}\text{P}$  Spectrum of  $[\text{Mo}(\text{SODPdiphos})(\text{CO})_3]$

KJS\_WPSO2P\_13072010  
Espectre 31P amb desacoblament de 1H

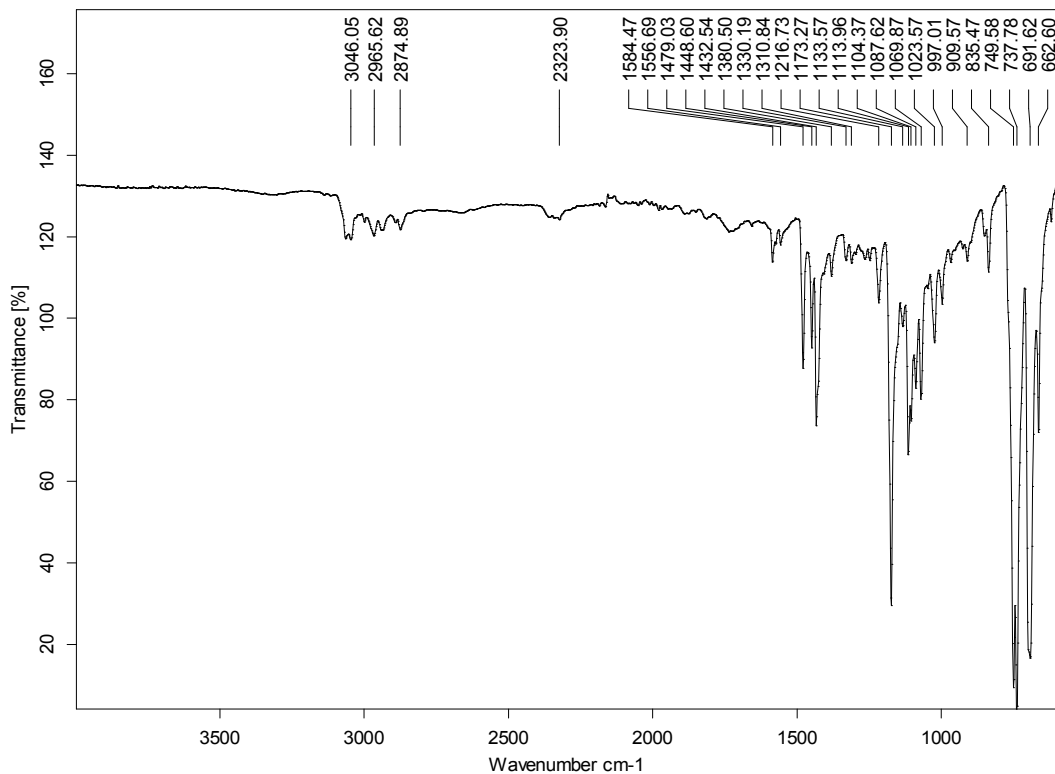


**Annex 1.22.**  $^{31}\text{P}\{\text{H}\}$  NMR of  $[\text{W}(\text{SODPdiphos})(\text{CO})_3]$

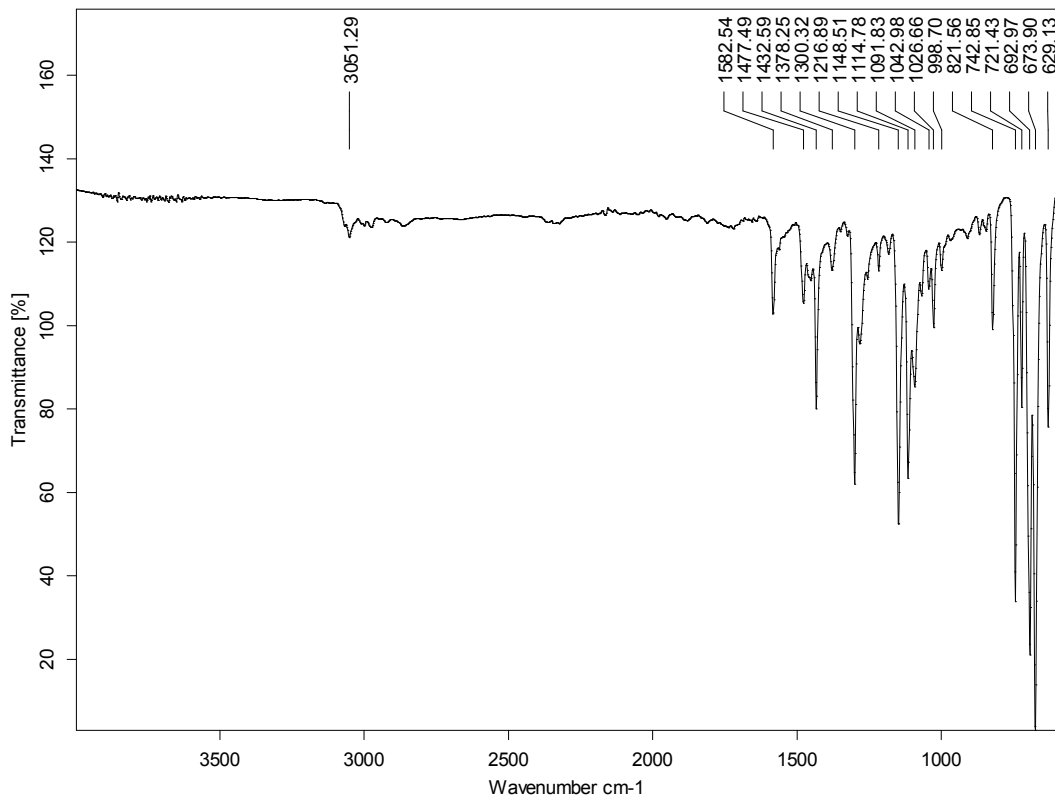
## ANNEX II. IR Spectra



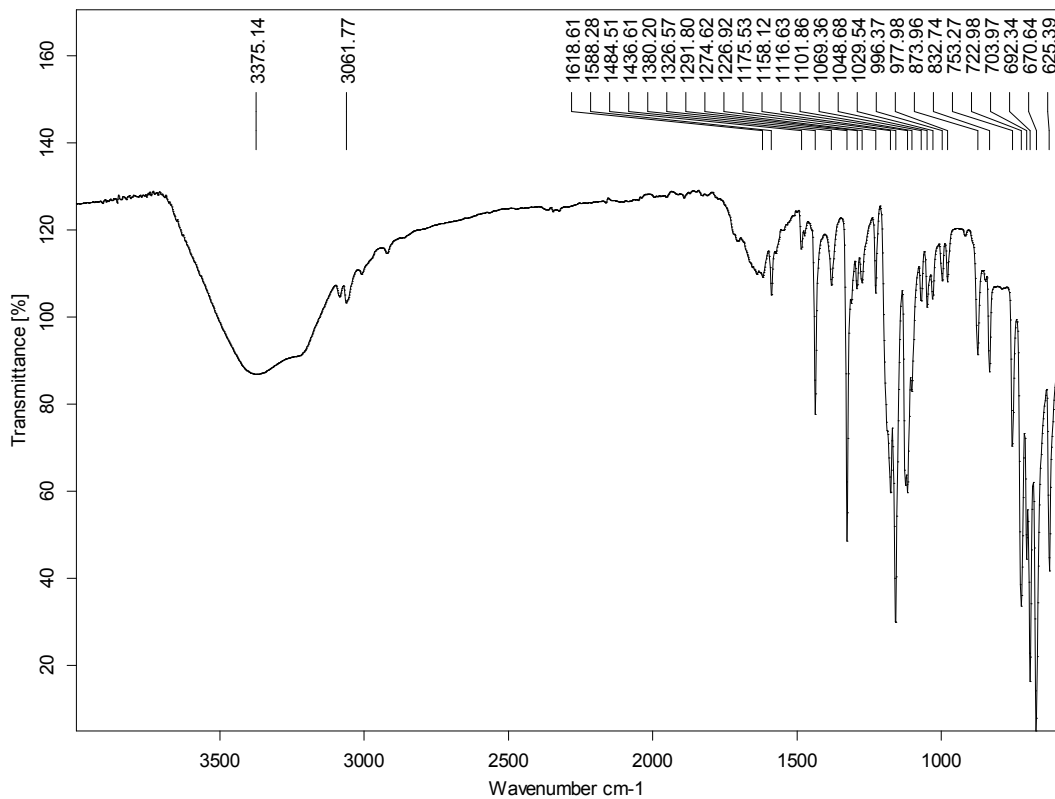
**Annex 2.1.** IR spectrum of TPOdiphos, **L1**



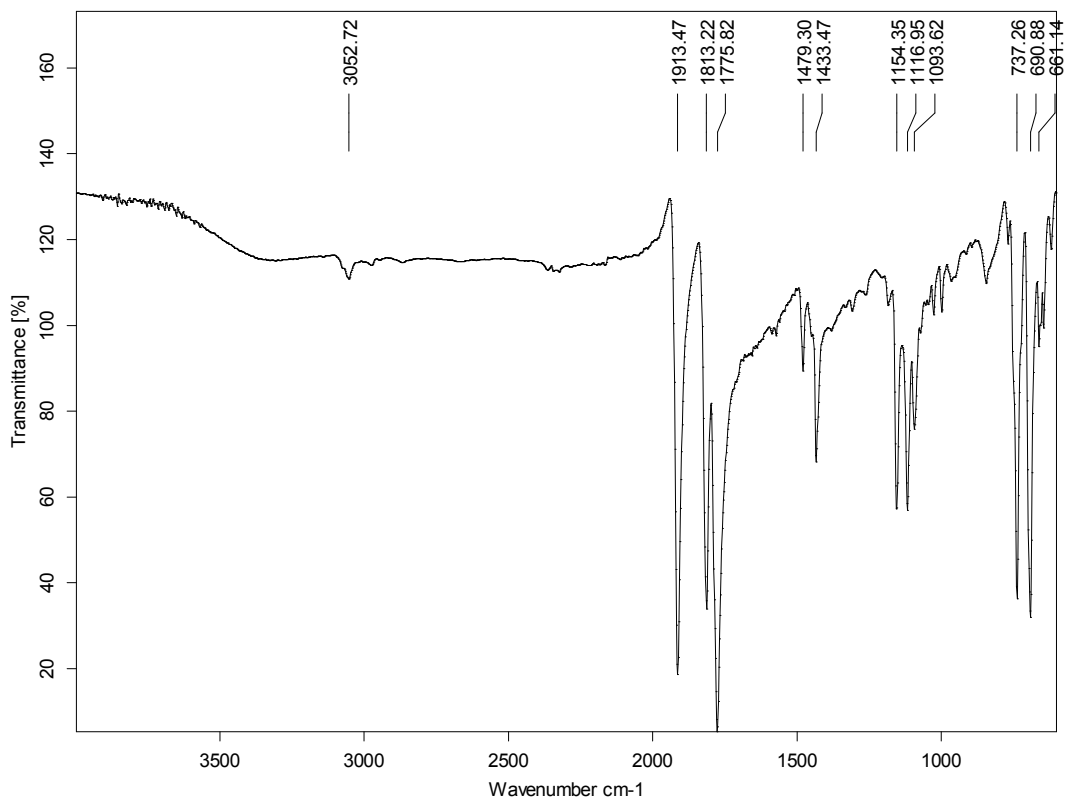
**Annex 2.2.** IR spectrum of DPPrPOdiphos, **L2**



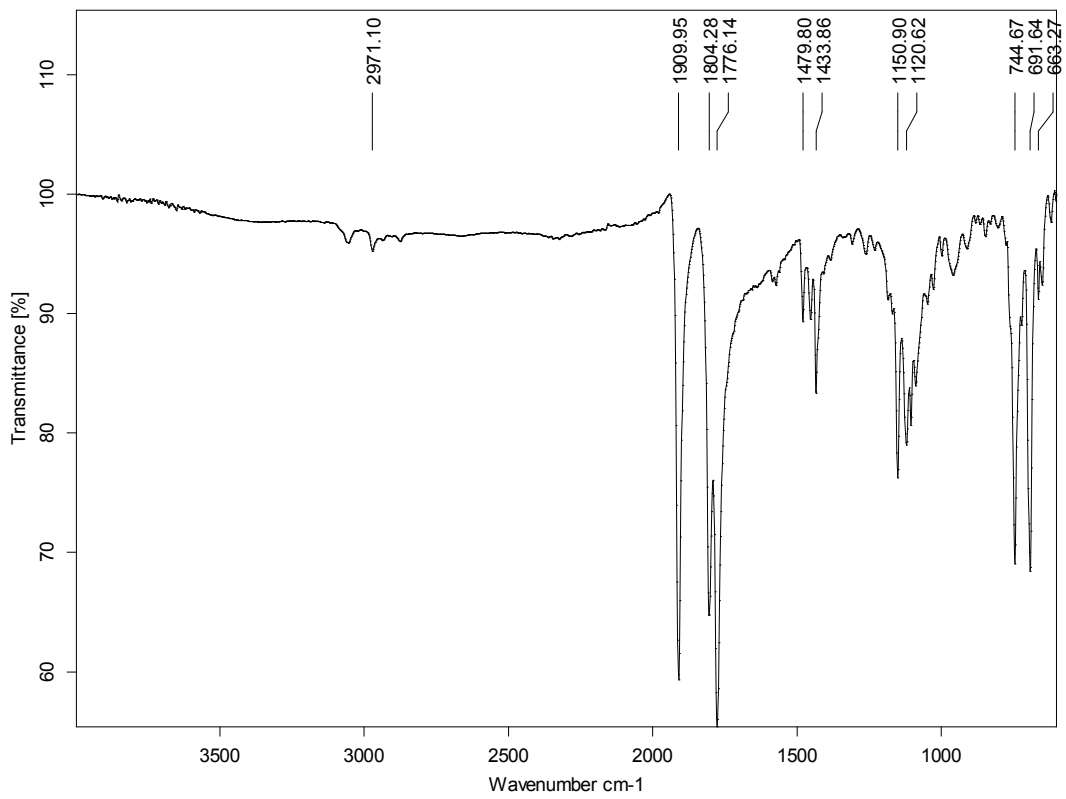
**Annex 2.3.** IR spectrum of SODPdiphos, **L3**



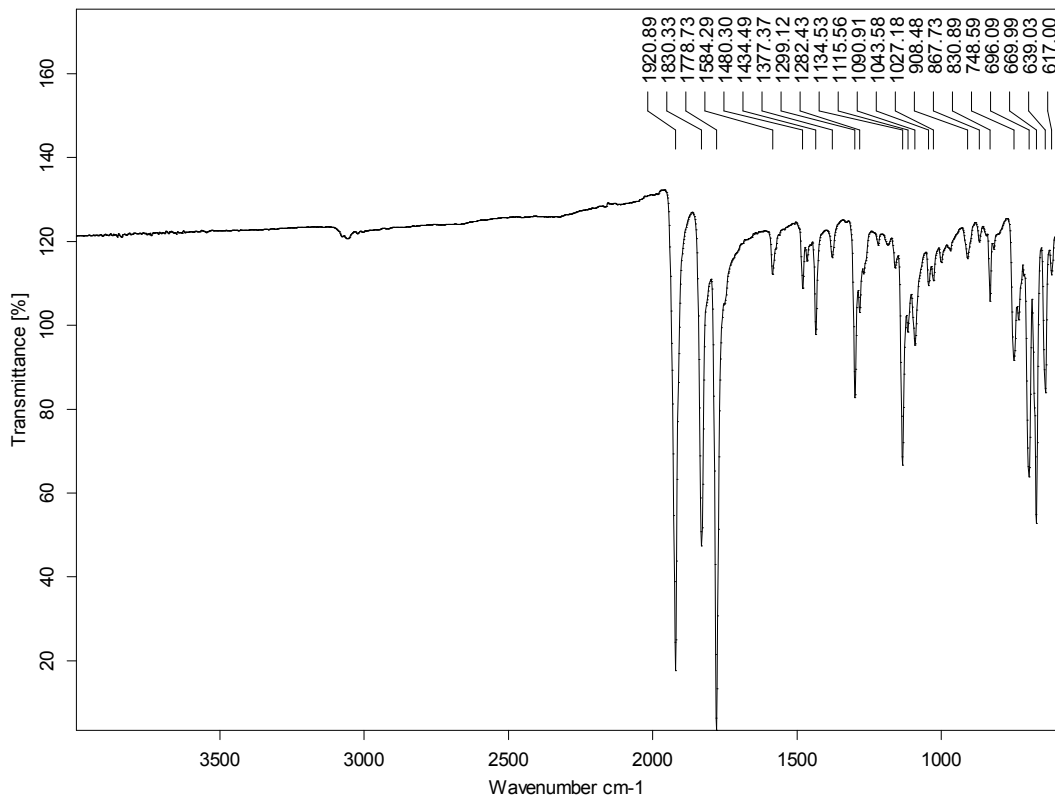
**Annex 2.4.** IR spectrum of SODPdiphos oxide, **L3O<sub>2</sub>**



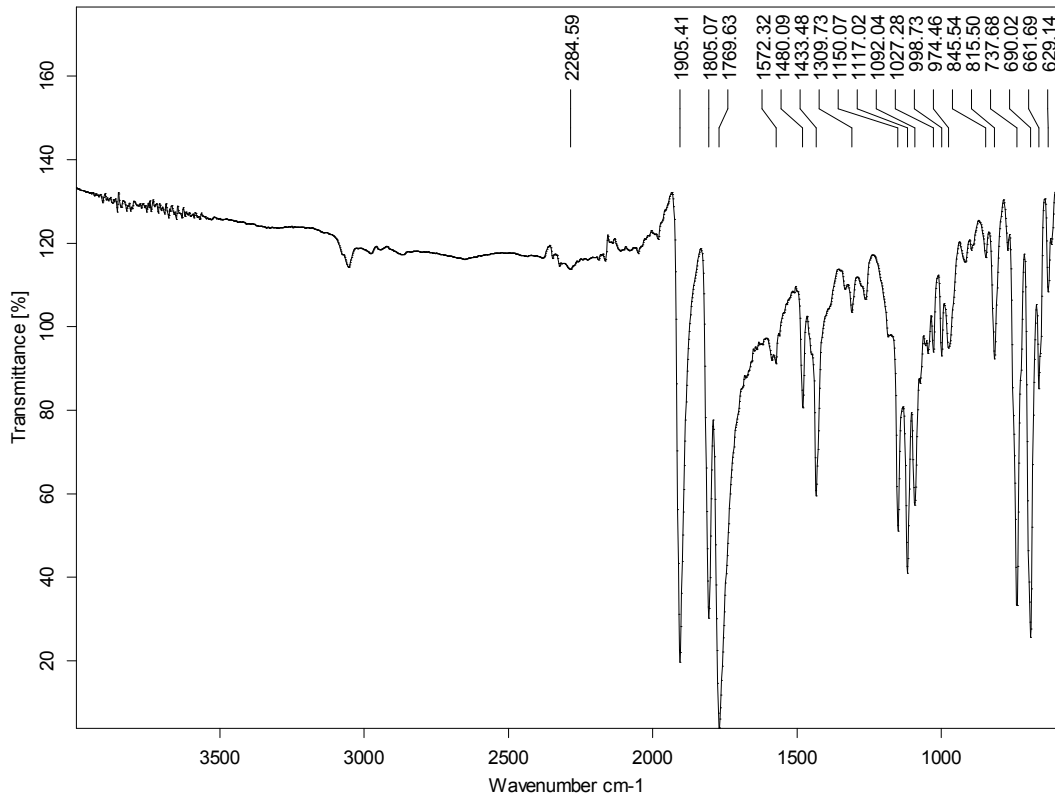
**Annex 2.5.** IR spectrum of  $[\text{Mo}(\text{TPOdiphos})(\text{CO})_3]$



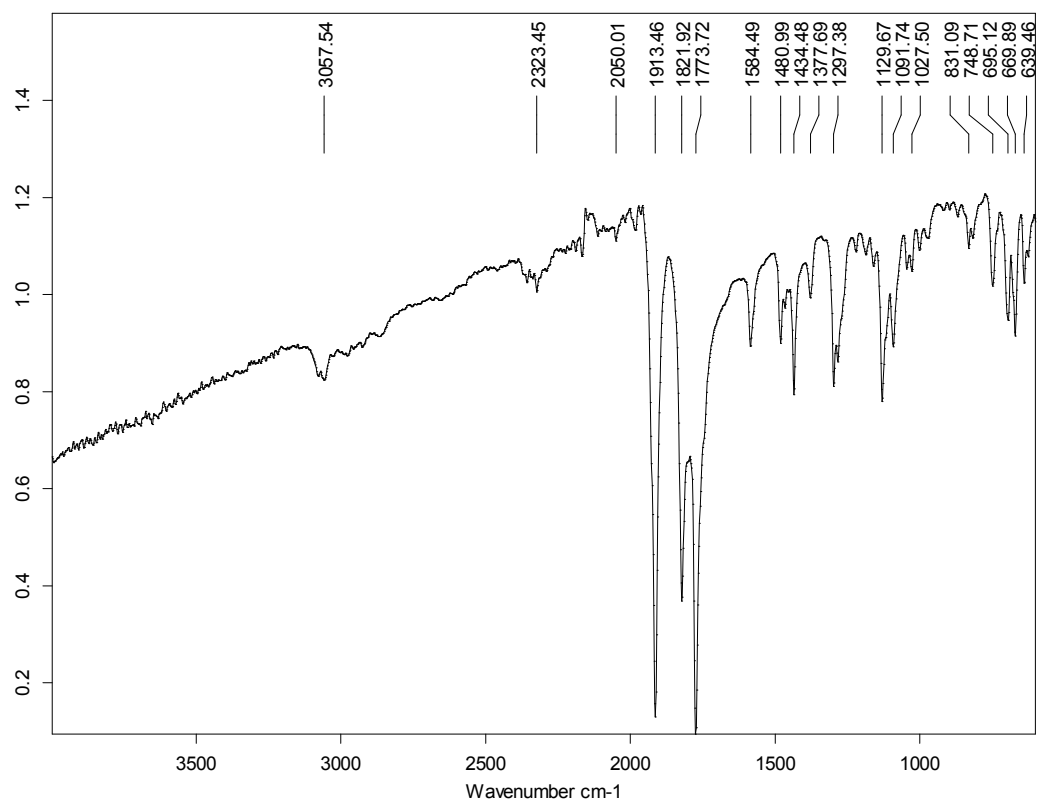
**Annex 2.5.** IR spectrum of  $[\text{Mo}(\text{DPPrPOdiphos})(\text{CO})_3]$



**Annex 2.6.** IR spectrum of  $[\text{Mo}(\text{SODPdiphos})(\text{CO})_3]$



**Annex 2.7.** IR spectrum of  $[\text{W}(\text{TPOdiphos})(\text{CO})_3]$

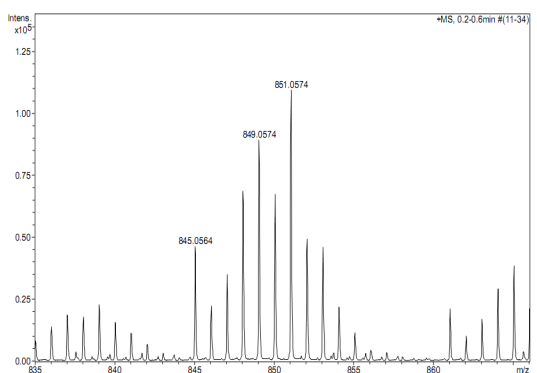


**Annex 2.7.** IR spectrum of  $[\text{W}(\text{SODPdiphos})(\text{CO})_3]$

### ANNEX III. HRMS-ESI<sup>+</sup> Spectra

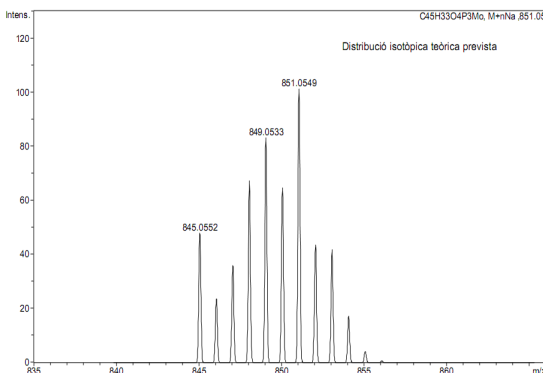
**Annex 3.1.** Experimental and Calculated High Resolution Mass Spectra of *fac*-[Mo(TPOdiphos)(CO)<sub>3</sub>]

#### 3.1.a. Experimental



#	m/z	I	I %
1	845.0564	46462	42.5
2	846.0614	22635	20.7
3	847.0565	35123	32.1
4	848.0577	68706	62.8
5	849.0574	89421	81.7
6	850.0592	67647	61.8
7	851.0574	109446	100.0
8	852.0631	49566	45.3
9	853.0600	46202	42.2
10	854.0659	22158	20.2
11	855.0609	11689	10.7
12	856.0692	4110	3.8

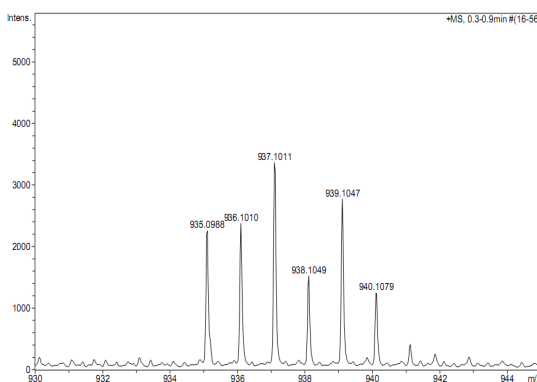
#### 3.1.b. Calculated



#	m/z	I	I %
1	845.0552	47	47.4
2	846.0586	23	23.3
3	847.0536	36	35.5
4	848.0543	66	66.4
5	849.0533	82	82.1
6	850.0546	64	63.8
7	851.0549	100	100.0
8	852.0572	43	43.1
9	853.0560	41	41.4
10	854.0592	17	17.0
11	855.0626	4	4.1
12	856.0659	1	0.7

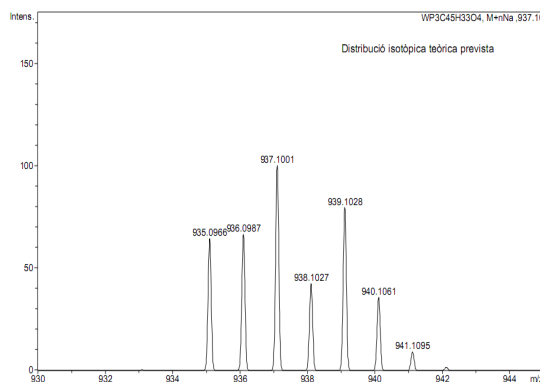
**Annex 3.2.** Experimental and Calculated High Resolution Mass Spectra of [W(TPOdiphos)(CO)<sub>3</sub>]

#### 3.2.a. Experimental



#	m/z	I	I %
1	935.0988	2269	67.4
2	936.1010	2384	70.9
3	937.1011	3365	100.0
4	938.1049	1528	45.4
5	939.1047	2775	82.5
6	940.1079	1264	37.6

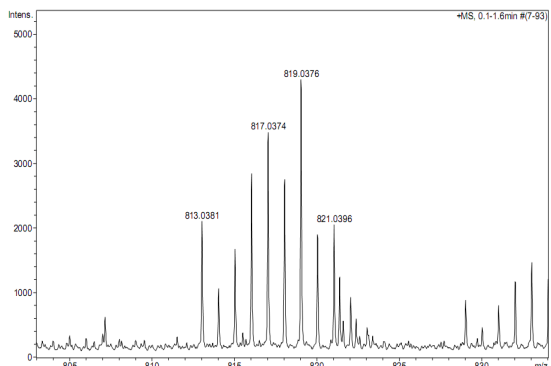
#### 3.2.b. Calculated



#	m/z	I	I %
1	935.0966	65	64.6
2	936.0987	67	66.7
3	937.1001	100	100.0
4	938.1027	43	42.6
5	939.1028	80	79.7
6	940.1061	36	35.9

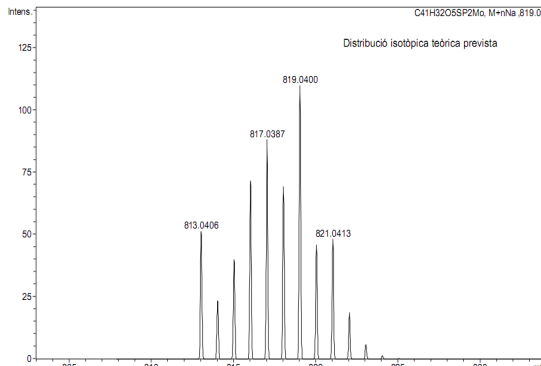
**Annex 3.3. Experimental and Calculated High Resolution Mass Spectra of [Mo(SODPdiphos)(CO)<sub>3</sub>]**

**3.5.a. Experimental**



#	m/z	I	I %
1	813.0381	2108	49.0
2	814.0419	1069	24.8
3	815.0382	1679	39.0
4	816.0385	2845	66.1
5	817.0374	3486	81.0
6	818.0380	2756	64.1
7	819.0376	4302	100.0
8	820.0398	1907	44.3
9	821.0396	2054	47.7
10	821.3751	1250	29.1
11	822.0458	935	21.7
12	822.3789	601	14.0

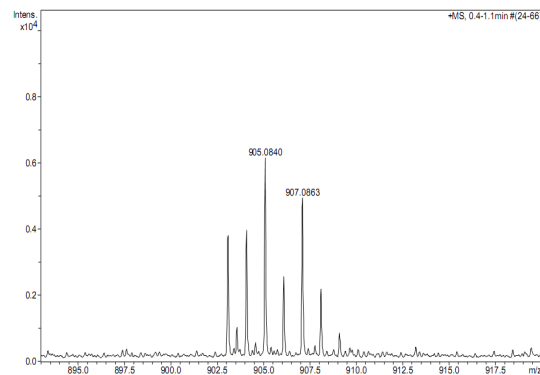
**3.5.b. Calculated**



#	m/z	I	I %
1	813.0406	47	46.6
2	814.0440	21	21.3
3	815.0389	36	36.4
4	816.0397	65	65.2
5	817.0387	80	80.2
6	818.0399	63	63.0
7	819.0400	100	100.0
8	820.0426	42	41.9
9	821.0413	44	43.8
10	822.0446	17	17.1
11	823.0479	5	5.4
12	824.0404	1	1.3

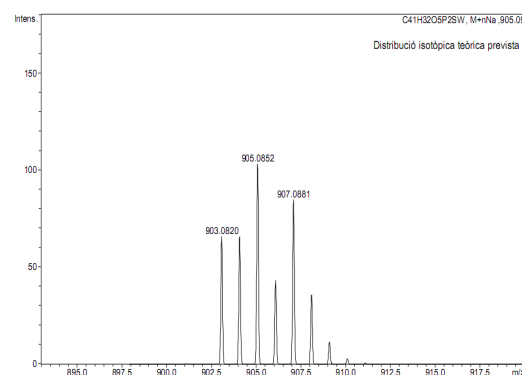
**Annex 3.4. Experimental and Calculated High Resolution Mass Spectra of [W(SODPdiphos)(CO)<sub>3</sub>]**

**3.6.a. Experimental**



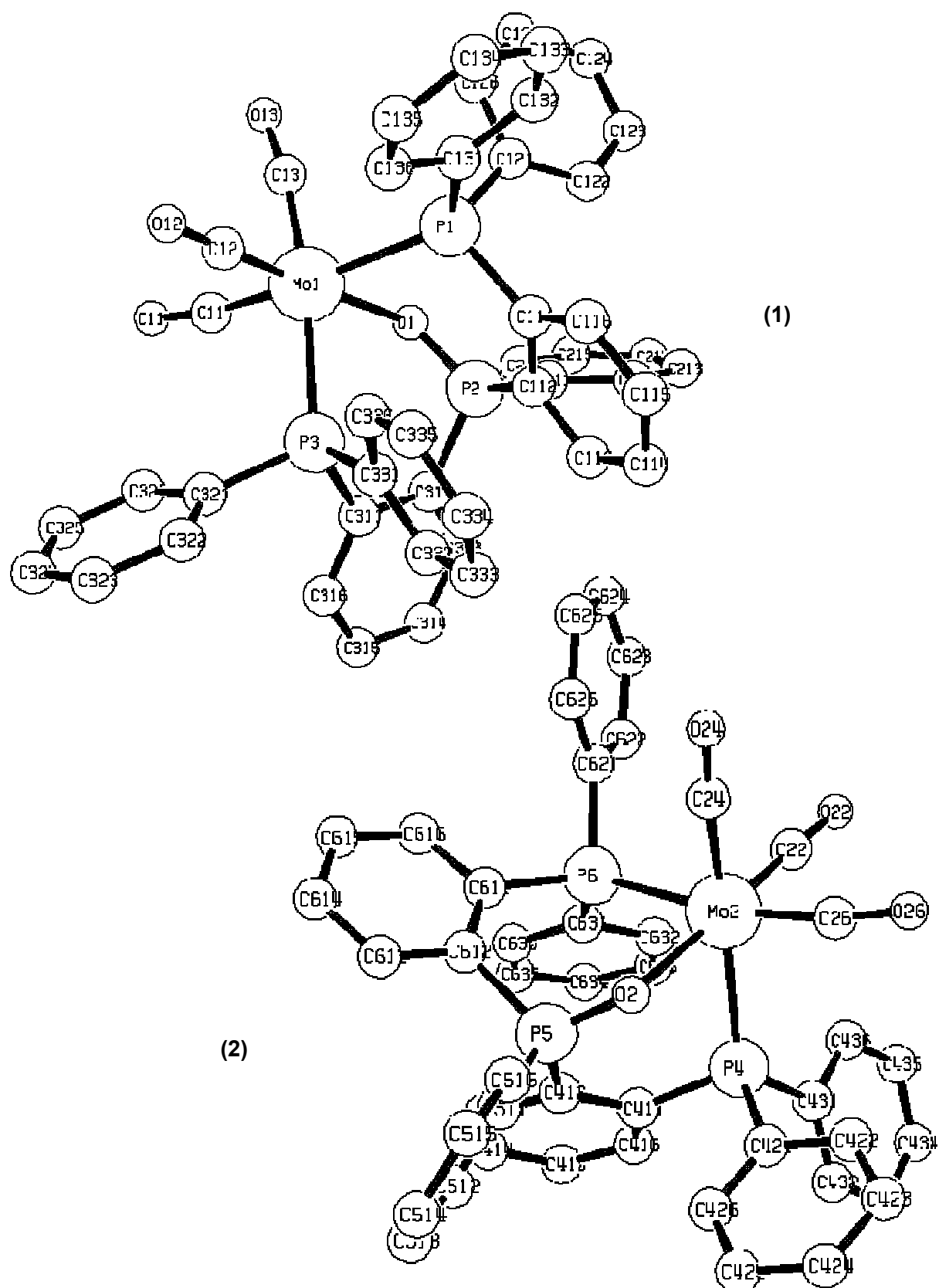
#	m/z	I	I %
1	903.0808	3614	58.7
2	904.0825	3785	61.5
3	905.0840	6158	100.0
4	906.0858	2372	38.5
5	907.0863	4753	77.2
6	908.0886	2000	32.5
7	909.0919	669	10.9

**3.6.b. Calculated**



#	m/z	I	I %
1	903.0820	64	64.1
2	904.0841	64	63.9
3	905.0852	100	100.0
4	906.0881	42	41.9
5	907.0881	82	82.3
6	908.0915	35	34.7
7	909.0948	11	11.4

ANNEX IV. Crystallographic Data, CIF file for *fac*-[Mo(TPOdiphos)(CO)<sub>3</sub>]



#\#CIF\_1.1

```

# CIF produced by WinGX routine CIF_UPDATE
# Created on 2007-07-14 at 12:51:17
# Using CIFtbx version 2.6.2 16 Jun 1998

# Dictionary name : cif_core.dic
# Dictionary vers : 2.3
# Request file   : c:\wingx\files\archive.dat
# CIF files read : kml1 struct

data_kml1

_audit_creation_date          2007-07-14T12:51:17-00:00
_audit_creation_method         'WinGX routine CIF_UPDATE'
_audit_conform_dict_name       cif_core.dic
_audit_conform_dict_version    2.3
_audit_conform_dict_location   ftp://ftp.iucr.org/pub/cif_core.dic
_publ_requested_category       FM

#-----#
#           CHEMICAL INFORMATION
#-----#

_chemical_name_systematic
;
?
;
_chemical_formula_moiety      'C45 H35 Mo1 O4 P3'
_chemical_formula_sum          'C45 H35 Mo O4 P3'
_chemical_formula_weight       828.58
_chemical_compound_source     'synthesis as described'

#-----#
#           UNIT CELL INFORMATION
#-----#

_symmetry_cell_setting        monoclinic
_symmetry_space_group_name_H-M 'P 21/a'
_symmetry_space_group_name_Hall '-P 2yab'
_symmetry_Int_Tables_number   14
loop_
    _symmetry_equiv_pos_as_xyz
'x, y, z'
'-x+1/2, y+1/2, -z'
'-x, -y, -z'
'x-1/2, -y-1/2, z'

_cell_length_a                19.7966(14)
_cell_length_b                9.8803(7)
_cell_length_c                39.196(3)
_cell_angle_alpha              90
_cell_angle_beta              95.880(2)
_cell_angle_gamma              90
_cell_volume                  7626.3(10)
_cell_formula_units_Z          8
_cell_measurement_temperature  293(2)
_cell_measurement_reflns_used 0
_cell_measurement_theta_min    0
_cell_measurement_theta_max    0
_cell_measurement_wavelength   0.71073

#-----#
#           CRYSTAL INFORMATION
#-----#

_exptl_crystal_description     prism

```

```

_exptl_crystal_colour          orange
_exptl_crystal_size_max        0.18
_exptl_crystal_size_mid        0.13
_exptl_crystal_size_min        0.12
_exptl_crystal_density_diffrn 1.443
_exptl_crystal_density_method  'not measured'
_exptl_crystal_F_000           3392
_exptl_special_details
;
?
;

#-----#
#          ABSORPTION CORRECTION #
#-----#


_exptl_absorpt_coefficient_mu 0.514
_exptl_absorpt_correction_type none

#-----#
#          DATA COLLECTION #
#-----#


_diffrn_ambient_temperature    293(2)
_diffrn_radiation_wavelength   0.71073
_diffrn_radiation_type         MoK\alpha
_diffrn_radiation_monochromator graphite
_diffrn_radiation_probe        x-ray
_diffrn_reflns_av_R_equivalents 0.1414
_diffrn_reflns_av_unetI/netI   0.2194
_diffrn_reflns_number          51199
_diffrn_reflns_limit_h_min     -26
_diffrn_reflns_limit_h_max     24
_diffrn_reflns_limit_k_min     -13
_diffrn_reflns_limit_k_max     13
_diffrn_reflns_limit_l_min     -53
_diffrn_reflns_limit_l_max     46
_diffrn_reflns_theta_min       1.57
_diffrn_reflns_theta_max       29.11
_diffrn_reflns_theta_full      29.11
_diffrn_measured_fraction_theta_full 0.91
_diffrn_measured_fraction_theta_max 0.91
_reflns_number_total          18654
_reflns_number_gt              7583
_reflns_threshold_expression   >2sigma(I)

#-----#
#          COMPUTER PROGRAMS USED #
#-----#


_computing_structure_solution  'SHELXS-86 (Sheldrick, 1986)'
_computing_structure_refinement 'SHELXL-97 (Sheldrick, 1997)'
_computing_molecular_graphics   'Ortep-3 for Windows (Farrugia, 1997)'
_computing_publication_material 'WinGX publication routines (Farrugia, 1999)'

#-----#
#          REFINEMENT INFORMATION #
#-----#


_refine_special_details
;

Refinement of F^2^ against ALL reflections. The weighted R-factor wR and
goodness of fit S are based on F^2^, conventional R-factors R are based
on F, with F set to zero for negative F^2^. The threshold expression of
F^2^ > 2sigma(F^2^) is used only for calculating R-factors(gt) etc. and is

```

not relevant to the choice of reflections for refinement. R-factors based on F<sup>2</sup> are statistically about twice as large as those based on F, and R-factors based on ALL data will be even larger.

```
;
_refine_ls_structure_factor_coef      Fsqd
_refine_ls_matrix_type               full
_refine_ls_weighting_scheme         calc
_refine_ls_weighting_details
'calc w=1/[s^2^(Fo^2^)+(0.0854P)^2^+7.9807P] where P=(Fo^2^+2Fc^2^)/3'
_atom_sites_solution_primary        direct
_atom_sites_solution_secondary     difmap
_atom_sites_solution_hydrogens     geom
_refine_ls_hydrogen_treatment       mixed
_refine_ls_extinction_method       none
_refine_ls_number_reflns           18654
_refine_ls_number_parameters        955
_refine_ls_number_restraints       0
_refine_ls_R_factor_all            0.2143
_refine_ls_R_factor_gt              0.0795
_refine_ls_wR_factor_ref           0.219
_refine_ls_wR_factor_gt             0.16
_refine_ls_goodness_of_fit_ref     0.867
_refine_ls_restrained_S_all        0.867
_refine_ls_shift/su_max            0.059
_refine_ls_shift/su_mean           0.004
_refine_diff_density_max           0.877
_refine_diff_density_min           -1.355
_refine_diff_density_rms           0.096

#-----#
#          ATOMIC TYPES, COORDINATES AND THERMAL PARAMETERS #
#-----#
```

loop\_
  \_atom\_type\_symbol
  \_atom\_type\_description
  \_atom\_type\_scat\_dispersion\_real
  \_atom\_type\_scat\_dispersion\_imag
  \_atom\_type\_scat\_source
C C 0.0033 0.0016 'International Tables Vol C Tables 4.2.6.8 and 6.1.1.4'
H H 0 0 'International Tables Vol C Tables 4.2.6.8 and 6.1.1.4'
Mo Mo -1.6832 0.6857 'International Tables Vol C Tables 4.2.6.8 and 6.1.1.4'
O O 0.0106 0.006 'International Tables Vol C Tables 4.2.6.8 and 6.1.1.4'
P P 0.1023 0.0942 'International Tables Vol C Tables 4.2.6.8 and 6.1.1.4'

loop\_
  \_atom\_site\_label
  \_atom\_site\_type\_symbol
  \_atom\_site\_fract\_x
  \_atom\_site\_fract\_y
  \_atom\_site\_fract\_z
  \_atom\_site\_U\_iso\_or\_equiv
  \_atom\_site\_adp\_type
  \_atom\_site\_occupancy
  \_atom\_site\_symmetry\_multiplicity
  \_atom\_site\_calc\_flag
  \_atom\_site\_refinement\_flags
  \_atom\_site\_disorder\_assembly
  \_atom\_site\_disorder\_group

Mo1	Mo	0.10065(3)	0.27287(6)	0.119198(16)	0.04196(19)	Uani	1	1	d	.	.	.
Mo2	Mo	0.28649(3)	0.54472(6)	0.379096(16)	0.04184(18)	Uani	1	1	d	.	.	.
P1	P	0.20852(11)	0.22043(19)	0.09046(5)	0.0464(5)	Uani	1	1	d	.	.	.
P2	P	0.10340(11)	-0.04805(18)	0.09148(5)	0.0469(5)	Uani	1	1	d	.	.	.
P3	P	0.11836(11)	0.10075(19)	0.16839(5)	0.0463(5)	Uani	1	1	d	.	.	.
P4	P	0.32092(10)	0.36346(18)	0.33753(5)	0.0440(5)	Uani	1	1	d	.	.	.

P5 P	0.43965(11)	0.60605(18)	0.35273(5)	0.0436(5)	Uani	1	1	d	.	.	.
P6 P	0.38369(10)	0.51090(18)	0.42619(5)	0.0429(5)	Uani	1	1	d	.	.	.
O1 O	0.0754(2)	0.0917(4)	0.08490(11)	0.0448(12)	Uani	1	1	d	.	.	.
O2 O	0.3654(2)	0.6365(4)	0.34803(12)	0.0466(12)	Uani	1	1	d	.	.	.
C11 C	0.0118(4)	0.3147(7)	0.1319(2)	0.051(2)	Uani	1	1	d	.	.	.
C12 C	0.1326(4)	0.4192(7)	0.14803(19)	0.052(2)	Uani	1	1	d	.	.	.
C13 C	0.0738(4)	0.4085(7)	0.08481(19)	0.055(2)	Uani	1	1	d	.	.	.
C22 C	0.2262(4)	0.4553(8)	0.4064(2)	0.058(2)	Uani	1	1	d	.	.	.
C24 C	0.2633(4)	0.7108(8)	0.40216(19)	0.053(2)	Uani	1	1	d	.	.	.
C26 C	0.2035(5)	0.5767(8)	0.3501(2)	0.056(2)	Uani	1	1	d	.	.	.
O11 O	-0.0411(3)	0.3577(6)	0.13774(17)	0.0789(19)	Uani	1	1	d	.	.	.
O12 O	0.1513(3)	0.5124(6)	0.16544(16)	0.0826(19)	Uani	1	1	d	.	.	.
O13 O	0.0528(4)	0.4946(6)	0.06683(16)	0.090(2)	Uani	1	1	d	.	.	.
O22 O	0.1859(3)	0.4037(6)	0.42223(17)	0.0845(19)	Uani	1	1	d	.	.	.
O24 O	0.2443(4)	0.8069(6)	0.41497(16)	0.089(2)	Uani	1	1	d	.	.	.
O26 O	0.1479(3)	0.5931(7)	0.33686(18)	0.094(2)	Uani	1	1	d	.	.	.
C111 C	0.2394(4)	0.0477(7)	0.10005(18)	0.0489(19)	Uani	1	1	d	.	.	.
C112 C	0.1927(4)	-0.0602(7)	0.10213(18)	0.0449(18)	Uani	1	1	d	.	.	.
C113 C	0.2175(5)	-0.1874(8)	0.1125(2)	0.060(2)	Uani	1	1	d	.	.	.
H113 H	0.1868	-0.2577	0.1143	0.072	Uiso	1	1	calc	R	.	.
C114 C	0.2850(5)	-0.2124(9)	0.1199(2)	0.076(3)	Uani	1	1	d	.	.	.
H114 H	0.3005	-0.2982	0.1266	0.091	Uiso	1	1	calc	R	.	.
C115 C	0.3304(5)	-0.1062(9)	0.1173(3)	0.079(3)	Uani	1	1	d	.	.	.
H115 H	0.3768	-0.1217	0.1219	0.095	Uiso	1	1	calc	R	.	.
C116 C	0.3077(5)	0.0205(8)	0.1082(2)	0.067(2)	Uani	1	1	d	.	.	.
H116 H	0.339	0.0903	0.1073	0.081	Uiso	1	1	calc	R	.	.
C121 C	0.1953(4)	0.2169(7)	0.04343(19)	0.0485(19)	Uani	1	1	d	.	.	.
C122 C	0.2039(4)	0.1025(8)	0.0242(2)	0.063(2)	Uani	1	1	d	.	.	.
H122 H	0.2182	0.0224	0.0351	0.076	Uiso	1	1	calc	R	.	.
C123 C	0.1915(5)	0.1061(10)	-0.0111(2)	0.078(3)	Uani	1	1	d	.	.	.
H123 H	0.1953	0.0264	-0.0234	0.094	Uiso	1	1	calc	R	.	.
C124 C	0.1741(5)	0.2213(10)	-0.0284(2)	0.078(3)	Uani	1	1	d	.	.	.
H124 H	0.1669	0.2224	-0.0522	0.094	Uiso	1	1	calc	R	.	.
C125 C	0.1675(5)	0.3363(10)	-0.0096(2)	0.077(3)	Uani	1	1	d	.	.	.
H125 H	0.156	0.4173	-0.0208	0.093	Uiso	1	1	calc	R	.	.
C126 C	0.1774(5)	0.3343(8)	0.0257(2)	0.063(2)	Uani	1	1	d	.	.	.
H126 H	0.1719	0.4138	0.0379	0.076	Uiso	1	1	calc	R	.	.
C131 C	0.2864(4)	0.3216(7)	0.0982(2)	0.052(2)	Uani	1	1	d	.	.	.
C132 C	0.3367(5)	0.3223(8)	0.0758(2)	0.067(2)	Uani	1	1	d	.	.	.
H132 H	0.3296	0.2751	0.0553	0.081	Uiso	1	1	calc	R	.	.
C133 C	0.3954(5)	0.3900(9)	0.0833(3)	0.073(3)	Uani	1	1	d	.	.	.
H133 H	0.428	0.3905	0.0678	0.087	Uiso	1	1	calc	R	.	.
C134 C	0.4071(5)	0.4580(8)	0.1138(3)	0.078(3)	Uani	1	1	d	.	.	.
H134 H	0.4478	0.5041	0.1191	0.094	Uiso	1	1	calc	R	.	.
C135 C	0.3589(4)	0.4583(8)	0.1365(2)	0.066(2)	Uani	1	1	d	.	.	.
H135 H	0.3674	0.5033	0.1574	0.079	Uiso	1	1	calc	R	.	.
C136 C	0.2975(4)	0.3919(7)	0.1287(2)	0.059(2)	Uani	1	1	d	.	.	.
H136 H	0.2642	0.3947	0.1438	0.07	Uiso	1	1	calc	R	.	.
C211 C	0.0824(4)	-0.1488(7)	0.05348(19)	0.051(2)	Uani	1	1	d	.	.	.
C212 C	0.1300(5)	-0.2288(8)	0.0391(2)	0.070(3)	Uani	1	1	d	.	.	.
H212 H	0.1739	-0.237	0.0499	0.084	Uiso	1	1	calc	R	.	.
C213 C	0.1114(6)	-0.2957(9)	0.0088(2)	0.079(3)	Uani	1	1	d	.	.	.
H213 H	0.1431	-0.3495	-0.0007	0.094	Uiso	1	1	calc	R	.	.
C214 C	0.0485(6)	-0.2850(10)	-0.0073(2)	0.081(3)	Uani	1	1	d	.	.	.
H214 H	0.0367	-0.3325	-0.0275	0.097	Uiso	1	1	calc	R	.	.
C215 C	0.0020(5)	-0.2044(10)	0.0060(2)	0.083(3)	Uani	1	1	d	.	.	.
H215 H	-0.0414	-0.1959	-0.0053	0.1	Uiso	1	1	calc	R	.	.
C216 C	0.0195(5)	-0.1347(9)	0.0365(2)	0.077(3)	Uani	1	1	d	.	.	.
H216 H	-0.0121	-0.0782	0.0453	0.092	Uiso	1	1	calc	R	.	.
C311 C	0.0732(4)	-0.0604(7)	0.16044(19)	0.0467(18)	Uani	1	1	d	.	.	.
C312 C	0.0696(4)	-0.1245(6)	0.12786(19)	0.0451(18)	Uani	1	1	d	.	.	.
C313 C	0.0368(4)	-0.2497(7)	0.1235(2)	0.056(2)	Uani	1	1	d	.	.	.
H313 H	0.0351	-0.2933	0.1024	0.067	Uiso	1	1	calc	R	.	.
C314 C	0.0073(4)	-0.3089(8)	0.1496(2)	0.066(2)	Uani	1	1	d	.	.	.
H314 H	-0.0139	-0.3926	0.1463	0.079	Uiso	1	1	calc	R	.	.
C315 C	0.0087(5)	-0.2459(8)	0.1806(2)	0.073(3)	Uani	1	1	d	.	.	.
H315 H	-0.0127	-0.2854	0.1982	0.088	Uiso	1	1	calc	R	.	.
C316 C	0.0418(5)	-0.1237(8)	0.1860(2)	0.068(2)	Uani	1	1	d	.	.	.

H316	H	0.0429	-0.0828	0.2074	0.081	Uiso	1	1	calc	R	.	.
C321	C	0.0872(4)	0.1565(7)	0.20876(19)	0.0480(19)	Uani	1	1	d	.	.	.
C322	C	0.1271(5)	0.1562(8)	0.2397(2)	0.063(2)	Uani	1	1	d	.	.	.
H322	H	0.1719	0.1268	0.2407	0.076	Uiso	1	1	calc	R	.	.
C323	C	0.1007(5)	0.1998(9)	0.2696(2)	0.074(3)	Uani	1	1	d	.	.	.
H323	H	0.1284	0.1981	0.2902	0.089	Uiso	1	1	calc	R	.	.
C324	C	0.0368(5)	0.2439(9)	0.2692(2)	0.071(3)	Uani	1	1	d	.	.	.
H324	H	0.02	0.2739	0.2892	0.085	Uiso	1	1	calc	R	.	.
C325	C	-0.0029(5)	0.2436(10)	0.2389(2)	0.087(3)	Uani	1	1	d	.	.	.
H325	H	-0.0474	0.2746	0.2383	0.105	Uiso	1	1	calc	R	.	.
C326	C	0.0205(5)	0.1987(10)	0.2086(2)	0.080(3)	Uani	1	1	d	.	.	.
H326	H	-0.0085	0.197	0.1884	0.096	Uiso	1	1	calc	R	.	.
C331	C	0.2040(4)	0.0460(8)	0.18462(19)	0.054(2)	Uani	1	1	d	.	.	.
C332	C	0.2212(5)	-0.0841(8)	0.1951(2)	0.078(3)	Uani	1	1	d	.	.	.
H332	H	0.1891	-0.1531	0.1935	0.093	Uiso	1	1	calc	R	.	.
C333	C	0.2888(7)	-0.1091(12)	0.2081(3)	0.109(4)	Uani	1	1	d	.	.	.
H333	H	0.3012	-0.1961	0.2153	0.13	Uiso	1	1	calc	R	.	.
C334	C	0.3362(6)	-0.0112(15)	0.2104(3)	0.107(4)	Uani	1	1	d	.	.	.
H334	H	0.3806	-0.0312	0.2189	0.129	Uiso	1	1	calc	R	.	.
C335	C	0.3192(6)	0.1161(14)	0.2004(3)	0.103(4)	Uani	1	1	d	.	.	.
H335	H	0.3516	0.1845	0.2023	0.124	Uiso	1	1	calc	R	.	.
C336	C	0.2542(5)	0.1433(10)	0.1876(2)	0.074(3)	Uani	1	1	d	.	.	.
H336	H	0.2431	0.2311	0.1805	0.089	Uiso	1	1	calc	R	.	.
C411	C	0.4117(4)	0.3239(7)	0.34541(17)	0.0415(17)	Uani	1	1	d	.	.	.
C412	C	0.4605(4)	0.4269(7)	0.35244(18)	0.0420(17)	Uani	1	1	d	.	.	.
C413	C	0.5280(4)	0.3959(8)	0.36220(19)	0.055(2)	Uani	1	1	d	.	.	.
H413	H	0.5596	0.4653	0.3663	0.066	Uiso	1	1	calc	R	.	.
C414	C	0.5488(4)	0.2621(8)	0.3658(2)	0.059(2)	Uani	1	1	d	.	.	.
H414	H	0.594	0.2415	0.3728	0.071	Uiso	1	1	calc	R	.	.
C415	C	0.5024(5)	0.1609(8)	0.3592(2)	0.061(2)	Uani	1	1	d	.	.	.
H415	H	0.5163	0.0711	0.3613	0.074	Uiso	1	1	calc	R	.	.
C416	C	0.4351(4)	0.1904(7)	0.34929(19)	0.053(2)	Uani	1	1	d	.	.	.
H416	H	0.4044	0.1196	0.3451	0.063	Uiso	1	1	calc	R	.	.
C421	C	0.3123(4)	0.4221(7)	0.29300(17)	0.0436(18)	Uani	1	1	d	.	.	.
C422	C	0.2471(5)	0.4414(8)	0.2776(2)	0.065(2)	Uani	1	1	d	.	.	.
H422	H	0.2108	0.4237	0.2903	0.078	Uiso	1	1	calc	R	.	.
C423	C	0.2337(5)	0.4860(10)	0.2442(2)	0.078(3)	Uani	1	1	d	.	.	.
H423	H	0.1893	0.4977	0.2344	0.093	Uiso	1	1	calc	R	.	.
C424	C	0.2874(6)	0.5127(9)	0.2257(2)	0.082(3)	Uani	1	1	d	.	.	.
H424	H	0.2792	0.5418	0.2031	0.099	Uiso	1	1	calc	R	.	.
C425	C	0.3523(5)	0.4971(10)	0.2400(2)	0.076(3)	Uani	1	1	d	.	.	.
H425	H	0.3885	0.5168	0.2275	0.092	Uiso	1	1	calc	R	.	.
C426	C	0.3643(5)	0.4505(8)	0.27416(19)	0.064(2)	Uani	1	1	d	.	.	.
H426	H	0.4087	0.4392	0.2839	0.077	Uiso	1	1	calc	R	.	.
C431	C	0.2820(4)	0.1969(7)	0.3324(2)	0.053(2)	Uani	1	1	d	.	.	.
C432	C	0.2900(5)	0.1137(8)	0.3052(2)	0.070(3)	Uani	1	1	d	.	.	.
H432	H	0.3158	0.1434	0.2882	0.084	Uiso	1	1	calc	R	.	.
C433	C	0.2609(5)	-0.0118(9)	0.3024(3)	0.084(3)	Uani	1	1	d	.	.	.
H433	H	0.2658	-0.0652	0.2832	0.101	Uiso	1	1	calc	R	.	.
C434	C	0.2246(6)	-0.0588(10)	0.3279(3)	0.095(4)	Uani	1	1	d	.	.	.
H434	H	0.2065	-0.1457	0.3265	0.114	Uiso	1	1	calc	R	.	.
C435	C	0.2149(5)	0.0206(10)	0.3552(3)	0.093(3)	Uani	1	1	d	.	.	.
H435	H	0.189	-0.0109	0.3721	0.112	Uiso	1	1	calc	R	.	.
C436	C	0.2442(4)	0.1519(8)	0.3581(2)	0.060(2)	Uani	1	1	d	.	.	.
H436	H	0.2382	0.2067	0.3768	0.072	Uiso	1	1	calc	R	.	.
C511	C	0.4788(4)	0.6902(7)	0.31890(18)	0.049(2)	Uani	1	1	d	.	.	.
C512	C	0.5331(5)	0.6427(9)	0.3034(2)	0.071(3)	Uani	1	1	d	.	.	.
H512	H	0.551	0.5579	0.3093	0.085	Uiso	1	1	calc	R	.	.
C513	C	0.5618(5)	0.7191(11)	0.2790(2)	0.082(3)	Uani	1	1	d	.	.	.
H513	H	0.5986	0.6862	0.2687	0.099	Uiso	1	1	calc	R	.	.
C514	C	0.5350(7)	0.8441(12)	0.2704(2)	0.091(4)	Uani	1	1	d	.	.	.
H514	H	0.5545	0.8963	0.2543	0.11	Uiso	1	1	calc	R	.	.
C515	C	0.4805(6)	0.8931(10)	0.2850(3)	0.091(3)	Uani	1	1	d	.	.	.
H515	H	0.4625	0.9773	0.2785	0.109	Uiso	1	1	calc	R	.	.
C516	C	0.4522(5)	0.8164(8)	0.3095(2)	0.075(3)	Uani	1	1	d	.	.	.
H516	H	0.4152	0.8496	0.3197	0.09	Uiso	1	1	calc	R	.	.
C611	C	0.4600(4)	0.6176(7)	0.42485(18)	0.0428(17)	Uani	1	1	d	.	.	.
C612	C	0.4817(4)	0.6622(7)	0.39362(18)	0.0440(18)	Uani	1	1	d	.	.	.

C613	C	0.5368(4)	0.7490(8)	0.3937(2)	0.056(2)	Uani	1	1	d	.	.	.
H613	H	0.5499	0.7806	0.373	0.068	Uiso	1	1	calc	R	.	.
C614	C	0.5724(4)	0.7890(8)	0.4239(2)	0.068(2)	Uani	1	1	d	.	.	.
H614	H	0.6099	0.8456	0.4237	0.082	Uiso	1	1	calc	R	.	.
C615	C	0.5522(4)	0.7446(8)	0.4546(2)	0.063(2)	Uani	1	1	d	.	.	.
H615	H	0.5754	0.7728	0.4752	0.076	Uiso	1	1	calc	R	.	.
C616	C	0.4976(4)	0.6584(8)	0.4548(2)	0.056(2)	Uani	1	1	d	.	.	.
H616	H	0.4857	0.6265	0.4756	0.068	Uiso	1	1	calc	R	.	.
C621	C	0.3557(4)	0.5591(7)	0.46772(18)	0.0474(19)	Uani	1	1	d	.	.	.
C622	C	0.3359(4)	0.4643(9)	0.4903(2)	0.066(2)	Uani	1	1	d	.	.	.
H622	H	0.3399	0.3728	0.4853	0.079	Uiso	1	1	calc	R	.	.
C623	C	0.3101(6)	0.5028(12)	0.5206(2)	0.092(3)	Uani	1	1	d	.	.	.
H623	H	0.2961	0.4371	0.5354	0.111	Uiso	1	1	calc	R	.	.
C624	C	0.3054(5)	0.6338(12)	0.5286(2)	0.083(3)	Uani	1	1	d	.	.	.
H624	H	0.2894	0.6589	0.5492	0.1	Uiso	1	1	calc	R	.	.
C625	C	0.3240(5)	0.7308(10)	0.5066(2)	0.075(3)	Uani	1	1	d	.	.	.
H625	H	0.3202	0.8219	0.512	0.091	Uiso	1	1	calc	R	.	.
C626	C	0.3483(4)	0.6944(8)	0.4764(2)	0.062(2)	Uani	1	1	d	.	.	.
H626	H	0.3601	0.7613	0.4614	0.074	Uiso	1	1	calc	R	.	.
C631	C	0.4172(4)	0.3410(7)	0.43526(17)	0.0437(18)	Uani	1	1	d	.	.	.
C632	C	0.3703(4)	0.2357(7)	0.4306(2)	0.059(2)	Uani	1	1	d	.	.	.
H632	H	0.3256	0.2547	0.4224	0.071	Uiso	1	1	calc	R	.	.
C633	C	0.3893(5)	0.1040(8)	0.4380(2)	0.074(3)	Uani	1	1	d	.	.	.
H633	H	0.3575	0.0345	0.4348	0.088	Uiso	1	1	calc	R	.	.
C634	C	0.4546(6)	0.0762(9)	0.4500(2)	0.078(3)	Uani	1	1	d	.	.	.
H634	H	0.467	-0.012	0.4561	0.094	Uiso	1	1	calc	R	.	.
C635	C	0.5019(5)	0.1753(10)	0.4530(2)	0.078(3)	Uani	1	1	d	.	.	.
H635	H	0.5471	0.1542	0.4597	0.093	Uiso	1	1	calc	R	.	.
C636	C	0.4831(5)	0.3084(8)	0.4463(2)	0.061(2)	Uani	1	1	d	.	.	.
H636	H	0.5156	0.3765	0.4492	0.074	Uiso	1	1	calc	R	.	.

loop\_

	_atom_site_aniso_label											
	_atom_site_aniso_U_11											
	_atom_site_aniso_U_22											
	_atom_site_aniso_U_33											
	_atom_site_aniso_U_23											
	_atom_site_aniso_U_13											
	_atom_site_aniso_U_12											
Mo1	0.0541(4)	0.0320(3)	0.0394(4)	-0.0021(3)	0.0030(3)	0.0009(3)						
Mo2	0.0501(4)	0.0382(3)	0.0374(4)	0.0044(3)	0.0053(3)	0.0057(3)						
P1	0.0568(13)	0.0380(10)	0.0442(11)	-0.0044(9)	0.0044(10)	-0.0038(10)						
P2	0.0577(13)	0.0335(10)	0.0490(12)	-0.0073(9)	0.0034(10)	-0.0004(10)						
P3	0.0562(13)	0.0379(10)	0.0436(11)	-0.0008(9)	-0.0004(10)	-0.0014(10)						
P4	0.0535(13)	0.0372(10)	0.0408(11)	0.0023(8)	0.0028(9)	0.0001(9)						
P5	0.0542(13)	0.0383(10)	0.0386(11)	0.0025(8)	0.0058(9)	-0.0028(10)						
P6	0.0554(13)	0.0386(10)	0.0349(10)	0.0028(8)	0.0060(9)	0.0024(9)						
O1	0.058(3)	0.032(2)	0.043(3)	-0.007(2)	-0.001(2)	0.003(2)						
O2	0.053(3)	0.044(3)	0.043(3)	0.007(2)	0.005(2)	0.005(2)						
C11	0.047(5)	0.043(4)	0.062(5)	-0.008(4)	0.006(4)	-0.002(4)						
C12	0.066(6)	0.043(4)	0.045(5)	-0.006(4)	-0.011(4)	0.008(4)						
C13	0.082(6)	0.038(4)	0.044(5)	0.002(4)	-0.005(4)	0.017(4)						
C22	0.072(6)	0.056(5)	0.051(5)	0.024(4)	0.024(4)	0.006(5)						
C24	0.069(6)	0.050(5)	0.041(4)	0.010(4)	0.005(4)	0.029(4)						
C26	0.064(6)	0.058(5)	0.047(5)	0.000(4)	0.004(4)	0.012(4)						
O11	0.061(4)	0.061(4)	0.116(5)	0.003(4)	0.016(4)	0.007(3)						
O12	0.096(5)	0.060(4)	0.086(5)	-0.024(3)	-0.022(4)	0.005(4)						
O13	0.132(6)	0.058(4)	0.078(4)	0.011(3)	0.000(4)	0.021(4)						
O22	0.075(5)	0.095(5)	0.087(5)	0.031(4)	0.027(4)	0.005(4)						
O24	0.132(6)	0.063(4)	0.074(4)	-0.001(3)	0.016(4)	0.042(4)						
O26	0.070(5)	0.108(5)	0.097(5)	0.004(4)	-0.023(4)	0.027(4)						
C111	0.065(6)	0.043(4)	0.037(4)	-0.006(3)	-0.001(4)	0.006(4)						
C112	0.055(5)	0.032(4)	0.048(4)	-0.002(3)	0.002(4)	0.002(4)						
C113	0.068(6)	0.042(4)	0.069(6)	0.004(4)	0.000(5)	0.000(4)						
C114	0.073(7)	0.062(6)	0.090(7)	0.001(5)	-0.004(6)	0.015(6)						
C115	0.066(7)	0.064(6)	0.106(8)	0.000(6)	-0.004(6)	0.013(5)						
C116	0.063(6)	0.053(5)	0.085(7)	-0.004(5)	0.003(5)	-0.003(5)						
C121	0.056(5)	0.044(4)	0.047(4)	-0.003(4)	0.011(4)	-0.008(4)						

C122	0.081 (6)	0.057 (5)	0.051 (5)	-0.013 (4)	0.010 (5)	0.001 (5)
C123	0.119 (9)	0.062 (6)	0.056 (6)	-0.018 (5)	0.016 (6)	-0.006 (6)
C124	0.099 (8)	0.093 (7)	0.045 (5)	-0.013 (5)	0.020 (5)	0.000 (6)
C125	0.102 (8)	0.080 (6)	0.051 (6)	0.023 (5)	0.015 (5)	0.001 (6)
C126	0.097 (7)	0.048 (5)	0.046 (5)	0.002 (4)	0.020 (5)	-0.002 (5)
C131	0.060 (5)	0.042 (4)	0.054 (5)	0.000 (4)	-0.001 (4)	-0.001 (4)
C132	0.083 (7)	0.065 (5)	0.059 (6)	-0.001 (4)	0.025 (5)	-0.014 (5)
C133	0.064 (6)	0.072 (6)	0.084 (7)	0.016 (5)	0.015 (5)	-0.025 (5)
C134	0.075 (7)	0.053 (5)	0.099 (8)	0.018 (5)	-0.022 (6)	-0.023 (5)
C135	0.059 (6)	0.058 (5)	0.077 (6)	0.001 (5)	-0.010 (5)	-0.005 (5)
C136	0.066 (6)	0.050 (5)	0.059 (5)	0.003 (4)	0.004 (4)	-0.011 (4)
C211	0.062 (6)	0.043 (4)	0.048 (5)	-0.010 (4)	0.008 (4)	-0.003 (4)
C212	0.086 (7)	0.055 (5)	0.070 (6)	-0.014 (5)	0.013 (5)	0.000 (5)
C213	0.110 (9)	0.062 (6)	0.068 (7)	-0.026 (5)	0.031 (6)	-0.007 (6)
C214	0.106 (9)	0.081 (7)	0.058 (6)	-0.028 (5)	0.019 (6)	-0.041 (7)
C215	0.074 (7)	0.105 (8)	0.068 (7)	-0.030 (6)	-0.008 (5)	-0.008 (6)
C216	0.081 (7)	0.082 (6)	0.067 (6)	-0.028 (5)	0.003 (5)	-0.002 (6)
C311	0.056 (5)	0.034 (4)	0.050 (5)	0.001 (3)	0.003 (4)	-0.005 (4)
C312	0.049 (5)	0.029 (4)	0.057 (5)	-0.001 (3)	0.004 (4)	0.003 (3)
C313	0.066 (6)	0.038 (4)	0.063 (5)	-0.008 (4)	0.009 (5)	-0.009 (4)
C314	0.072 (6)	0.035 (4)	0.090 (7)	0.001 (5)	0.006 (5)	-0.014 (4)
C315	0.095 (8)	0.061 (6)	0.063 (6)	0.012 (5)	0.005 (5)	-0.029 (5)
C316	0.082 (7)	0.060 (5)	0.061 (6)	-0.002 (4)	0.007 (5)	-0.012 (5)
C321	0.058 (5)	0.046 (4)	0.042 (4)	-0.003 (3)	0.013 (4)	0.007 (4)
C322	0.067 (6)	0.081 (6)	0.042 (5)	-0.010 (4)	0.005 (4)	0.007 (5)
C323	0.084 (7)	0.086 (7)	0.050 (6)	0.001 (5)	-0.003 (5)	-0.013 (6)
C324	0.094 (8)	0.067 (6)	0.053 (6)	-0.001 (4)	0.008 (5)	0.018 (5)
C325	0.085 (8)	0.123 (9)	0.058 (6)	0.017 (6)	0.021 (6)	0.041 (7)
C326	0.091 (8)	0.097 (7)	0.053 (6)	0.006 (5)	0.013 (5)	0.012 (6)
C331	0.061 (5)	0.049 (4)	0.049 (5)	-0.002 (4)	-0.001 (4)	0.007 (4)
C332	0.096 (8)	0.047 (5)	0.084 (7)	-0.011 (5)	-0.021 (6)	0.018 (5)
C333	0.117 (10)	0.083 (8)	0.114 (9)	-0.025 (7)	-0.046 (8)	0.038 (8)
C334	0.067 (8)	0.138 (11)	0.108 (9)	-0.034 (9)	-0.032 (7)	0.037 (8)
C335	0.066 (8)	0.131 (11)	0.106 (9)	-0.002 (8)	-0.022 (6)	-0.003 (8)
C336	0.073 (7)	0.080 (6)	0.066 (6)	0.012 (5)	-0.014 (5)	-0.004 (6)
C411	0.046 (5)	0.041 (4)	0.036 (4)	0.000 (3)	0.001 (3)	0.005 (4)
C412	0.041 (4)	0.044 (4)	0.042 (4)	0.005 (3)	0.010 (3)	0.005 (3)
C413	0.058 (6)	0.051 (5)	0.054 (5)	-0.003 (4)	0.000 (4)	0.000 (4)
C414	0.054 (5)	0.062 (5)	0.063 (6)	0.003 (4)	0.010 (4)	0.014 (5)
C415	0.076 (7)	0.048 (5)	0.061 (5)	0.006 (4)	0.010 (5)	0.014 (5)
C416	0.067 (6)	0.044 (4)	0.049 (5)	-0.001 (4)	0.014 (4)	0.005 (4)
C421	0.061 (5)	0.037 (4)	0.033 (4)	0.002 (3)	0.005 (4)	-0.005 (4)
C422	0.072 (6)	0.072 (6)	0.049 (5)	-0.003 (4)	-0.005 (5)	0.001 (5)
C423	0.094 (8)	0.098 (7)	0.037 (5)	0.004 (5)	-0.010 (5)	0.009 (6)
C424	0.124 (10)	0.073 (6)	0.047 (6)	0.012 (5)	-0.004 (7)	-0.007 (7)
C425	0.080 (7)	0.101 (7)	0.050 (6)	0.008 (5)	0.016 (5)	-0.017 (6)
C426	0.073 (6)	0.081 (6)	0.038 (5)	0.007 (4)	0.006 (4)	0.000 (5)
C431	0.065 (6)	0.039 (4)	0.053 (5)	0.001 (4)	-0.001 (4)	-0.008 (4)
C432	0.086 (7)	0.048 (5)	0.074 (6)	-0.004 (5)	-0.001 (5)	-0.007 (5)
C433	0.100 (8)	0.058 (6)	0.089 (8)	-0.002 (5)	-0.015 (7)	-0.009 (6)
C434	0.115 (10)	0.047 (6)	0.116 (10)	0.004 (6)	-0.023 (8)	-0.025 (6)
C435	0.083 (8)	0.069 (7)	0.125 (10)	0.035 (7)	-0.004 (7)	-0.016 (6)
C436	0.061 (6)	0.052 (5)	0.065 (6)	0.011 (4)	-0.004 (5)	-0.006 (4)
C511	0.066 (6)	0.049 (4)	0.034 (4)	0.001 (3)	0.015 (4)	-0.010 (4)
C512	0.093 (7)	0.068 (6)	0.054 (5)	0.003 (5)	0.016 (5)	-0.004 (5)
C513	0.097 (8)	0.095 (7)	0.059 (6)	-0.009 (6)	0.031 (6)	-0.026 (7)
C514	0.130 (11)	0.100 (9)	0.043 (6)	0.009 (6)	0.003 (6)	-0.055 (8)
C515	0.133 (11)	0.070 (6)	0.070 (7)	0.018 (6)	0.007 (7)	-0.025 (7)
C516	0.105 (8)	0.055 (5)	0.065 (6)	0.010 (5)	0.011 (6)	-0.008 (5)
C611	0.044 (4)	0.040 (4)	0.045 (4)	-0.001 (3)	0.003 (4)	0.004 (3)
C612	0.052 (5)	0.041 (4)	0.039 (4)	0.001 (3)	0.007 (4)	-0.005 (4)
C613	0.069 (6)	0.060 (5)	0.042 (5)	-0.007 (4)	0.010 (4)	-0.001 (4)
C614	0.058 (6)	0.064 (5)	0.081 (7)	-0.006 (5)	-0.001 (5)	-0.013 (5)
C615	0.057 (6)	0.063 (6)	0.067 (6)	-0.012 (5)	-0.006 (5)	0.003 (5)
C616	0.071 (6)	0.052 (5)	0.045 (5)	-0.003 (4)	-0.002 (4)	-0.001 (4)
C621	0.061 (5)	0.043 (4)	0.038 (4)	0.002 (3)	0.004 (4)	0.011 (4)
C622	0.089 (7)	0.068 (5)	0.045 (5)	0.000 (4)	0.025 (5)	-0.001 (5)
C623	0.125 (10)	0.104 (8)	0.056 (6)	0.005 (6)	0.049 (6)	-0.006 (7)

```

C624 0.096(8) 0.106(8) 0.053(6) -0.011(6) 0.035(6) -0.001(7)
C625 0.086(7) 0.073(6) 0.069(6) -0.020(5) 0.014(6) 0.013(5)
C626 0.074(6) 0.057(5) 0.055(5) 0.000(4) 0.012(5) 0.006(5)
C631 0.056(5) 0.040(4) 0.035(4) 0.006(3) 0.004(4) 0.005(4)
C632 0.059(6) 0.041(4) 0.074(6) 0.004(4) -0.002(5) 0.003(4)
C633 0.090(8) 0.043(5) 0.088(7) 0.006(5) 0.009(6) 0.002(5)
C634 0.107(9) 0.047(5) 0.082(7) 0.010(5) 0.017(6) 0.019(6)
C635 0.077(7) 0.071(6) 0.084(7) 0.013(5) 0.003(6) 0.026(6)
C636 0.074(6) 0.054(5) 0.054(5) 0.003(4) -0.007(5) 0.006(5)

#-----#
#          MOLECULAR GEOMETRY      #
#-----#
_geom_special_details
;
All esds (except the esd in the dihedral angle between two l.s. planes)
are estimated using the full covariance matrix. The cell esds are taken
into account individually in the estimation of esds in distances, angles
and torsion angles; correlations between esds in cell parameters are only
used when they are defined by crystal symmetry. An approximate (isotropic)
treatment of cell esds is used for estimating esds involving l.s. planes.
;
loop_
    _geom_bond_atom_site_label_1
    _geom_bond_atom_site_label_2
    _geom_bond_distance
    _geom_bond_site_symmetry_2
    _geom_bond_publ_flag

Mo1 C12      1.902(8) . ?
Mo1 C11      1.922(8) . ?
Mo1 C13      1.936(8) . ?
Mo1 O1       2.263(4) . ?
Mo1 P1       2.567(2) . ?
Mo1 P3       2.568(2) . ?
Mo2 C22      1.899(8) . ?
Mo2 C26      1.925(9) . ?
Mo2 C24      1.951(8) . ?
Mo2 O2       2.266(5) . ?
Mo2 P6       2.548(2) . ?
Mo2 P4       2.560(2) . ?
P1 C121     1.836(8) . ?
P1 C111     1.838(7) . ?
P1 C131     1.836(8) . ?
P2 O1       1.501(5) . ?
P2 C112     1.779(8) . ?
P2 C312     1.802(7) . ?
P2 C211     1.804(7) . ?
P3 C331     1.830(8) . ?
P3 C321     1.841(7) . ?
P3 C311     1.836(7) . ?
P4 C431     1.819(7) . ?
P4 C411     1.833(7) . ?
P4 C421     1.830(7) . ?
P5 O2       1.493(5) . ?
P5 C511     1.806(7) . ?
P5 C612     1.815(7) . ?
P5 C412     1.818(7) . ?
P6 C631     1.827(7) . ?
P6 C621     1.836(7) . ?
P6 C611     1.847(7) . ?
C11 O11     1.174(8) . ?
C12 O12     1.183(8) . ?
C13 O13     1.155(8) . ?
C22 O22     1.176(8) . ?
C24 O24     1.154(8) . ?
C26 O26     1.179(9) . ?

```

C111	C116	1.385(11)	.	?
C111	C112	1.418(10)	.	?
C112	C113	1.394(10)	.	?
C113	C114	1.362(11)	.	?
C114	C115	1.391(12)	.	?
C115	C116	1.366(11)	.	?
C121	C122	1.378(10)	.	?
C121	C126	1.379(10)	.	?
C122	C123	1.381(11)	.	?
C123	C124	1.352(12)	.	?
C124	C125	1.369(12)	.	?
C125	C126	1.378(11)	.	?
C131	C136	1.381(10)	.	?
C131	C132	1.392(11)	.	?
C132	C133	1.348(11)	.	?
C133	C134	1.370(12)	.	?
C134	C135	1.371(12)	.	?
C135	C136	1.388(11)	.	?
C211	C216	1.356(11)	.	?
C211	C212	1.392(11)	.	?
C212	C213	1.377(11)	.	?
C213	C214	1.340(13)	.	?
C214	C215	1.360(13)	.	?
C215	C216	1.394(11)	.	?
C311	C316	1.382(10)	.	?
C311	C312	1.421(10)	.	?
C312	C313	1.400(9)	.	?
C313	C314	1.362(11)	.	?
C314	C315	1.362(11)	.	?
C315	C316	1.379(11)	.	?
C321	C326	1.384(11)	.	?
C321	C322	1.378(10)	.	?
C322	C323	1.398(11)	.	?
C323	C324	1.337(12)	.	?
C324	C325	1.358(12)	.	?
C325	C326	1.388(12)	.	?
C331	C336	1.379(11)	.	?
C331	C332	1.381(10)	.	?
C332	C333	1.404(13)	.	?
C333	C334	1.343(15)	.	?
C334	C335	1.350(15)	.	?
C335	C336	1.360(13)	.	?
C411	C416	1.402(9)	.	?
C411	C412	1.411(9)	.	?
C412	C413	1.387(10)	.	?
C413	C414	1.388(10)	.	?
C414	C415	1.365(11)	.	?
C415	C416	1.379(11)	.	?
C421	C426	1.356(10)	.	?
C421	C422	1.379(10)	.	?
C422	C423	1.383(11)	.	?
C423	C424	1.371(13)	.	?
C424	C425	1.357(12)	.	?
C425	C426	1.412(11)	.	?
C431	C432	1.368(10)	.	?
C431	C436	1.387(11)	.	?
C432	C433	1.367(11)	.	?
C433	C434	1.372(14)	.	?
C434	C435	1.357(14)	.	?
C435	C436	1.421(12)	.	?
C511	C512	1.371(11)	.	?
C511	C516	1.388(11)	.	?
C512	C513	1.383(12)	.	?
C513	C514	1.372(14)	.	?
C514	C515	1.360(14)	.	?
C515	C516	1.387(12)	.	?
C611	C616	1.383(10)	.	?
C611	C612	1.409(9)	.	?

C612	C613	1.389(10)	. . ?
C613	C614	1.371(11)	. . ?
C614	C615	1.378(11)	. . ?
C615	C616	1.376(11)	. . ?
C621	C622	1.373(10)	. . ?
C621	C626	1.390(10)	. . ?
C622	C623	1.394(11)	. . ?
C623	C624	1.337(13)	. . ?
C624	C625	1.367(12)	. . ?
C625	C626	1.370(11)	. . ?
C631	C636	1.369(10)	. . ?
C631	C632	1.394(10)	. . ?
C632	C633	1.377(10)	. . ?
C633	C634	1.359(12)	. . ?
C634	C635	1.351(12)	. . ?
C635	C636	1.385(11)	. . ?

loop\_  
  \_geom\_angle\_atom\_site\_label\_1  
  \_geom\_angle\_atom\_site\_label\_2  
  \_geom\_angle\_atom\_site\_label\_3  
  \_geom\_angle  
  \_geom\_angle\_site\_symmetry\_1  
  \_geom\_angle\_site\_symmetry\_3  
  \_geom\_angle\_publ\_flag

C12	Mo1	C11	86.6(3)	. . ?
C12	Mo1	C13	86.5(3)	. . ?
C11	Mo1	C13	80.7(3)	. . ?
C12	Mo1	O1	173.4(3)	. . ?
C11	Mo1	O1	99.9(2)	. . ?
C13	Mo1	O1	96.1(2)	. . ?
C12	Mo1	P1	100.0(3)	. . ?
C11	Mo1	P1	169.0(2)	. . ?
C13	Mo1	P1	90.9(3)	. . ?
O1	Mo1	P1	73.90(13)	. . ?
C12	Mo1	P3	92.6(2)	. . ?
C11	Mo1	P3	90.4(2)	. . ?
C13	Mo1	P3	171.1(3)	. . ?
O1	Mo1	P3	85.82(12)	. . ?
P1	Mo1	P3	98.05(7)	. . ?
C22	Mo2	C26	82.0(3)	. . ?
C22	Mo2	C24	86.5(3)	. . ?
C26	Mo2	C24	84.7(3)	. . ?
C22	Mo2	O2	174.8(3)	. . ?
C26	Mo2	O2	102.1(3)	. . ?
C24	Mo2	O2	96.9(3)	. . ?
C22	Mo2	P6	90.2(3)	. . ?
C26	Mo2	P6	169.8(2)	. . ?
C24	Mo2	P6	88.3(2)	. . ?
O2	Mo2	P6	86.03(13)	. . ?
C22	Mo2	P4	104.8(2)	. . ?
C26	Mo2	P4	90.3(2)	. . ?
C24	Mo2	P4	166.9(2)	. . ?
O2	Mo2	P4	72.24(12)	. . ?
P6	Mo2	P4	97.97(6)	. . ?
C121	P1	C111	101.4(3)	. . ?
C121	P1	C131	101.9(3)	. . ?
C111	P1	C131	102.5(4)	. . ?
C121	P1	Mo1	113.9(3)	. . ?
C111	P1	Mo1	111.8(3)	. . ?
C131	P1	Mo1	122.7(3)	. . ?
O1	P2	C112	116.3(3)	. . ?
O1	P2	C312	111.2(3)	. . ?
C112	P2	C312	103.1(3)	. . ?
O1	P2	C211	108.4(3)	. . ?
C112	P2	C211	107.2(4)	. . ?
C312	P2	C211	110.4(3)	. . ?

C331	P3	C321	99.8(4)	. . ?
C331	P3	C311	102.7(3)	. . ?
C321	P3	C311	101.9(3)	. . ?
C331	P3	Mo1	120.5(3)	. . ?
C321	P3	Mo1	114.5(2)	. . ?
C311	P3	Mo1	114.8(2)	. . ?
C431	P4	C411	102.9(3)	. . ?
C431	P4	C421	100.6(3)	. . ?
C411	P4	C421	102.8(3)	. . ?
C431	P4	Mo2	124.5(3)	. . ?
C411	P4	Mo2	111.2(2)	. . ?
C421	P4	Mo2	112.4(2)	. . ?
O2	P5	C511	107.9(3)	. . ?
O2	P5	C612	113.8(3)	. . ?
C511	P5	C612	108.4(3)	. . ?
O2	P5	C412	114.6(3)	. . ?
C511	P5	C412	109.2(3)	. . ?
C612	P5	C412	102.7(3)	. . ?
C631	P6	C621	101.7(3)	. . ?
C631	P6	C611	104.4(3)	. . ?
C621	P6	C611	101.5(3)	. . ?
C631	P6	Mo2	119.6(2)	. . ?
C621	P6	Mo2	109.5(3)	. . ?
C611	P6	Mo2	117.6(2)	. . ?
P2	O1	Mo1	124.8(3)	. . ?
P5	O2	Mo2	125.2(3)	. . ?
O11	C11	Mo1	170.7(7)	. . ?
O12	C12	Mo1	178.3(7)	. . ?
O13	C13	Mo1	172.2(7)	. . ?
O22	C22	Mo2	176.2(7)	. . ?
O24	C24	Mo2	174.7(8)	. . ?
O26	C26	Mo2	169.7(7)	. . ?
C116	C111	C112	117.9(7)	. . ?
C116	C111	P1	121.6(6)	. . ?
C112	C111	P1	120.3(6)	. . ?
C113	C112	C111	118.9(7)	. . ?
C113	C112	P2	116.2(6)	. . ?
C111	C112	P2	125.0(5)	. . ?
C114	C113	C112	122.3(8)	. . ?
C113	C114	C115	118.3(8)	. . ?
C116	C115	C114	120.9(9)	. . ?
C115	C116	C111	121.7(8)	. . ?
C122	C121	C126	117.1(7)	. . ?
C122	C121	P1	123.4(6)	. . ?
C126	C121	P1	119.5(6)	. . ?
C121	C122	C123	120.5(8)	. . ?
C124	C123	C122	122.4(8)	. . ?
C123	C124	C125	117.5(8)	. . ?
C124	C125	C126	121.2(9)	. . ?
C121	C126	C125	121.3(8)	. . ?
C136	C131	C132	118.7(8)	. . ?
C136	C131	P1	118.2(6)	. . ?
C132	C131	P1	122.8(6)	. . ?
C133	C132	C131	121.5(8)	. . ?
C132	C133	C134	119.9(9)	. . ?
C135	C134	C133	120.0(9)	. . ?
C134	C135	C136	120.6(9)	. . ?
C131	C136	C135	119.2(8)	. . ?
C216	C211	C212	119.0(8)	. . ?
C216	C211	P2	118.0(6)	. . ?
C212	C211	P2	122.6(7)	. . ?
C213	C212	C211	119.3(9)	. . ?
C214	C213	C212	121.4(9)	. . ?
C213	C214	C215	119.9(9)	. . ?
C214	C215	C216	120.0(9)	. . ?
C211	C216	C215	120.3(9)	. . ?
C316	C311	C312	117.7(7)	. . ?
C316	C311	P3	121.1(6)	. . ?

C312	C311	P3	121.2(6)	. . ?
C313	C312	C311	119.0(7)	. . ?
C313	C312	P2	118.6(6)	. . ?
C311	C312	P2	122.4(5)	. . ?
C314	C313	C312	121.1(8)	. . ?
C313	C314	C315	120.2(7)	. . ?
C314	C315	C316	120.1(8)	. . ?
C311	C316	C315	121.9(8)	. . ?
C326	C321	C322	117.7(8)	. . ?
C326	C321	P3	119.4(6)	. . ?
C322	C321	P3	122.9(6)	. . ?
C321	C322	C323	120.4(8)	. . ?
C324	C323	C322	121.8(9)	. . ?
C323	C324	C325	118.0(9)	. . ?
C324	C325	C326	122.4(10)	. . ?
C321	C326	C325	119.6(9)	. . ?
C336	C331	C332	118.1(8)	. . ?
C336	C331	P3	117.2(6)	. . ?
C332	C331	P3	124.8(7)	. . ?
C331	C332	C333	117.9(10)	. . ?
C334	C333	C332	122.0(10)	. . ?
C333	C334	C335	120.0(11)	. . ?
C334	C335	C336	119.3(11)	. . ?
C335	C336	C331	122.7(10)	. . ?
C416	C411	C412	116.4(7)	. . ?
C416	C411	P4	121.8(6)	. . ?
C412	C411	P4	121.3(5)	. . ?
C413	C412	C411	121.1(6)	. . ?
C413	C412	P5	115.2(6)	. . ?
C411	C412	P5	123.5(5)	. . ?
C412	C413	C414	120.4(8)	. . ?
C415	C414	C413	119.5(8)	. . ?
C414	C415	C416	120.7(8)	. . ?
C415	C416	C411	121.9(8)	. . ?
C426	C421	C422	117.5(7)	. . ?
C426	C421	P4	125.6(6)	. . ?
C422	C421	P4	116.8(6)	. . ?
C421	C422	C423	122.5(9)	. . ?
C424	C423	C422	118.6(9)	. . ?
C425	C424	C423	120.8(9)	. . ?
C424	C425	C426	119.2(9)	. . ?
C421	C426	C425	121.4(8)	. . ?
C432	C431	C436	119.1(7)	. . ?
C432	C431	P4	123.3(7)	. . ?
C436	C431	P4	117.6(6)	. . ?
C433	C432	C431	121.8(9)	. . ?
C432	C433	C434	119.7(10)	. . ?
C435	C434	C433	120.5(9)	. . ?
C434	C435	C436	119.9(10)	. . ?
C431	C436	C435	118.9(9)	. . ?
C512	C511	C516	118.9(8)	. . ?
C512	C511	P5	125.6(6)	. . ?
C516	C511	P5	115.4(6)	. . ?
C511	C512	C513	121.0(9)	. . ?
C514	C513	C512	119.1(10)	. . ?
C515	C514	C513	121.3(10)	. . ?
C514	C515	C516	119.4(10)	. . ?
C515	C516	C511	120.4(10)	. . ?
C616	C611	C612	117.4(7)	. . ?
C616	C611	P6	120.9(6)	. . ?
C612	C611	P6	121.7(5)	. . ?
C613	C612	C611	120.0(7)	. . ?
C613	C612	P5	118.8(6)	. . ?
C611	C612	P5	121.3(6)	. . ?
C614	C613	C612	121.0(8)	. . ?
C613	C614	C615	119.5(8)	. . ?
C614	C615	C616	119.9(8)	. . ?
C611	C616	C615	122.2(8)	. . ?

C622	C621	C626	117.0(7)	. . ?
C622	C621	P6	121.8(6)	. . ?
C626	C621	P6	121.0(6)	. . ?
C621	C622	C623	121.1(8)	. . ?
C624	C623	C622	120.3(9)	. . ?
C623	C624	C625	120.0(9)	. . ?
C624	C625	C626	120.2(9)	. . ?
C625	C626	C621	121.2(8)	. . ?
C636	C631	C632	117.8(7)	. . ?
C636	C631	P6	126.4(6)	. . ?
C632	C631	P6	115.9(6)	. . ?
C633	C632	C631	120.9(8)	. . ?
C634	C633	C632	119.5(9)	. . ?
C635	C634	C633	120.7(9)	. . ?
C634	C635	C636	120.0(9)	. . ?
C631	C636	C635	120.9(9)	. . ?